



universität
wien

DISSERTATION

Titel der Dissertation

Designing & Characterization of Plastic Antibodies as
Chemical Sensor Materials for Pesticides Detection

Verfasserin

Mag. Sadaf Yaqub

angestrebter akademischer Grad

Doktorin der Naturwissenschaften der.(Dr. rer.nat.)

Wien, 2010

Studienkennzahl lt. A 0419

Studienblatt:

Dissertationsgebiet lt. Chemie

Studienblatt:

Betreuerin / Betreuer: O. Univ. Prof. Dr. Franz Ludwig Dickert

Preface

This work is done in the department of Chemical Sensors and Optical Molecular Spectroscopy since the official commencement date of the approved research program from Mar 2007 till Sep 2010 under the supervision of O. Univ. Prof. Dr. Franz Ludwig Dickert at the Institute of Analytical Chemistry, University of Vienna, Währingerstraße 38, 1090-Vienna, Austria.

To

Maan Jee (Late)

&

My Parents

Acknowledgements

I would like to express sincere gratitude to my supervisor, *O. Univ. Prof. Dr. Franz Ludwig Dickert*. He has not only been a fantastic scientific mentor but also an effervescent personality who kept me going during the most challenging times. His wisdom and enthusiasm has been a beacon for me. With his positive approach, he always had solutions for problems whether academic or personal. I gratefully acknowledge the impact that he has made to this research and to my own scientific development.

More importantly, I owe a debt of gratitude to *Ao. Univ. Prof. Mag. Dr. Peter A. Lieberzeit* for the many stimulating discussions where his wisdom and insightful observations have contributed to my critical thinking. He was always there to help in academic as well as administrative matters out of his busy schedules. I sincerely thank him for his consistent guidance and support throughout my stay in Vienna.

I thank my colleagues; *Mr. Alexander Biedermann* and *Mr. Pual Grilberger* for making efficient oscillator circuits for the present work.

I'm obliged to the Higher Education Commission (HEC) of Pakistan for the grant of scholarship to pursue PhD studies in Austria. I would like to acknowledge the support of my *employers in Pakistan* to grant me study leave. It would have been definitely impossible to complete the dream of my life to pursue PhD studies without their assistance.

I have been lucky to be surrounded by intellectuals and talented people who influenced positively in my professional and spiritual growth. In this regard, my heartfelt gratitude is to *Dr. Touqeer, Mrs. Yabqua Anwar* and *Mrs. Al-Awami Sawsan* for their encouragement and mentoring role they played in my life.

I believe strongly in expending interaction outside of work circle for developing broader outlook in the learning process. On this note, I would like to thank *Dr. Yahsinta, Dr. Fida* and *Dr. Flora* for sharing ideas, advice and cheerful company, which, throughout this journey have played a major part. My Special thanks are due to *Isabella, Christina and Carole* for their love and care, making my stay in Austria memorable.

My gratitude also goes to *Fabiha, Gul and all Pakistani friends and families* here, for their love and hospitality, enabling me periodic escapes from the world of scientific inquiry. It was due to all of them that I felt at home in Vienna.

Finally, I am also forever thankful to *(Late) Maan jee* my life role model, *my parents and family*, for their unconditional love and unwavering support. Living apart, far away from them was very tough. Indeed, it was their sincere prayers and encouragement that led me to accomplish my PhD journey.

Table of Contents

ACKNOWLEDGEMENTS.....	5
ABBREVIATIONS & ACRONYMS	11
CHAPTER 1.....	13
INTRODUCTION	13
1.1 PESTICIDES	14
1.2 CLASSIFICATION OF PESTICIDES.....	15
1.3 TRIAZINE HERBICIDES	16
1.4 CHLOROTRIAZINE HERBICIDES	16
1.4.1 ATRAZINE	18
1.4.2 SIMAZINE.....	19
1.4.3 PROPАЗINE.....	19
1.4.4 TERT-BUTHYLАЗINE	20
1.5 MECHANISM OF PESTICIDES ACTION	20
1.6 ENVIRONMENTAL FATE OF TRIAZINES	22
1.7 CHEMICAL SENSORS	23
1.8 QUARTZ CRYSTAL MICROBALANCES (QMB).....	24
1.9 SYNTHETIC ANTIBODIES AS SENSOR LAYERS	25
1.10 ROLE OF ATR-IR IN MIP PREPARATION.....	26
1.11 ATOMIC FORCE MICROSCOPY (AFM).....	27
1.12 STATE OF ART.....	29
CHAPTER 2.....	31
METHODOLOGY	31
2.1 PIEZOACOUSTIC DEVICES & MEASUREMENT SET UP.....	31
2.2. GRAVIMETRIC SET UP.....	32
2.3 SYNTHESIS OF MIP COMPOSITIONS.....	33
2.4 IMMOBILIZATION OF MIPs ON GOLD SURFACE.....	34

2.5	TEMPLATE REMOVAL	35
2.6	IR ANALYSIS FOR TEMPLATE REMOVAL.....	39
CHAPTER 3.....		41
SENSOR MEASUREMENTS WITH MOLECULARLY IMPRINTED POLYMER LAYERS.....		41
3.1	SENSITIVITY MEASUREMENTS.....	41
3.1.1	MIP-MA30 [POLYMETHACRYLIC ACID] OF ATRAZINE	41
3.1.2	MIP-MA30 [POLYMETHACRYLIC ACID] OF PROPAZINE.....	43
3.1.3	MIP-VP [POLYVINYLPIRROLIDONE] OF PROPAZINE.....	46
3.1.4	EFFECT OF ACID CONTENT OF MIP-MA [POLYMETHACRYLIC ACID] ON SENSITIVITY.....	49
3.1.5	MIP-MA46 [POLYMETHACRYLIC ACID]	51
3.2	SELECTIVITY MEASUREMENTS.....	55
3.2.1	MIP-MA30 [POLYMETHACRYLIC ACID]	55
3.2.2	MIP-ME35 & ME42 MIP [CO-POLYMER OF METHACRYLIC ACID & METHYL ACRYLATE]	57
3.3	TEMPERATURE EFFECTS ON SENSOR RESPONSE.....	63
3.4	EFFECT OF METHANOL ON MIP LAYERS FOR TEMPLATE REMOVAL.....	64
3.5	COMPARISON OF SENSOR RESPONSE OF MIP LAYERS	65
CHAPTER 4.....		67
DETECTION WITH MOLECULARLY IMPRINTED NANOPARTICLES.....		67
4.1	NANOPARTICLES AS CHEMICAL SENSOR COATINGS	67
4.2	SYNTHESIS & EXTRACTION OF IMPRINTED PARTICLES	68
4.3	ATOMIC FORCE MICROSCOPE STUDIES	69
4.4	TEMPLATE REMOVAL	73
4.5	IMMOBILIZATION OF IMPRINTED NANOPARTICLES ON QCM.....	74
4.6	SENSOR MEASUREMENTS.....	76
4.7	SIZE AND DISTRIBUTION OF IMPRINTED NANOPARTICLES.....	77
4.8	EFFECT OF SIZE OF NANOPARTICLES ON SENSOR RESPONSE.....	81
4.9	SENSITIVITY MEASUREMENTS	82
4.10	SELECTIVITY MEASUREMENTS	85
4.11	SURFACE ROUGHNESS OF IMPRINTED NPS LAYER	88

CHAPTER 5.....	91
QCM BASED SENSOR WITH NATURAL ANTIBODY	91
5.1 PIEZO ACOUSTIC DEVICES & MEASUREMENT SET-UP.....	91
5.2 SENSITIVITY MEASUREMENTS	91
5.3 SELECTIVITY MEASUREMENTS	95
5.4 AFM STUDIES OF SENSOR SURFACE.....	97
CONCLUSIONS	101
ABSTRACT.....	107
LIST OF FIGURES	111
REFERENCES	123

Abbreviations & Acronyms

ACN	Acetonitrile
AFM	Atomic force microscopy
AIBN	Azobisisobutyronitril
ATRIR	Attenuated total reflection infrared
ATR	Atrazine
DEA	Desethyl Atrazine
DIA	Desisopropyl Atrazine
DEDIA	Desethyl disopropyl Atrazine
EGDMA	Ethyleneglycoldiaminemethacrylate
GHz	Giga hertz
MA	Methacrylic acid
MA30	Polymer of Methacrylic acid (30%)
MA46	Polymer of Methacrylic acid (46%)
ME	Copolymer (MA & MMA)
ME42	Copolymer (42% of MA & MMA)
MeOH	Methanol
MHz	Mega hertz
MIPs	Molecularly imprinted polymers
MMA	Methylmethacrylate
NPs	Nanoparticles
Nm	Nanometre
λ	Wavelength
PDMS	Polydimethylsiloxane
PU	Polyurethane
PRO	Propazine
PROX	Propoxur
PVP	Polyvinylpyrrolidone

QCM	Quartz crystal micro balance
rpm	Rotations per minute
T	Temperature in °C
TBA	Terbuthylazine
THF	Tetrahydrofuran
UV	Ultraviolet
VP	Vinyl Pyrrolidone

Chapter 1

INTRODUCTION

Chemicals for crop protection and pest control - known collectively as Pesticides - are applied extensively in Europe and other parts of the world mainly to ensure sustainable agriculture with sufficient yield of food and fiber supplies¹. Some of these pesticides penetrate into soils and underground water² as a result of direct application or through indirect means into the food chain³. Potential hazards^{4,5,6} of pesticides for human health have derived serious concerns for researchers to develop methods and update techniques for detection of pesticides in the environment.

Monitoring data for pesticides are generally poor in much of the world and especially in developing countries. Key pesticides namely Atrazine, Simazine and Propazine are included in the monitoring schedule of most western countries, however the cost of analysis and the necessity to sample at critical times of the year (linked to periods of pesticide use) often preclude development of an extensive data set. Many developing countries have difficulty carrying out organic chemical analysis due to problems of inadequate facilities, impure reagents, and financial constraints.

According to European regulations⁷, the permissible amount of each pesticide is 0.1 μ g/L and collectively as sum of all pesticides is 0.5 μ g/L in water. Therefore need of the time is to develop cheap, frequent in use and durable analytical for on-line monitoring pesticides traces in water.

Though, instrumental analysis has proven to be an efficient strategy to detect all kinds of compounds generated by synthetic activities. But in case of pesticide continuous monitoring requires alternative tools and techniques to replace tedious procedures⁸ and expensive lab equipments⁹.

A well known technology of modern analytical chemistry is molecular recognition through artificial antibodies¹⁰. Mimics of natural antibody are products

of MIP (Molecularly imprinted polymer) that allow selective recognition of targeted molecules by cross-linked polymers¹¹⁻¹². Further, MIPs are combined with the sensitivity offered by QCM (Quartz Crystal Microbalances) sensors¹³ for transduction. The combination of molecular imprinting polymers with QCM transducers has proven to be a highly efficient sensing system in a wide range of analytical application¹⁴.

The process of combining MIP techniques with QCMs includes designing an active polymer system and on-chip polymerization of imprinting agents to provide MIP-functionalized QCM probes. MIP based QCM shows sensitivity for print molecules in form of negative frequency shift when the molecules interact with its surface, resulting in increase of mass. Therefore, QCMs can be considered as extremely sensitive mass-measuring device at nano scale making them highly suitable for dynamic monitoring of pesticides. Furthermore, by transforming such imprinted receptors into nanoparticles has the advantage of increased surface area to amplify sensor signals. Highly expensive natural antibodies for pesticides in market can be replaced by designing similar artificial receptors. By applying these artificial receptors to QCM sensor system, miniaturized, inexpensive and fast sensors can be produced for online monitoring of pesticides in water.

1.1 Pesticides

Generally, the term “pest” encompasses all unwanted organisms pertaining pathogenic properties which may cause health concerns, destroy or damage food, crops or other goods, significant for human consumption. Whereas “pesticides” are the chemicals used to destroy, prevent, or repel such organisms¹⁵.

Application of chemicals categorized as pesticides is also found in ancient history. For instance, Chinese were using Arsenic in A.D. 900 to eliminate garden insects¹⁸. Arsenic and tobacco as insecticides were also used in Europe in 17th century. In agriculture too, pest control has been practiced for centuries by adopting various methodologies to control weeds. However, by the expansion in world’s population the need for food and fiber production also increased drastically.

Therefore, application of pesticides for crop protection and pest control has continued and intensified with the course of time.

1.2 Classification of Pesticides

Based on the type of pests controlled by these chemicals, pesticides are generally divided into five classes as illustrated in **Fig. 1**.

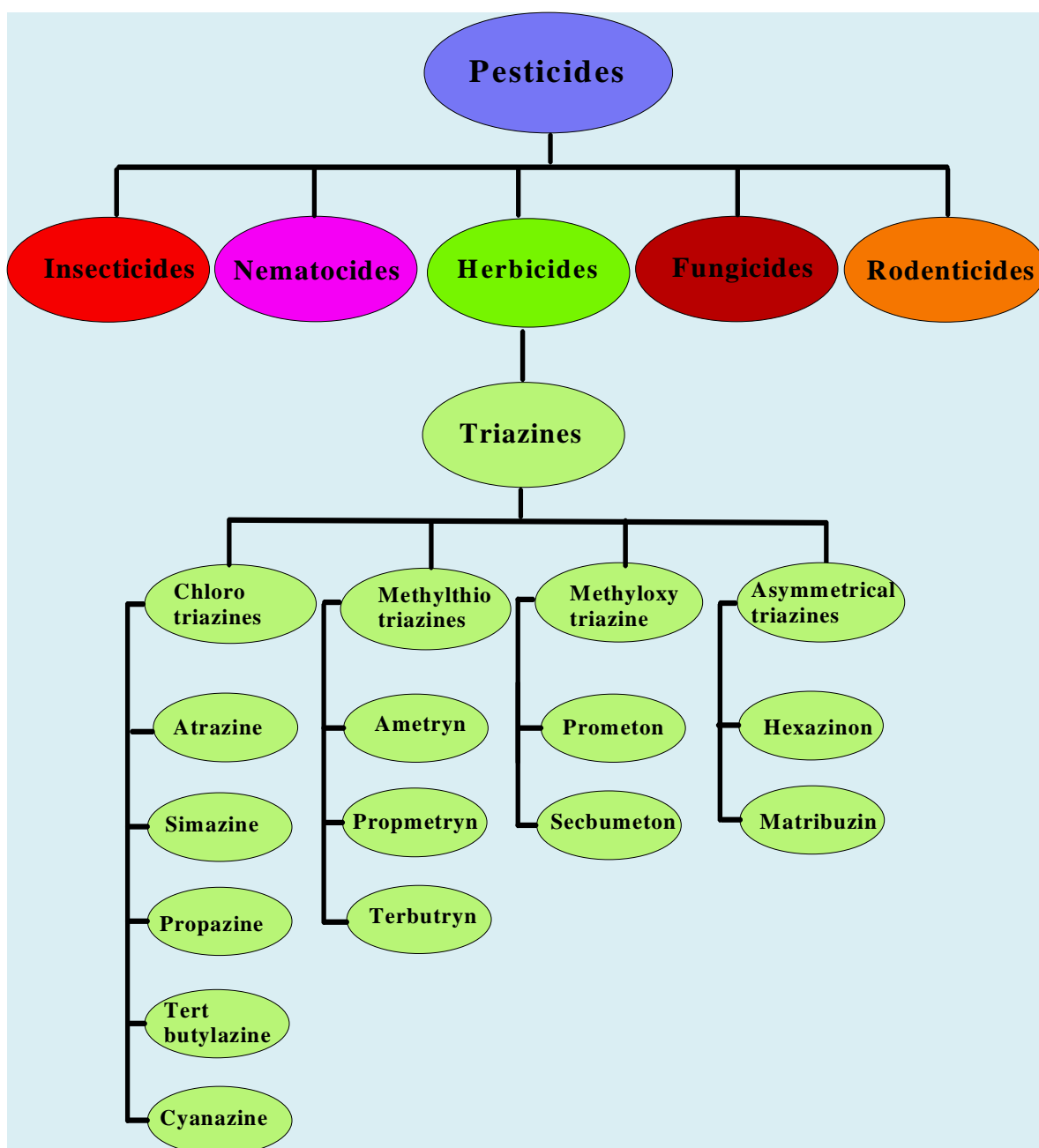


Figure 1: Classification of Pesticides

Among these, herbicides are group of chemicals used to destroy unwanted plants, categorized as weeds. Weeds occupy agricultural area or consume nutrients required for essential crops and other significant goods. The firstly developed herbicides of major importance belong to triazines family¹⁹.

1.3 Triazine Herbicides

The triazine herbicides are considered as the most significant category of herbicides since the time of their early development in 1950's. To fulfill the food demands of the global population, triazines played the key role in weed control. The discovery of first triazine was made in Switzerland in 1952, leading to evolutionary developments in the agriculture from scientific laboratories to the crop field. Being the main components in controlling weeds, the triazines brought major agricultural transformations in Europe. Due to extensive use for more than 50 crops in more than 100 countries, these chemicals especially Atrazine, have been highly focused by researchers and regulatory authorities to monitor their impact on ecosystem. After positive reviews the regulatory authorities from United States, the European Union, Australia, and France and World Health Organization (WHO) continued their registration till date.

Triazines are used in combination with other active chemicals for controlling majority of weeds in a range of tillage systems for better growth of various crops. Most important features of triazines are their ability to conserve tillage, saving land from erosion and managing weed biotypes which are no more controllable by other herbicides due to genetic transformations. Keeping in view, the resulting benefits of triazines, even after decades of origin, their careful use is still essential for worldwide agricultural production.

1.4 Chlorotriazine Herbicides

Chlorotriazines are among the firstly discovered triazines used as legalized herbicides in 1960. Most commonly applied Chlorotriazines are Atrazine (ATR), Simazine (SIM), Propazine (PRO) and Terbutylazine (TBA). Metabolites of

Atrazine like des-ethyl atrazine (DEA), des-isopropyl-atrazine (DIA) and des-ethyl-des-isopropyl-atrazine (DEDIA) are found to be toxic as the parent Atrazine (ATR). The structures of Chlorotriazines analyzed in present work are illustrated in **Fig. 2**.

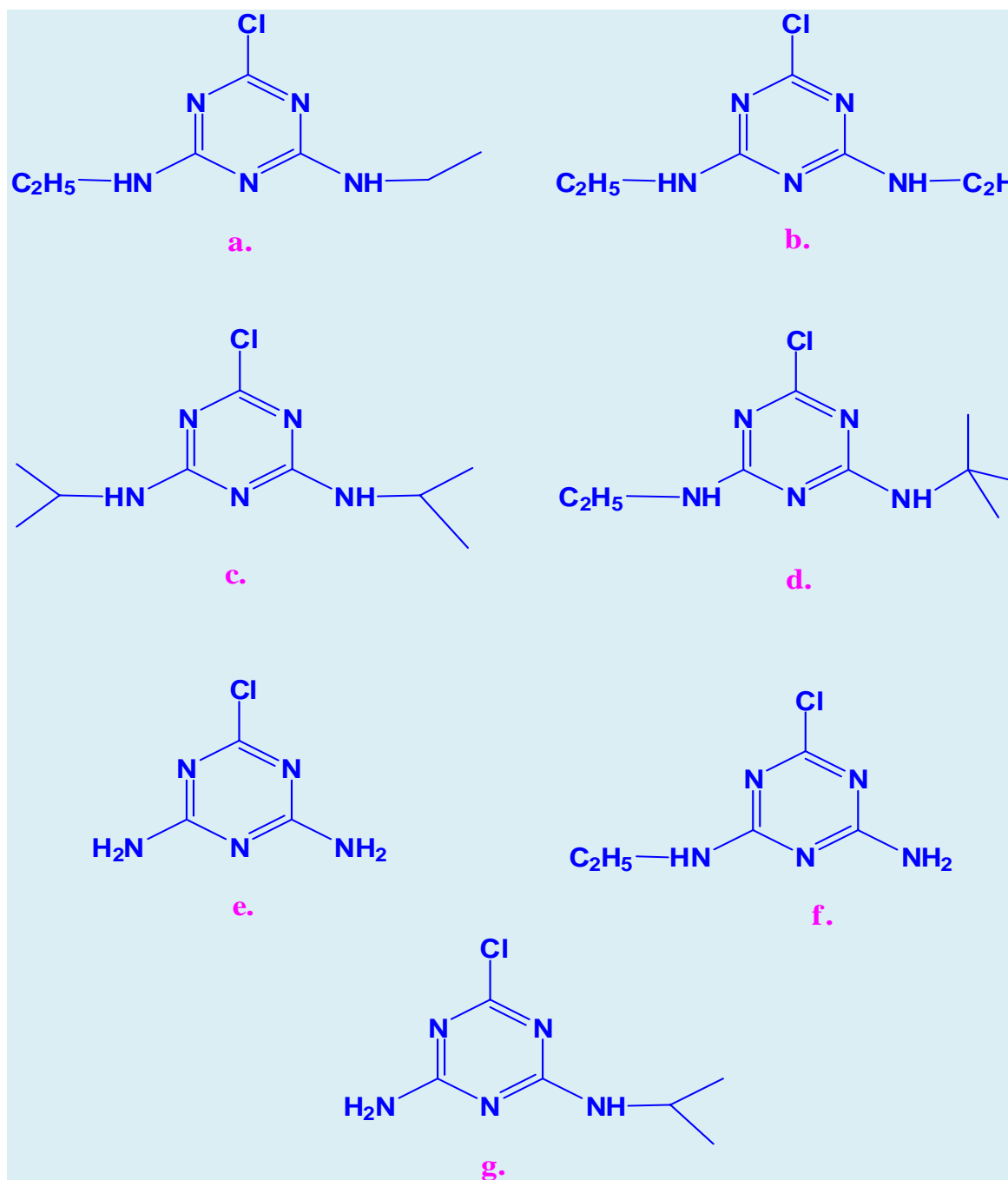


Figure 2: Chemical Structures of Chlorotriazine Herbicides; Atrazine (ATR), b. Simazine (SIM), c. Propazine (PRO). d. Terbutylazine (TBA), e. Des-ethyl-isopropyl atrazine (DEDIA), f. Des-iso propyl atrazine (DIA), g. Des-ethyl atrazine

Physical properties of these herbicides (**Table-1**) vary with alkyl substituent attached to triazine ring.

Analytes	Mol.For/ Mol.wt	M.P (°C)	Solubility at pH 7 & 20°C (ppm)				
			H ₂ O	C ₂ H ₅	Acetone	n-C ₆ H ₂₄	CH ₂ Cl ₂
Atrazine	C ₈ H ₁₄ ClN ₅ 215.7	173- 176	33	15000	31000		4000
Ter- buthylazine	C ₉ H ₁₆ ClN ₅ 229.7	174- 177	8.5	1400	41000	410	9800
Propazine	C ₉ H ₁₆ ClN ₅ 216.1	212- 214	5.0			CCl ₄ 2500	6.2
Simazine	C ₇ H ₁₂ ClN ₅ 201.7	224- 227	6.2	570	1500	3.1	130

Table 1: Physical properties of some Chlorotriazines commonly used as Herbicides

1.4.1 Atrazine

Atrazine, a Chloro-dialkyl- substituted triazine has been one of the most widely applied herbicide for pre- and post-emergence weed control in agriculture for more than five decades. Initially, Atrazine was allowed commercially for weed control on corn crops and non-cropland in Europe and the United States. By applying Atrazine, strenuous labor for hand weeding was no more required. With the excellent yield of corn, Atrazine became the most important member of Chlorotriazines transforming the corn production highly economical.

After testing the Atrazine residues in soil through available analytical techniques at 1969, the first US Atrazine tolerances were approved for corn, sorghum, macadamia nut, pineapple, sugarcane, and wheat.

Research work has been continued to determine toxicity and persistency of Atrazine residues in environment as potential groundwater contaminants. The harmful effects of such contamination on human life are possibility of cancer, injury to the nervous system, lung damage, reproductive dysfunction, and possible dysfunction of the endocrine and immune systems. Owing to its high risk factor, Atrazine thereby has been classified as Priority A chemical by the U.S. Environmental Protection agency (EPA)¹⁶.

1.4.2 Simazine

Simazine was the first triazine herbicide authorized for commercial use in non crop field and then for corn, after data acquisition of its metabolites and fate of deposits in soil. With a vast range of applicability, Simazine has been successfully used to control broad leaf weeds. In the course of time, it has been applied to eliminate weeds in number of fruit plants, ornamental, nursery stock, and corn crops. With growing needs of weed control, Simazine is also sprayed in industry and under guard rails. Not only for land but for aquatic systems also, Simazine proved to be effective. Use of Simazine even in presence of many other herbicides as well as its structural similarities with Atrazine makes it an important analyte for testing contaminations in water.

1.4.3 Propazine

Propazine belongs to triazine family with two propyl amino substituent. Being expensive and less applicable compared to other herbicides, the use of Propazine has been restricted to sorghum and corn crops. Analysis of such molecules helps in establishing the methodologies to trace triazines in water.

1.4.4 Tert-butylazine

Terbutylazine is another novel Chlorotriazines characterized by ethylamino and tert-butylamino side chains. It is applied in more than 45 countries and all over Europe in corn, vineyards and orchards, however not authorized in the United States, except for use in cooling towers against algae. Terbutylazine has substituted Atrazine and Simazine in many countries of Europe when combined with other herbicides. In countries with higher amounts of Atrazine (0.1 ppb) residue in ground water, Atrazine has been replaced by Terbutylazine.

1.5 Mechanism of Pesticides Action

Triazine herbicides can selectively diminish weeds without destroying crops like Corn, sorghum and sugar cane. A few members of triazine family are also applied to orchards, horticultural, and perennial crops, etc. for weed control.

Overall, herbicides have been helpful in managing a vast range of grass and broadleaf weed. However, triazine-resistant weeds are also developed in course of time. Triazines have ability to bind with QB proteins and selectively destroy weeds by stopping electronic flow in photosynthetic electron transport chain. Selective destruction of weeds by triazines occurs due to their fast metabolic detoxification. The main detoxification of triazine in crops like sorghum occurs by conjugation with a protein known as glutathione (GSH).

In case of Chlorotriazines when applied to corn crop, inactivation of herbicide occurs by hydrolytic dehalogenation or nucleophilic substitution of chloride with hydroxyl group. In Sorghum, triazines also get detoxified by N-dealkylation. Some members of triazines family destroy weeds with weak roots and cannot access deep in soil to crop roots.

Fig. 3 illustrates the metabolic pathways¹⁷ of Atrazine in Sorghum ending in degraded products like des-ethyl-atrazine (DEA), des-isopropyl-atrazine (DIA) and des-ethyl-des-isopropyl-atrazine (DEDIA) through dealkylation.

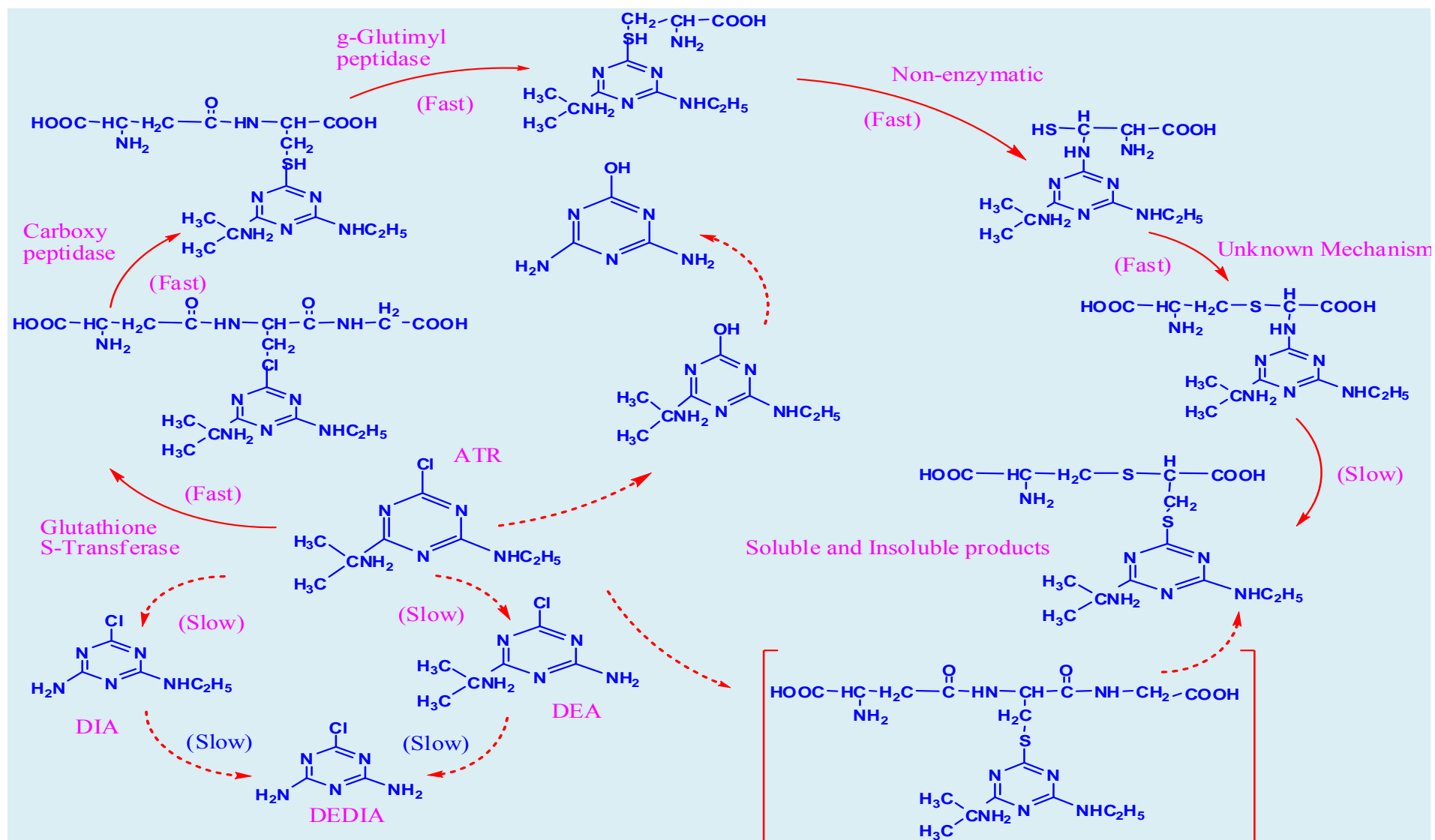


Figure 3: The metabolic pathways for Atrazine (ATR) in sorghum through N-dealkylation, hydrolytic dehalogenation, or nucleophilic displacement. Solid lines present major pathways and dashed lines show minor pathways of formation of Metabolites like des-ethyl atrazine (DEA), des-isopropyl atrazine (DIA) and des-ethyl des-isopropyl atrazine (DEDIA).

1.6 Environmental Fate of Triazines

Water plays an important role in transportation of pesticides from the areas where they are applied to other locations, where they may cause health problems. Even if pesticides are distributed throughout the landscape, water monitoring is important due to leaching of these chemicals from soil to wells, aquifers, and lakes. Ground water is used for drinking in many parts of the world. This especially concerns people living in the agricultural areas where pesticides are most often used, as most of that population relies upon ground water for drinking purpose. Earlier, it was assumed that soil acted as a protective filter to stop pesticides from reaching ground water. Studies¹⁸ have now shown that this is not the case. Pesticides can reach water-bearing aquifers below ground from applications onto crop fields, seepage of contaminated surface water, accidental spills and leaks, improper disposal, and even through injection waste material into wells. **Fig. 4** depicts an approximate time line for pesticides to appear in ground water.

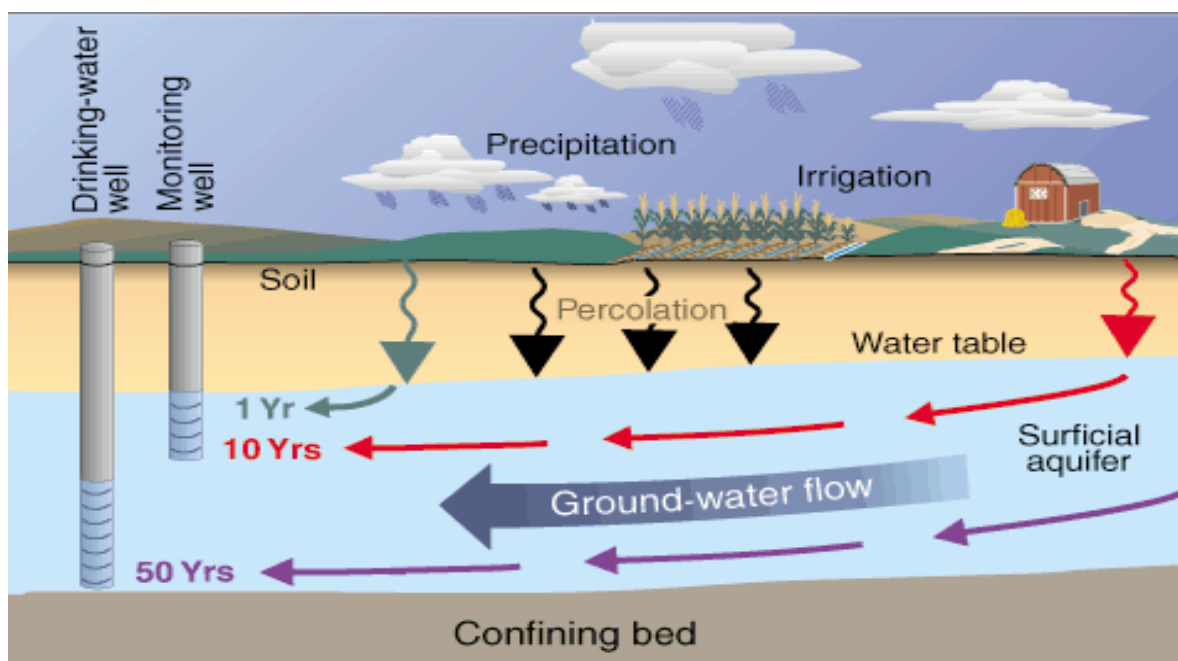


Figure 4: Scheme illustrates pathway of pesticides during the course of time from field to underground water.

1.7 Chemical Sensors

Chemical sensors¹⁹ are micro-sensing devices that detect or generate signal as a consequence of chemical interaction with an analyte²⁰. A chemical sensor comprises four main elements (**Fig.5**):

- Chemically sensitive layer capable to interact selectively and reversibly with the analyte to bring a physical change in mass or voltage or polarity etc.,
- Physical transducer which can transform this change into electrical signal.
- Electronic set up for signal processing to amplify and transfer the signal to data acquisition unit
- Data acquisition unit for storage of received signal and process it to demonstrate analytical information in form of data set points.

Owing to the nature of transduction element, chemical sensors can be optical, thermal, electrochemical or acoustic wave/mass sensors. Among these sensors, acoustic sensors based on oscillator technologies are primarily used for the detection of gaseous species²¹ and liquids^{22,23}

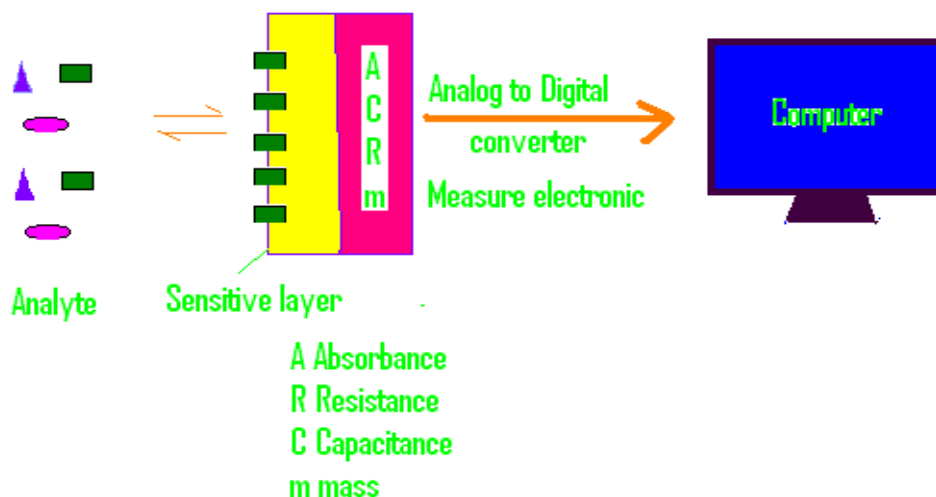


Figure 5: Schematic set up for Sensor Measurements

As interaction of chemical species occurs at the quartz surfaces through absorption or adsorption, a signal indicates the change caused by the additional

mass. The signal appears in form of frequency shift to detect presence or absence of the analyte and also its concentration within a limiting range. The acoustic sensors utilize Shear and Rayleigh waves at frequencies ranging from MHz to GHz. Depending upon the mode of vibration of elastic membrane or bulk material; acoustic sensors consist of a large variety of sensors. One of such device that uses vibrating piezoelectric crystal plate is known as Quartz Crystal Microbalances (QCM)²⁴.

1.8 Quartz Crystal Microbalances (QMB)

Crystalline Quartz exhibits piezoelectricity due to polar axes without centre of symmetry.

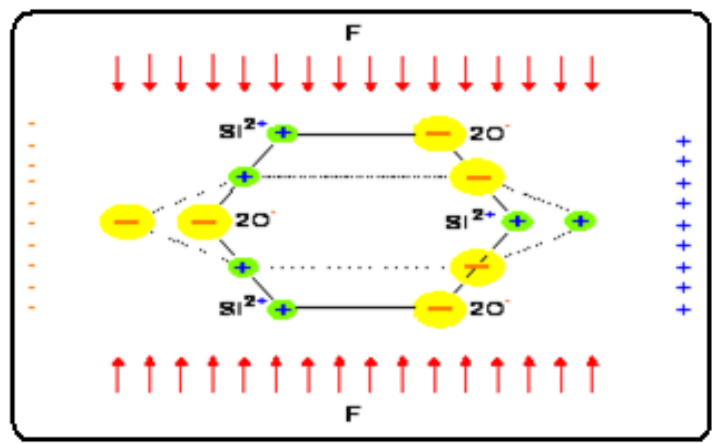


Figure 6: Generation of electric potential in QCM

With mechanical stress is applied on certain faces of QCM, shifting of charge centers occur within crystal creating a dipole and as a result an electric potential²⁵.

By cutting the crystalline quartz in different angles, different mode of vibrations can be achieved for various applications. QCM used in present work are AT cut to reduce temperature effects for their better performance in harsh environments²⁵. The commercial available QCM have resonance frequency 5-50 MHz depending on their thickness. The quartz crystals work as microbalances due to the correlation of deposited mass on their surface to the frequency shift as given by the Sauerbrey's equation²⁶ for QCM in liquid phase i.e.

$$\Delta f = -f_o^2 \frac{2}{(\rho_m C_q)^{1/2}} \sqrt{\frac{\rho_l \eta_l}{4\pi f_o}} \dots\dots \text{Eq. 1}$$

Where,

Δf = change in frequency,

f_o = fundamental resonance frequency of the crystal

Δm = change in mass, A_{cr} = area/size of the crystal

ρ_m = density of the chemical film, C_q = shear modulus of the quartz crystal

ρ_l = density of the surrounding liquid and η_l = viscosity of the surrounding liquid

1.9 Synthetic Antibodies as Sensor Layers

Synthetic antibodies as mimics of natural antibody can be synthesized by molecular imprinting²⁷ (**Fig. 7**).

Molecular imprinting involves polymerization of monomer units in presence of print molecules utilizing either non-covalent interactions such as hydrogen bonding, ion-pair interactions, etc. (non-covalent imprinting) or reversible covalent interactions (covalent imprinting). Extraction of the print molecules creates sites in the polymer that are chemically as well as physically complementary to the original print molecule²⁸.

In this way the biotype nature of MIPs makes them highly suitable for a broad range of applications from structural studies of ligand-receptor interactions to selective binding-matrices in detection, separation, and purification²⁹. Nanoparticles of MIP are advantageous over MIP thin films due to enhanced surface area of active sites. By extraction of pre-polymerized solution in a different phase, nanoparticles gel is collected and immobilized over the substrate to improve sensitivity of host molecules towards specific analyte³⁰.

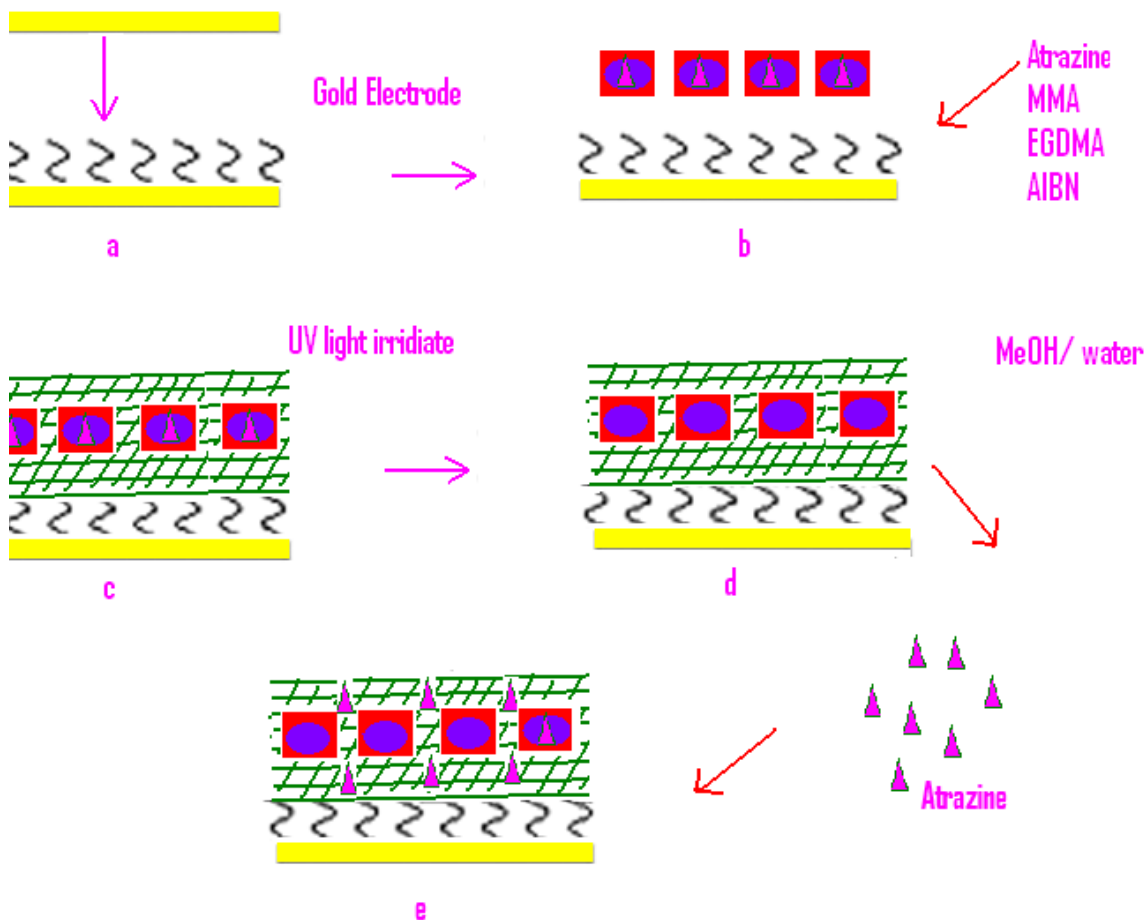


Figure 7: Schematic illustration of the MIP preparation for Sensor Layer on Gold electrode of QCM.

1.10 Role of ATR-IR in MIP Preparation

Attenuated total reflection (ATR) is an advance technique to examine in situ solid or liquid samples³¹. Infrared spectroscopic study of aqueous solutions is challenging due to the high infrared absorption of water. An alternate is attenuated total reflection technique that measures the change in infrared beam while in contact with a sample (**Fig.8a**). The infrared beam is first directed to a crystal with high refractive index like Zinc Selenide coated with diamond for chemical resistance (**Fig.8b**).

Total internal reflection generates an evanescent field only in range of few micrometers beyond the crystal surface and the sample. As the sample absorbs the energy in the region of infrared spectrum, the evanescent wave attenuates.

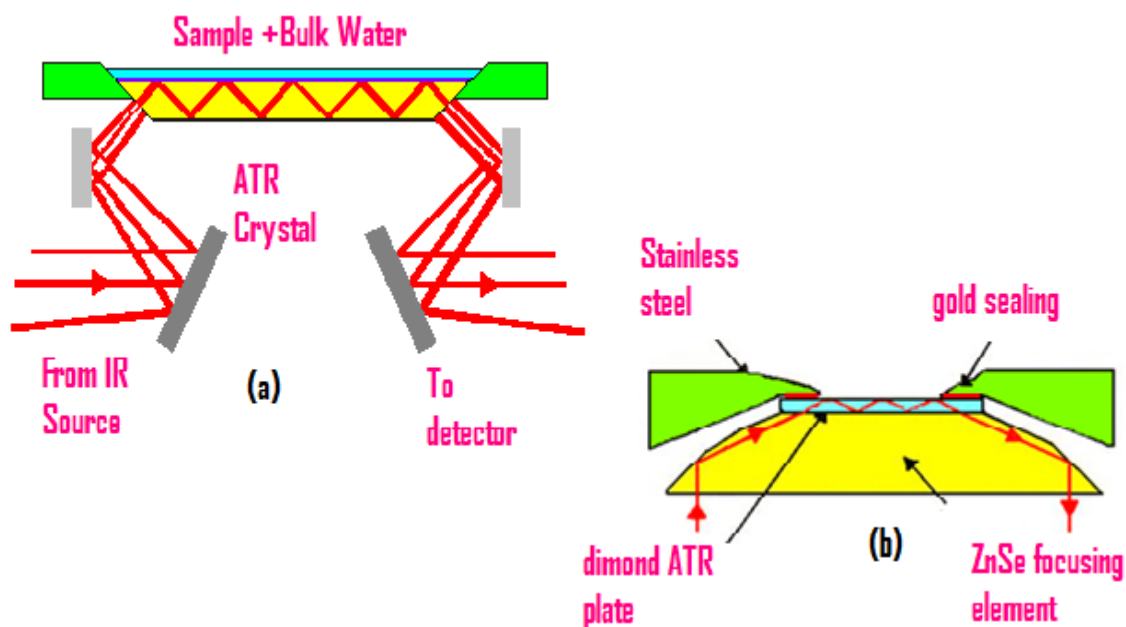


Figure 8: Schematic sketch of ATR

After exiting from the other end of crystal, the attenuated IR beam is detected and IR spectrum is obtained by the IR spectrometer. During the synthesis of MIP, ATR/IR studies in situ help to investigate the extent of polymerization and also interaction intensity of template molecule within the cross linked polymer. Removal of template from the polymer matrix can also be investigated through ATR spectra by using different solvents during the spectral analysis.

1.11 Atomic Force Microscopy (AFM)

Atomic force microscopy scans images at higher resolution down to few nanometers. A mechanical probe or tip at the end of a metallic frame ‘cantilever’ interacts with the sample surface (see **Fig. 9**). Depending upon the distance between tip and surface in range of 0.001 to 100 nm, coulombs or Van der Waal forces are generated. These attractive and repulsive forces lead to cantilever deflection.

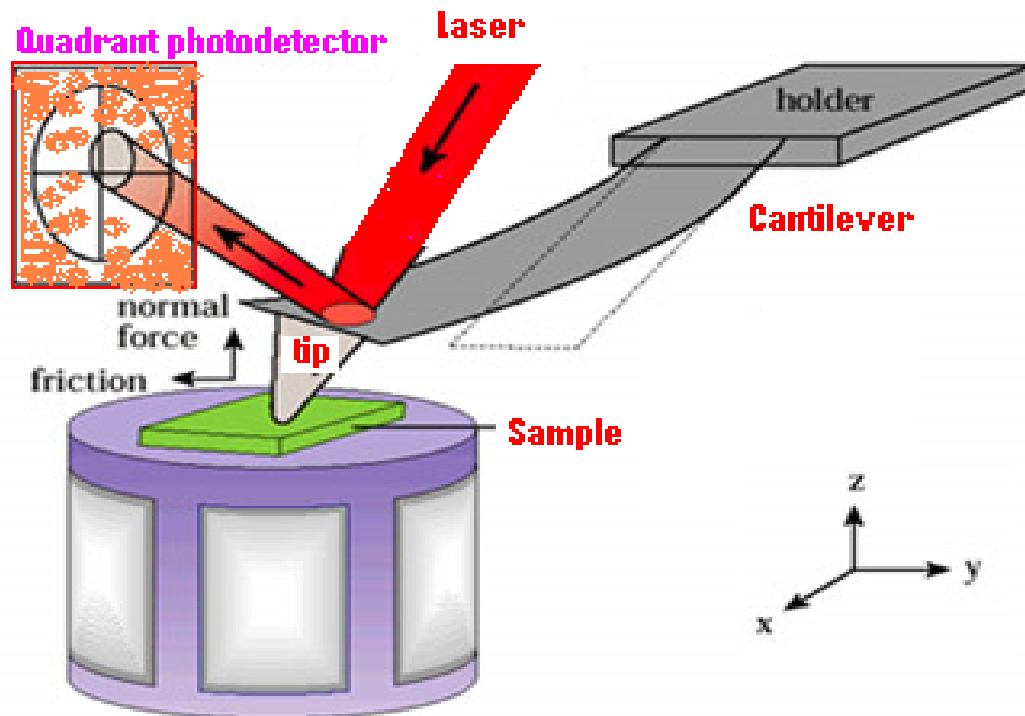


Figure 9: Working principle of AFM

The upper side of cantilever has a reflective coating exposed to laser from a solid state diode. By the laser light, intensity of deflection is measured in Contact or tapping mode. In contact mode, movement of tip is controlled by piezoelectric scanner located under the sample substrate.

Measurement can be made by keeping constant force or constant height. While in the tapping mode, deflection is measured at a certain frequency with short spans of tip in contact with the surface. Using this technique, data about surface topology is calculated without damaging the sample surface³². In present work, AFM images were taken to characterize MIP layer height and size of nanoparticles. The image below (**Fig. 10**) shows the AFM program window while scanning image of MIP-nanoparticles.

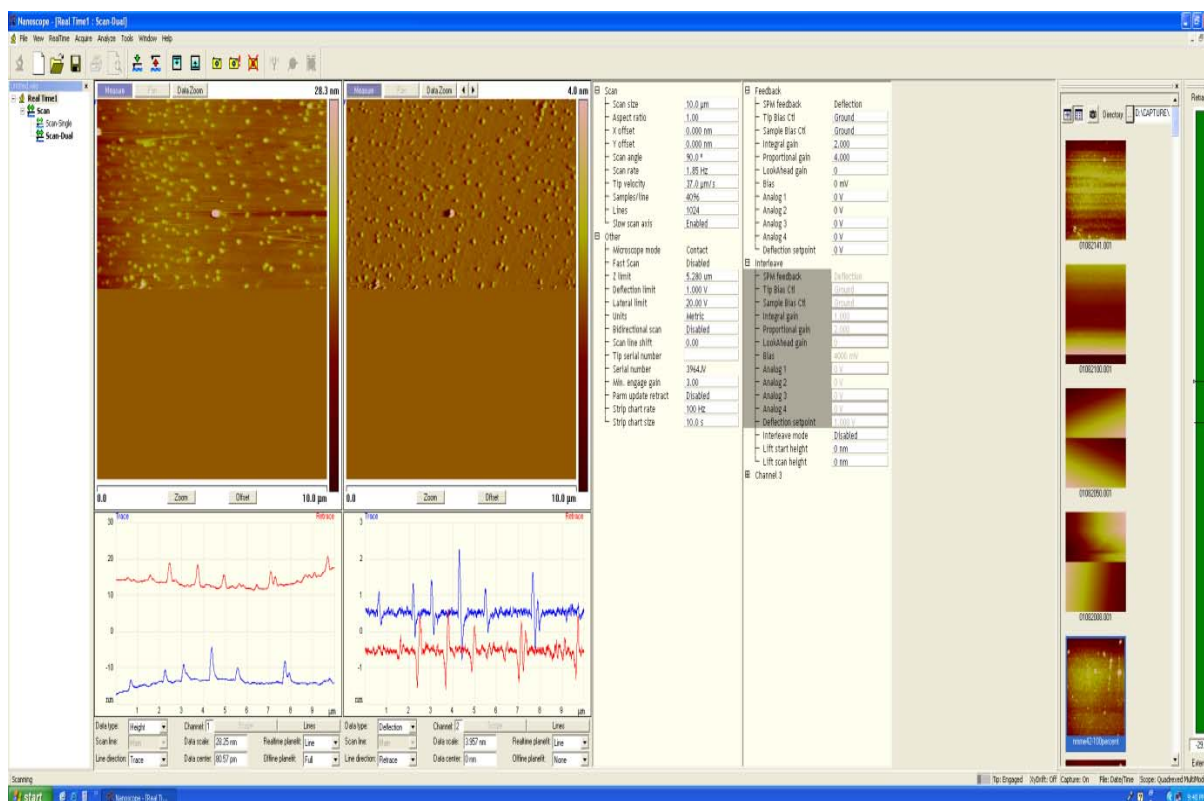


Figure 10: Screen image of AFM scan with “Nanoscale” software while probing imprinted nanoparticles film in contact mode

1.12 State of Art

To improve online pesticides testing methods in practice, an alternative technique is, to use artificial receptors which are mimics of the natural antibodies. The purpose of this dissertation is to develop sensitive layers by synthetic antibodies in form of imprinted polymers and nanoparticles on mass-sensitive quartz microbalances for the detection of s-triazines. In particular, the optimization of MIP compositions for better selectivity and comparison of their efficiency with natural antibodies as chemical sensor coatings is discussed

Chapter 2

METHODOLOGY

2.1 Piezoacoustic Devices & Measurement Set Up

Quartz crystals (Fundamental resonance frequency 10MHz) used in all the experiments, were purchased from Zhejiang Quartz Crystal Electronic Company, Shanghai, China. Dual electrode geometries (**Fig. 11**) were screen-printed (brilliant gold paste from Heraeus) onto quartz discs by gold paste using a silk sieve (mesh size: 41 μ m).

Printing sieve was fixed on a metallic frame and coated with UV photo-resist lacquer. After keeping it in dark for 20 min two-electrode sketch was patterned on it in UV-printer within 20 seconds. Electrodes design was prominent on the sieve after washing the unhardened lacquered areas with warm water. Two such sieves were prepared for each side of the electrodes by making electrode dia. 5 mm on side to be coated and 3mm for the other side for electronic connections. Gold was pasted using these sieves by creating vacuum to QCM on substrate. By keeping the QCM at 400 °C for 2 -3 hrs for each side coating, organic chemicals of paste were removed and gold electrodes were ready with low damping.

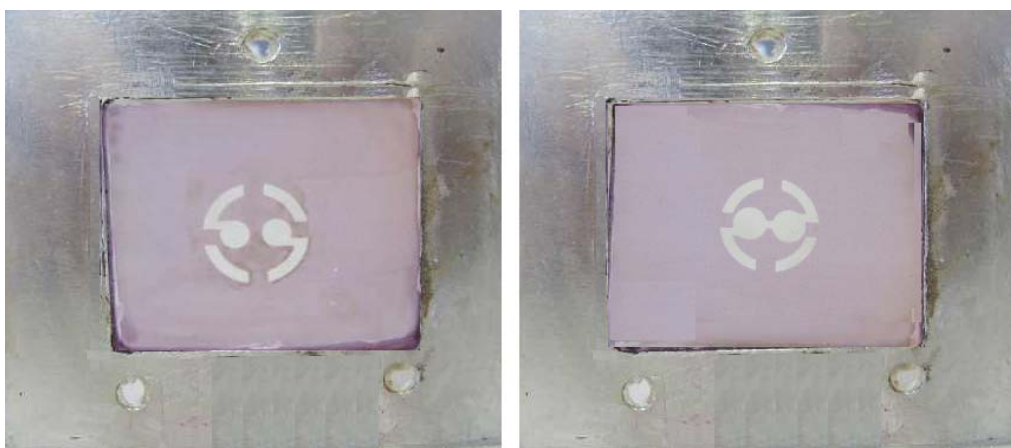


Figure 11: Photographs of silk-screen sieves showing dual-electrode structure printed for coating front and back sides of electrodes on QCM.

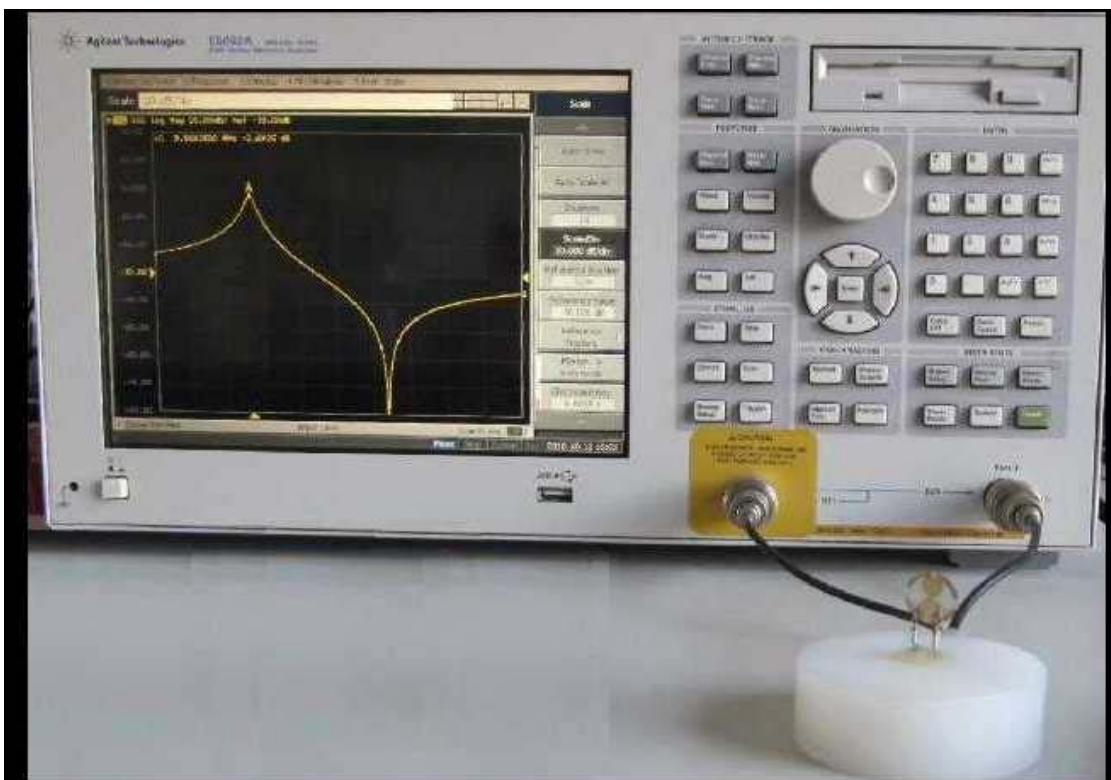


Figure 12: Network Analyzer generating damping and phase spectra for gold electrode of QCM.

2.2. Gravimetric Set Up

Gravimetric analysis was carried out by fixing the QCM with coated sensor layers in a flow cell. The purpose of flow cell is to provide thermally and mechanically stable measuring environment. The design of flow cell is simple with an inlet and outlet tubes for liquid flow and two connections to oscillator circuit. QCM are mounted horizontally in flow cell having volume of 150 μL . Custom built oscillator circuits are connected with the cell. Only one side of QCM was exposed to liquid to minimize damping effects. The frequency shifts of quartz were measured by a HP53131A frequency counter, and the data was transferred via a HP-IB bus to a computer. The whole experimental set up is illustrated in **Fig. 13** with a photographic image.

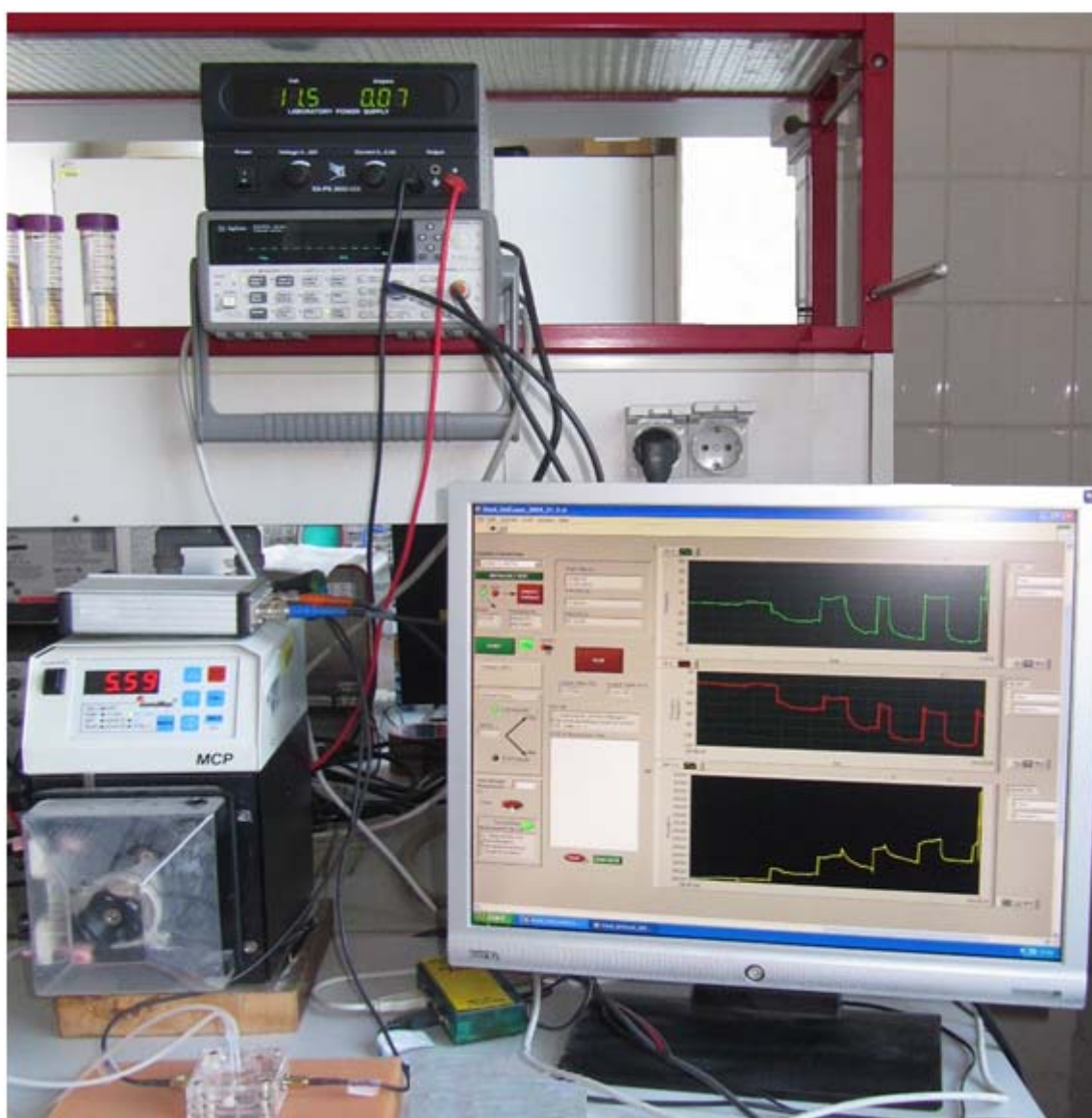


Figure 13: Chemical Sensor set up in running mode.

2.3 Synthesis of MIP Compositions

General procedure opted for synthesis was pre-polymerization of monomer mixtures with a cross-linker in presence of analyte by heating in water bath. Time of synthesis varied for different polymers depending on nature of monomers, amount of initiator, solvent and cross linker and temperature³³. On reaching near the gel point, polymer became viscous indicating pre-polymerization of the mixture. Following the same procedure a non-imprinted solution without template was

prepared in each case for reference electrode. **Fig.14** illustrates chemical structures of reagents used for synthesis of polymers.

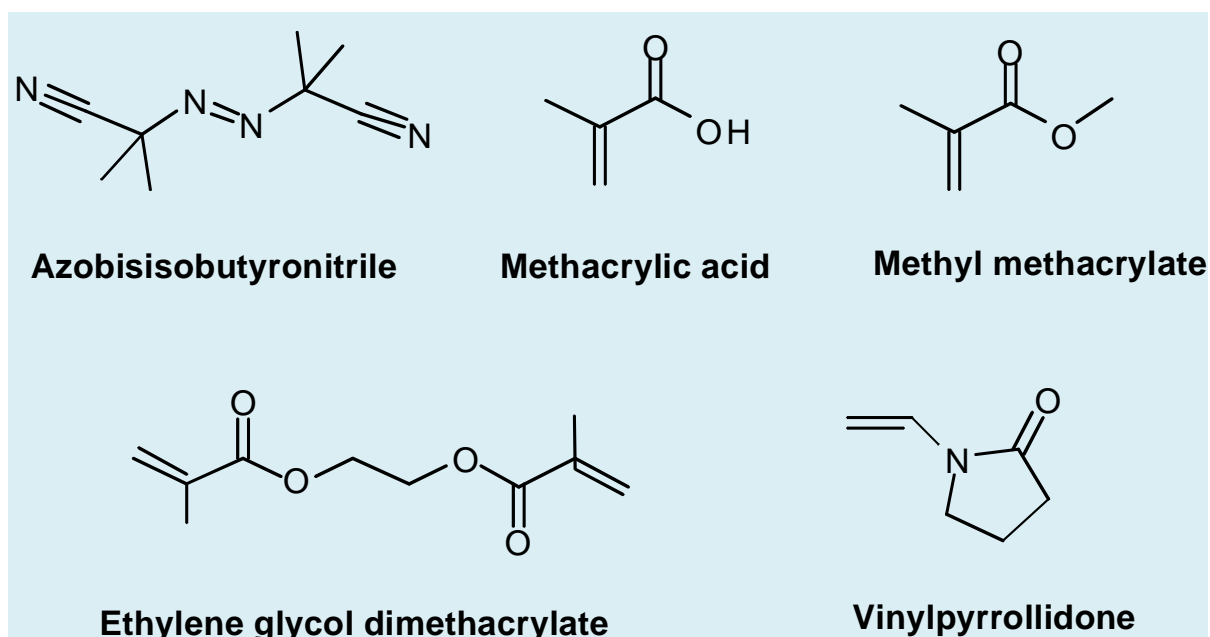


Figure 14: Chemical structures of reagents used for polymer synthesis

2.4 Immobilization of MIPs on Gold Surface

Imprinted and reference solutions were spin coated on the QCM electrodes. The thickness of coated layer was optimized by adjusting spinning speed and dilution ratio of solutions. Coated QCM was kept under UV in nitrogen atmosphere for 12 hrs at room temperature. Afterwards, thickness of the imprinted and non imprinted layers was determined from the frequency difference of the quartz crystal before and after coating the layer materials. In order to avoid cross-talk effects, the frequency of both channels should have at least a difference of 3 kHz.

A network analyzer of the ENA series of Agilent Technologies (model no. E5062A) was used to check frequency for the thickness of coated layers on each electrode.

2.5 Template Removal

Removal of Atrazine and related structural analogues from imprinted polymers was difficult with water due to strong interaction of polymeric acid with triazine moieties. There are some low affinity areas and high affinity areas in the imprinted layer. Low affinity areas got clean up easily while high affinity areas can only be cleaned by suitable solvents or conditions e.g. heating or vacuum drying. In case of Atrazine, different solvent systems were tested. The frequency of quartz electrodes was checked each time after using each solvent to determine any loss of mass. The effect of solvent on non imprinted layer was also observed to monitor loss of polymer mass. Theoretically, 1 kHz frequency shift is taken as mass load of 40 nm. Based upon this value, frequency shifts observed for imprinted and non imprinted layers were calculated for loss of layer height as presented in **Table 2**.

	Imprinted channel freq. (kHz)	Layer height in (nm)	Imprinted layer height (kHz)	Imprinted layer height (% decrease)	Non-imprinted channel freq. (kHz)	Non-imprinted layer height (kHz)	Layer height in(nm)	Non-imprinted layer height (% decrease)
Original Frequency /Solvents	9.886375	480	12	0	9.915813	12	480	0
Water	9.886734	464	11.64	3	9.916010	11.8	472	1
Methanol	9.890375	372	9.31	22.4	9.916156	11.65	466	3
Acetic acid & methanol (1:4)	9.891177	288	7.2	40	9.916409	10.08	403	16
Acetic acid	9.892369	240	6	50	9.917913	9.48	379	21

Table 2: Data illustrating increase in frequency of electrodes with mass loss of layers coated with imprinted MIP-ME42 [35% of methylacrylic acid & 7% of methylacrylate cross-linked with 58% ethylene glycol dimethacrylate by weight and imprinted with 10 % Atrazine] and Non-imprinted polymer [ME42] by different solvents applied to remove template.

As depicted in **Fig.15**, decrease in mass from frequency counts for imprinted polymer was pronounced as compared to loss in mass of non-imprinted polymer layer.

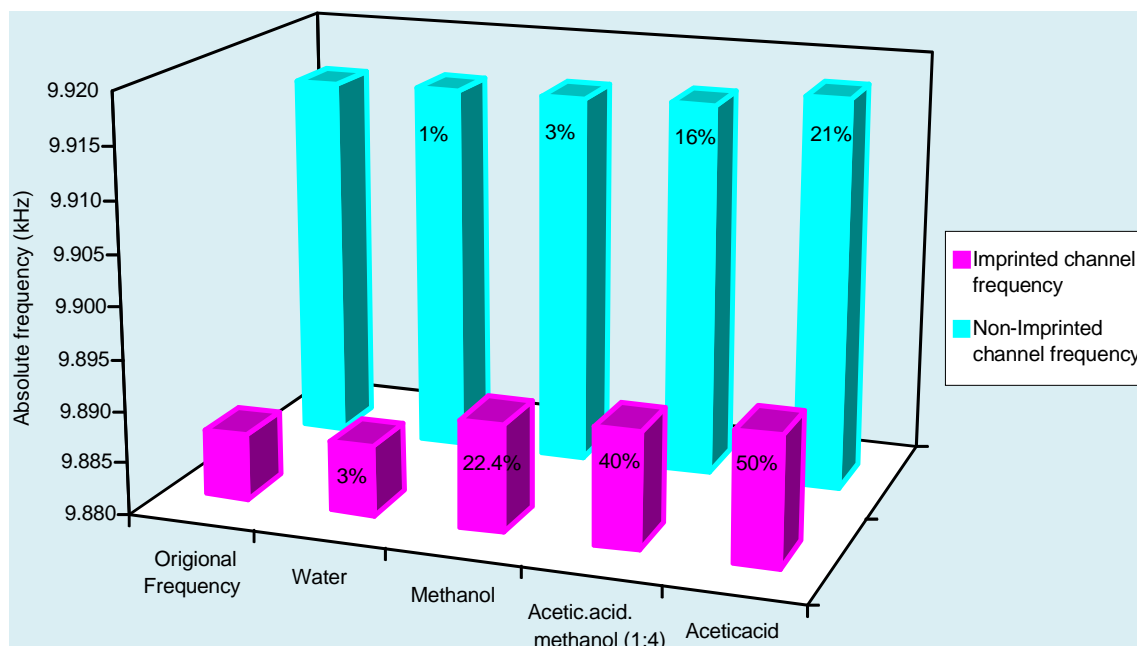
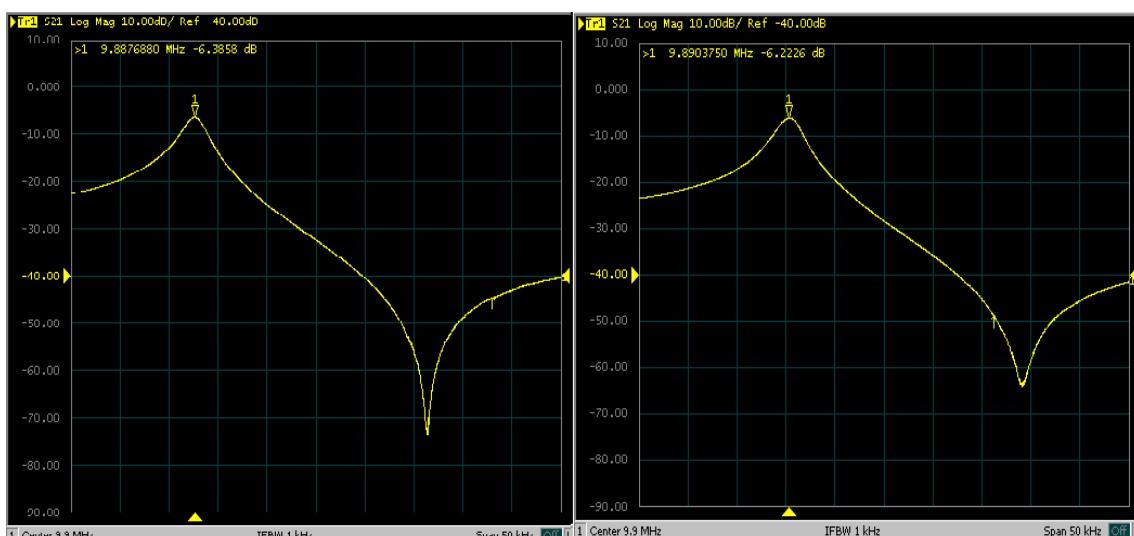


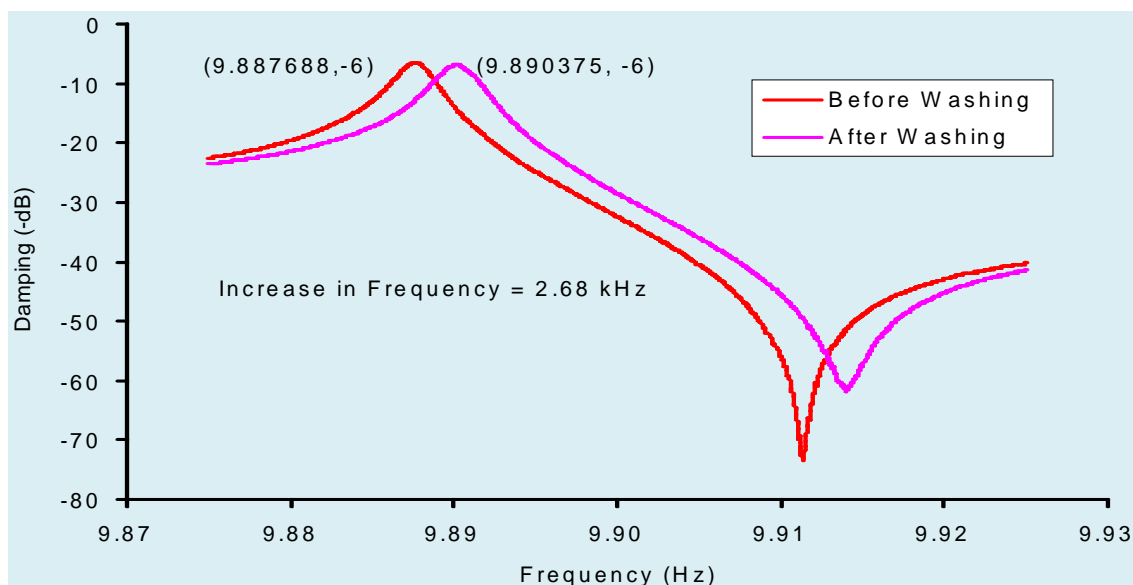
Figure 15: Graphic presentation of increase in frequency of electrodes due to loss in layer height (shown in percent) due to different solvents applied to remove (10%) Atrazine used as template. Imprinted and non imprinted layers each of 12 kHz composed of copolymer [35% of methylacrylic acid & 7% of methylacrylate cross-linked with 58% ethylene glycol dimethacrylate by weight].

In solvent system containing conc. acetic acid, the 16% and 40 % weight loss was observed for non imprinted & imprinted layers. Thus, indicating significant damage to polymer layer. The most suitable solvent for template removal was methanol as decrease in mass of polymer layer was only 3 % for reference, showing layer stability. Imprinted layer has 22% loss of layer mass indicating maximum extraction of analyte molecules with some loss of polymer. **Fig. 16** shows image of damping spectra by network analyzer of QCM before and after washing the

imprinted polymer layer of 12 kHz on gold electrode. The rise in frequency recorded after washing was 2.68 kHz.



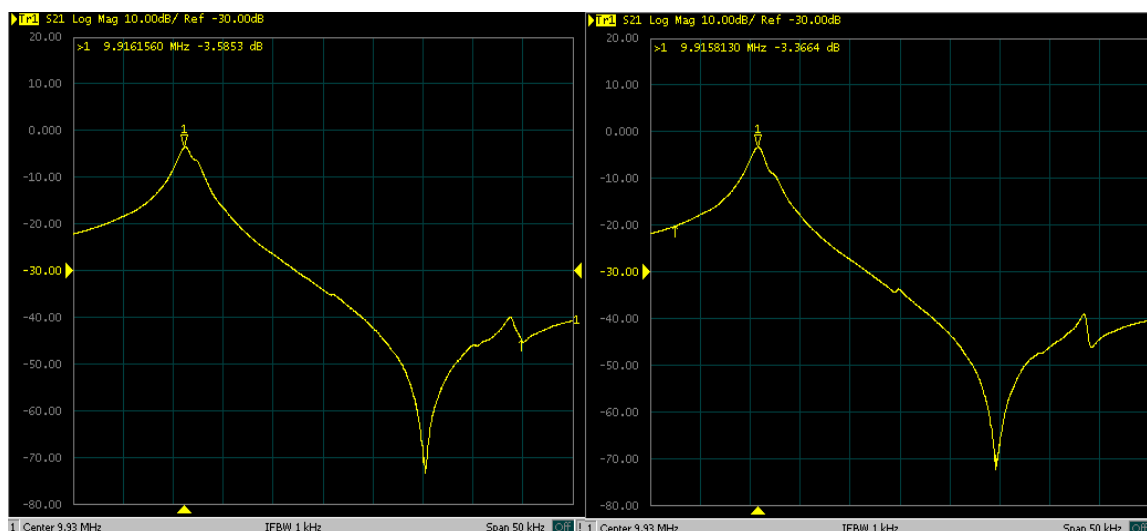
(a)



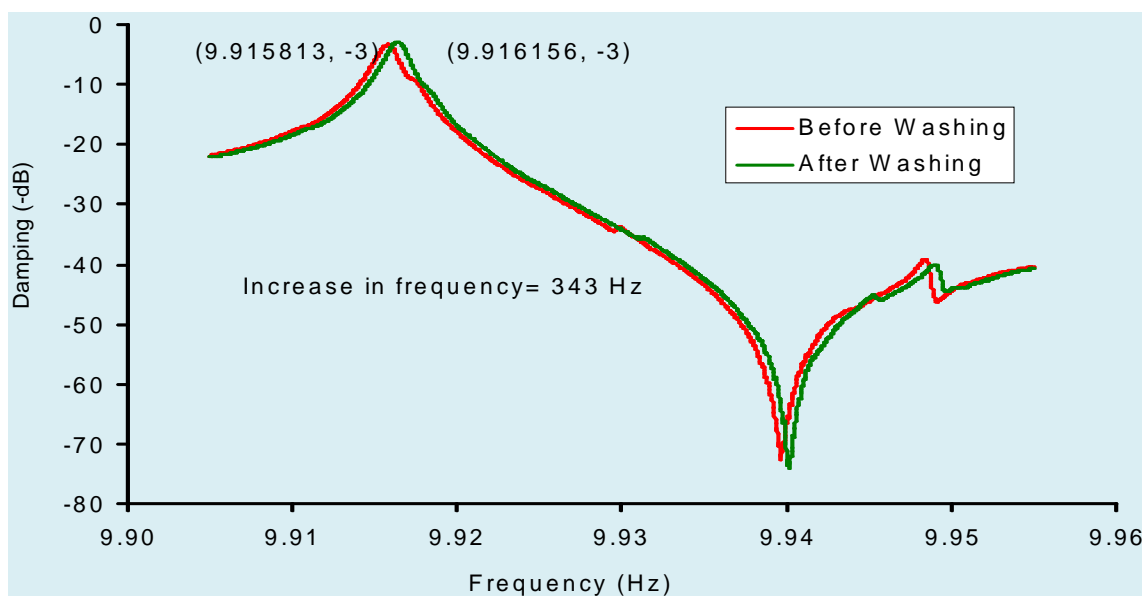
(b)

Figure 16: Damping spectra of QCM electrode taken at 50 kHz span, before and after washing with methanol, coated with MIP-ME42 [35% of methylacrylic acid & 7% of methylacrylate cross-linked with 58% ethylene glycol dimethacrylate by weight and 10% Atrazine as template]. Difference in the resonance frequencies was 2.68 kHz (a). Image of spectra by network analyzer (b). Graphic presentation

As shown in **Fig.17**, the damping spectra recorded by network analyzer for QCM electrode coated with non imprinted polymer layer [ME42], the difference of frequency after washing with methanol was only 343 Hz, indicating stability of polymer layer.



(a)



(b)

Figure 17: Damping spectra of QCM electrode taken at 50 kHz span before and after washing with methanol coated with non imprinted polymer ME42 [35% of methacrylic acid & 7% of methacrylate cross-linked with 58% ethylene glycol dimethacrylate by weight] layer with Methanol. Difference in the resonance frequencies was 343 Hz. (a) Image of spectra by network analyzer, (b). Graphic presentation

2.6 IR Analysis for Template Removal

Infrared studies were also carried out to confirm template removal from imprinted polymer film. Spectra were taken for imprinted and non imprinted polymer layer coated on glass surface, while taking glass spectra as background.

The ATR-IR spectra of imprinted and reference polymers are given in **Fig. 18**. The IR spectra of the imprinted polymer after washing with methanol showed the absence of amide band at 3270 cm^{-1} due to amide group of triazine. The absorptions for the symmetric stretching of —CH_3 and —CH_2 as well as for the deformations of the alkyl group were same in each case.

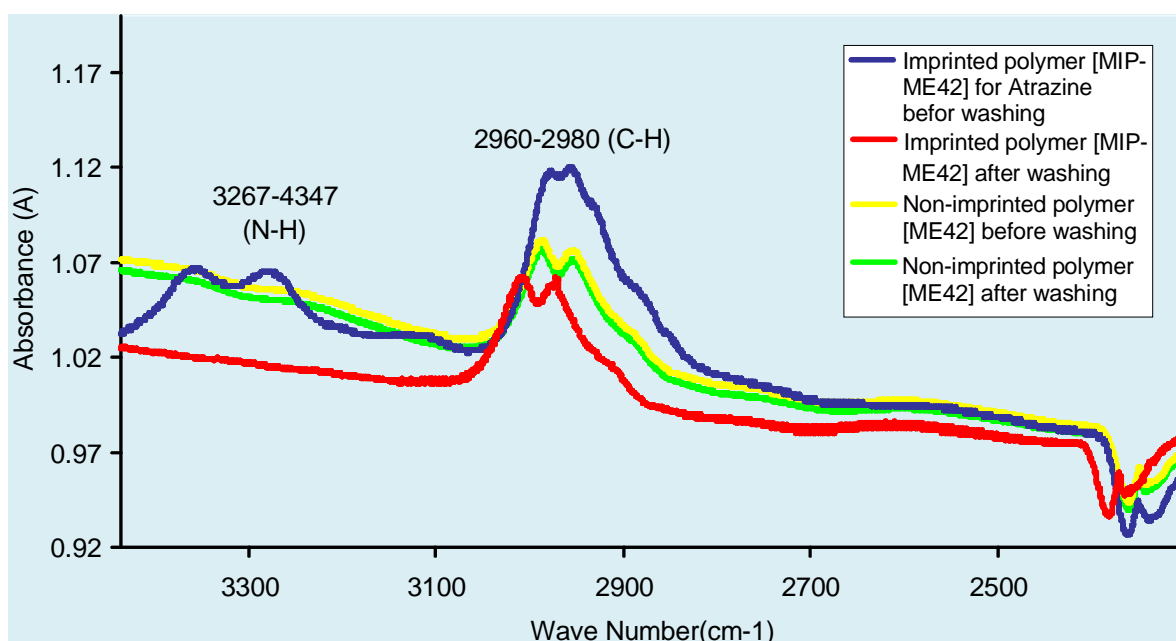


Figure 18: ATR-IR Spectra of copolymer [methacrylic acid (35%) & methylacrylate (7%) cross-linked with ethylene glycol dimethacrylate (58%) by weight] to analyze removal of Atrazine (10%) as template. Two absorption bands for —NH (at 3270 cm^{-1}) amino group of Atrazine and or the aliphatic —CH (at 3000 cm^{-1}) of methacrylic acid are observed. After washing with methanol, imprinted polymer peak for amino group disappeared indicating removal of Atrazine.

Chapter 3

SENSOR MEASUREMENTS WITH MOLECULARLY IMPRINTED POLYMER LAYERS

3.1 Sensitivity Measurements

Chemically sensitive layers were synthesized by molecular imprinting technique and analyzed for sensitivity measurements towards Atrazine (ATR) and other structural analogues namely Propazine (PRO), Terbutylazine (TBA), Des-ethyl atrazine (DEA), Des-isopropyl atrazine and Des-ethyl-des- isopropyl atrazine (DEDIA).

3.1.1 MIP-MA30 [Polymethacrylic acid] of Atrazine

Layers with artificial recognition sites for Atrazine were synthesized by pre-polymerization of methacrylic acid 30% by adding AIBN to initiate the reaction, adding 70% of Ethylene glycol dimethacrylate by weight for crosslinking and 10% Atrazine as template in 1mL of THF. Corresponding reference polymer was also prepared using the same procedure without Atrazine.

The pre-polymerized solutions were spin-coated on the dual electrodes of QCM, followed by polymerization under UV lamp overnight in Nitrogen atmosphere. The template molecules were washed out by keeping QCM in methanol for 30 min. The responses of the reference and imprinted polymer layers on electrodes were monitored by gravimetric analysis. The pre-polymerized solutions were spin-coated on QCM with two electrodes, followed by polymerization under ultra violet lamp over night in Nitrogen atmosphere. The template molecules were washed out by keeping QCM in methanol for 30 min. The responses of the reference and imprinted polymer layers on electrodes were monitored by gravimetric analysis.

For testing sensor response towards atrazine, saturated solution of Atrazine and further dilutions were prepared. A concentrated solution (5 mg/L) of Atrazine was prepared for sensor measurements. Distilled water was flushed through the cell at a rate of 1.5 mL/min to establish equilibrium in liquid phase before starting the analytical measurement.

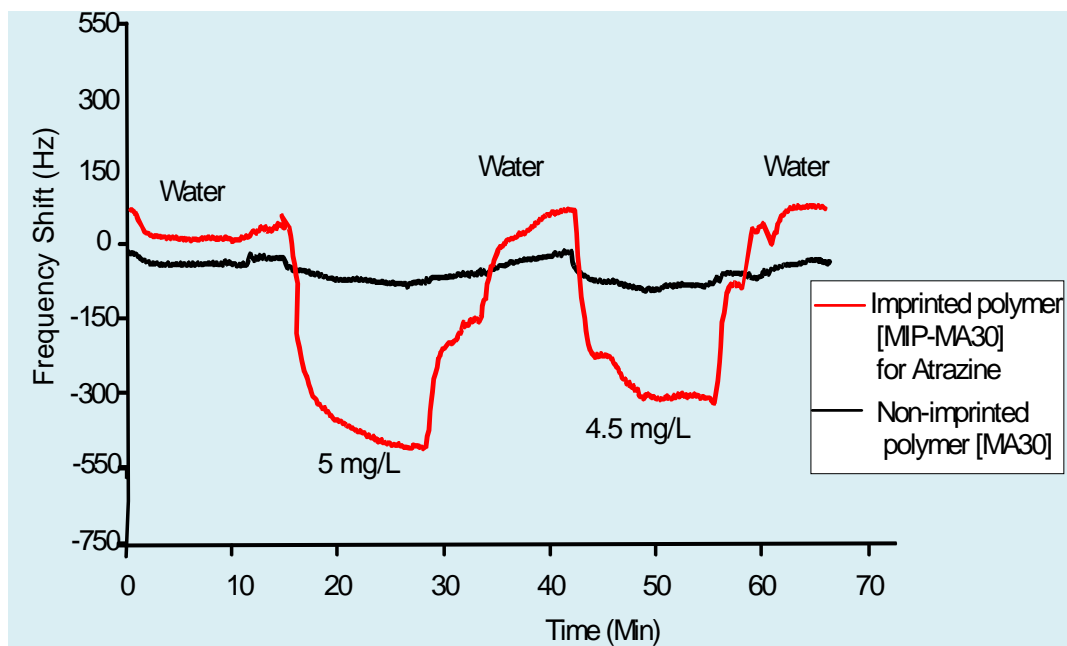


Figure 19: Sensor response of imprinted polymer MA30 [methacrylic acid 30% with 70% ethylene glycol dimetacrylate by weight crosslinked with 10% Atrazine as template] & Non-imprinted polymer MA30 at 28°C with flow rate of 1.5mL/min. The respective layer heights for the imprinted and non-imprinted layers are 480 nm and 375nm.

To minimize thermal instability, the temperature of flowing water and sample solutions was kept at 28 °C. The measurement was carried out by pumping liquids into cell housing QCM at a flow rate of 1.5mL/min. Sensor response of 503 Hz was recorded for 5 mg/L of Atrazine solution by the imprinted polymethacrylic acid layer. The reference electrode also showed frequency shift of 50 Hz that could occur due to surface absorption of analyte molecules by non imprinted polymer. The sensitivity of the imprinted film was further investigated for further dilutions of Atrazine down to 0.35 mg/L (signal to noise ratio ≥ 3). Reproducibility of sensor response was not possible below this concentration.

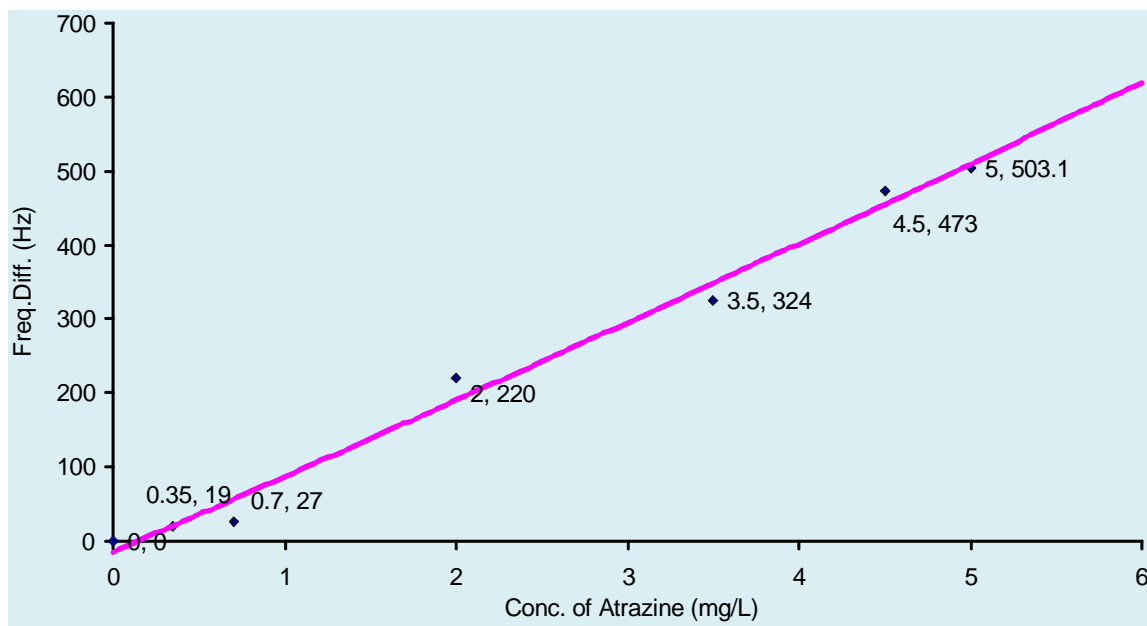


Figure 20: Difference of frequency shift from sensitivity responses of imprinted polymer MIP-MA30 [methacrylic acid 30% crosslinked with 70% ethylene glycol dimethacrylate by weight and 10% Atrazine as template] and non imprinted layer MA30 with thickness of 480 nm and 375 nm, respectively. The analysis was carried out at 28°C for different concentrations of Atrazine ranging from 0.35mg/L to 5 mg/L in water at flow rate of 1.5 mL/min.

A graph was plotted for sensor response against different concentrations of Atrazine recorded in the experiment. As demonstrated in Fig. 20, sensor response increased linearly with concentration of Atrazine in aqueous media.

3.1.2 MIP-MA30 [Polymethacrylic acid] of Propazine

Propazine is a triazine herbicide that may cause poisoning of livestock and diseases like anorexia, weight loss and muscle weakness. Additional Propyl group in Propazine make it hydrophobic than Atrazine with a solubility of 8 ppm in water.

Thereby, different polymer compositions were prepared to achieve sensor response for Propazine. As described in **Table-3**, MIP-MA30 was prepared using 8.5 mg of Propazine as template and a polymer layer of 250 nm thickness was

coated on QCM. After hardening of thin film overnight, template removal was tested with water and methanol.

Monomer	Methacrylic Acid	30 mg
Cross linker	EDMA	70 mg
Initiator	AIBN	3.5 mg
Solvent	THF	600 uL
Temperature	60 °C	
time	65 min	

Table 3: Chemical composition for MA30 along with reaction conditions

Finally, with a mixture of acetic acid and methanol (1:4), 2.2 kHz increase was observed in frequency of imprinted electrode due to loss of mass from 290 nm (6.2 kHz) thick layer reference layer showed an increment of 800 Hz. From the mass ratio of template (10 %), Propazine was expected to be removed from the imprinted layer and loss of polymer mass for both channels. Further sensor measurements were performed to investigate sensitivity of the imprinted layer.

Sensor measurement was carried out at 28 °C by pumping the sample solution at 1.5mL /min into the measuring cell containing QCM with imprinted and reference layer of 210 nm and 218 nm thickness, respectively.

Sensor response for Propazine (8.6 ppm) was 100 Hz. Frequency shift was less as observed for Atrazine by the same polymer composition. Propazine with relatively larger size of molecule than Atrazine required optimization of crosslinking network in polymer matrix for relatively larger pore size. As shown in **Fig. 21**, the reference channel showed a frequency shift of 15 Hz and 7Hz for 8.3 ppm and 4.3ppm of Propazine. While the imprinted channel generated sensor signal of 30 Hz for 4.3 ppm of Propazine solution. On change of phase to water, sensor response was observed fully reversible. The layer was not stable and was washed out after repeated measurements. The physical appearance indicated instability due to solvent system used for washing out template.

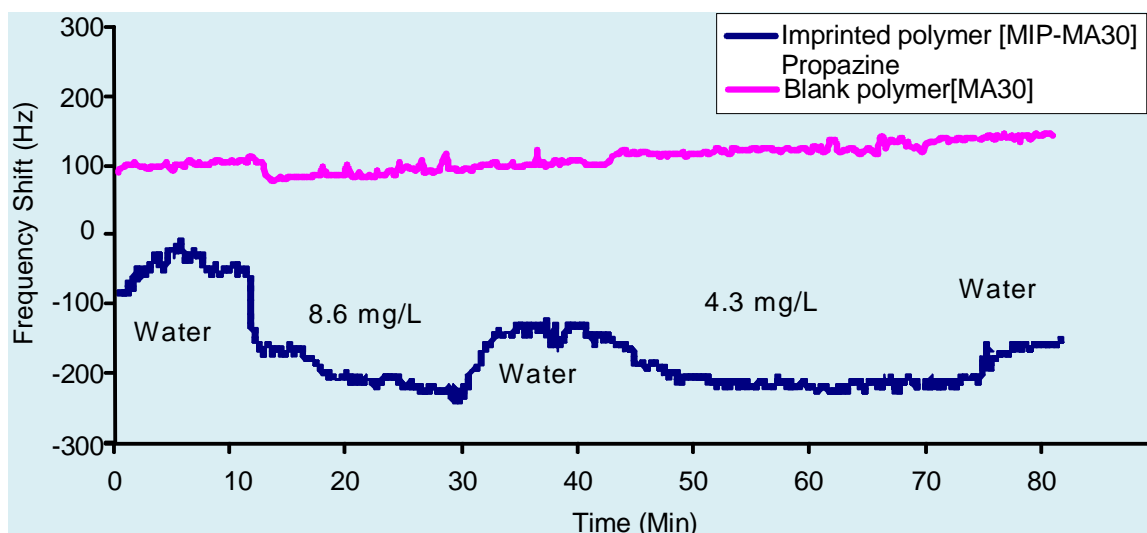


Figure 21: Sensitivity of imprinted polymer MA30 [methacrylic acid 30% crosslinked with 70% ethylene glycol dimethacrylate by weight and 8.5 % Propazine as template] after washing out template with Acetic acid & Methanol mixture (1:4), at 28°C with a layer height of 210 nm and 217nm of imprinted and non imprinted layers, respectively. Propazine solution (8.6ppm & 4.33ppm) was pumped at a flow rate of 1.5 mL/min.

To improve the porosity of polymer matrix, one approach was addition of Toluene to increase the cavities in polymer matrix at 60 °C (**Table-4**).

Methacrylic acid	30 mg
Toluene	100 uL
EDMA	70 mg
AIBN	3.5 mg
THF	400 uL
Propazine	8.5 mg

Table 4: Chemical composition of MA30

Washing for template removal was carried out with methanol. Toluene was expected to enhance sensitivity of polymer towards target molecules. But a similar sensor response of 120 Hz was observed. Though, the signal to noise ratio was improved as illustrated in **Fig. 22**.

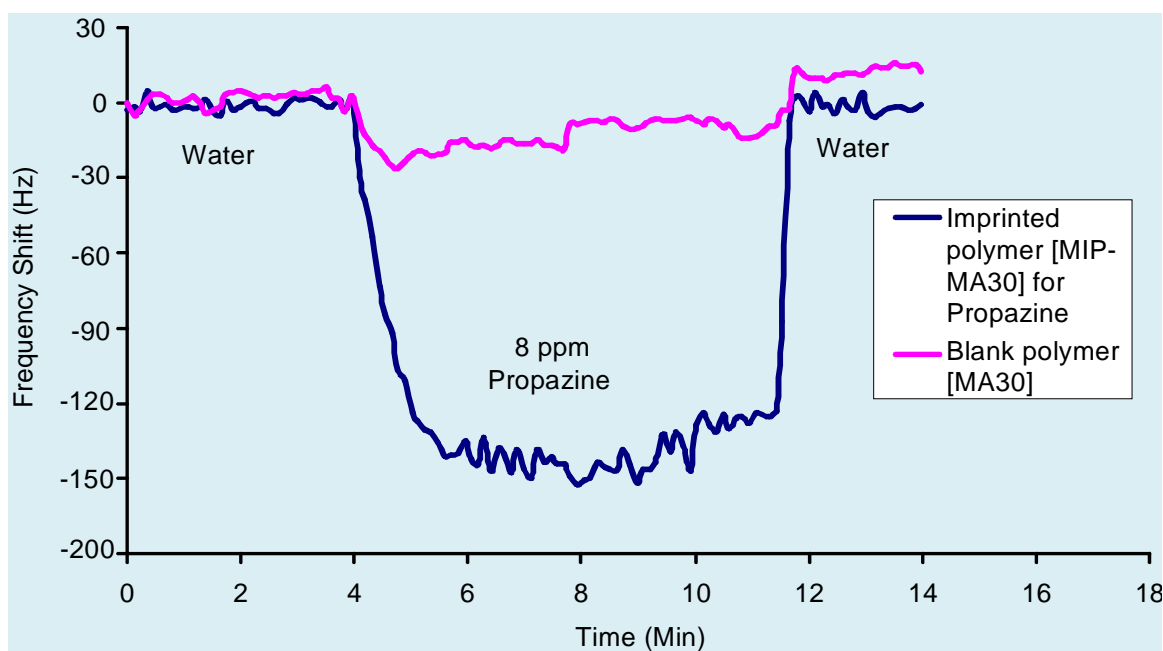


Figure 22: Sensitivity of imprinted polymer MA30 [methacrylic acid 30% by mass crosslinked by 70% ethylene glycol by weight and 8.5 % Propazine as template with addition of 100uL toluene] at 28°C. The layer thickness of imprinted and reference channel was 220 nm and 212 nm, respectively.

3.1.3 MIP-VP [Polyvinylpyrrolidone] of Propazine

Taking a step further to enhance sensitivity, imprinted polymer for Propazine was designed with Vinyl pyrrolidone as monomer crosslinked with Bis acrylamide. (See **Table 5**). The strong interaction of halogen atoms of Propazine to the highly polarizable aromatic ring also make it suitable for imprinting. Pre-polymerized solution was synthesized with conditions and quantities as given in table. Washing off the template was done within measuring cell by water.

Vinylpyrrolidone	95 mg
Bis acrylamide	5 mg
AIBN	1 mg
Propazine	7 mg
Temperature	60 °C
time	30 min

Table 5: Chemical composition of poly Vinyl pyrrolidone imprinted with Propazine

As shown in **Fig. 23**, frequency shift of 1.1 kHz of imprinted electrode was observed during washing step for template removal (6.5% by weight of polymer composition) from imprinted layer of 5.6 kHz.

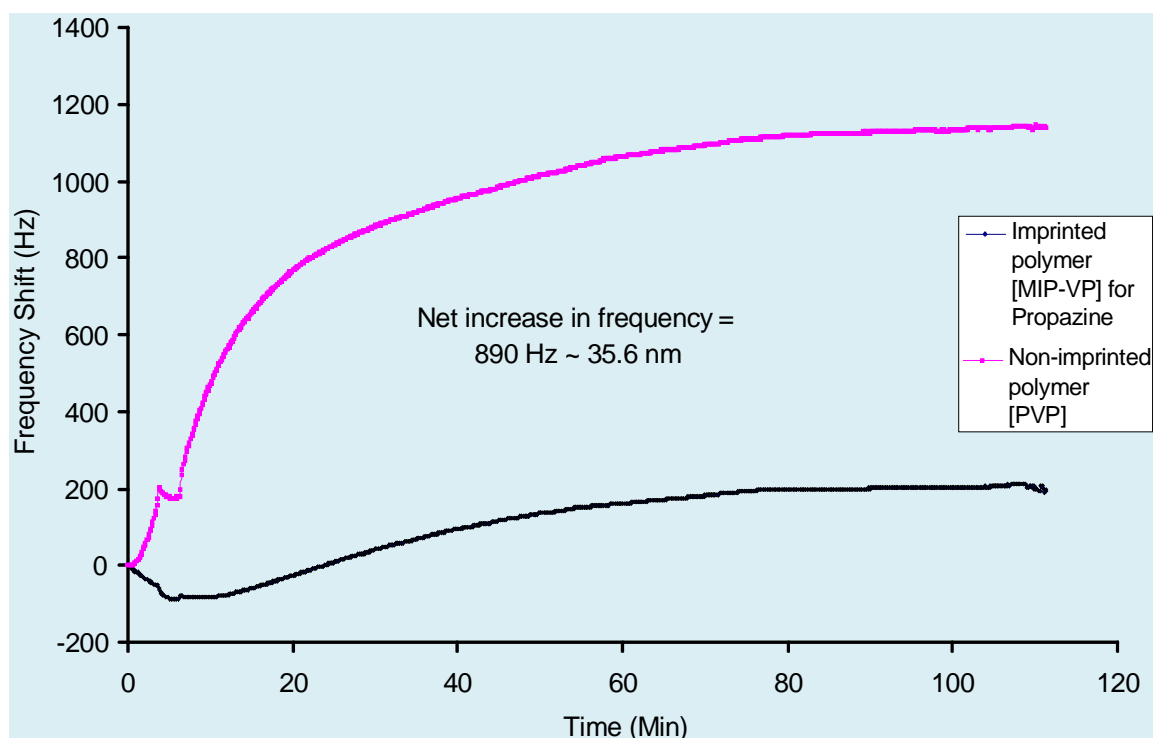


Figure 23: Washing of QCM by water at 28 °C with flow rate 0.5 mL/min coated with imprinted layer of polyurethane [197 mg Bisphenol A, 100 mg of 4,4methylene diphenyldiisocyanate and Pholoroglucinol 22 mg with propazine as template 9mg]. The layer thickness of imprinted and non-imprinted channel before washing was 5.6 kHz and 5.5 kHz, respectively.

In case of non-imprinted electrode, the rise in frequency was 200 Hz by a layer height of 5.5 kHz. Thus, the shift in frequency of 890 Hz (approximately 35.6 nm) indicated removal of Propazine from the imprinted layer.

Sensor response of 350 Hz for Imprinted layer was recorded with polyvinylpyrrolidone for 8.6 ppm of Propazine. Previously, imprinted MA30 (methacrylic acid 30 % by weight crosslinked by 7 % ethylene glycol dimethacrylate with 8.5 % Propazine) responded to Atrazine (5ppm) & Propazine (8.6ppm) with frequency shift of 550 Hz and 100 Hz (see **Fig. 24**).

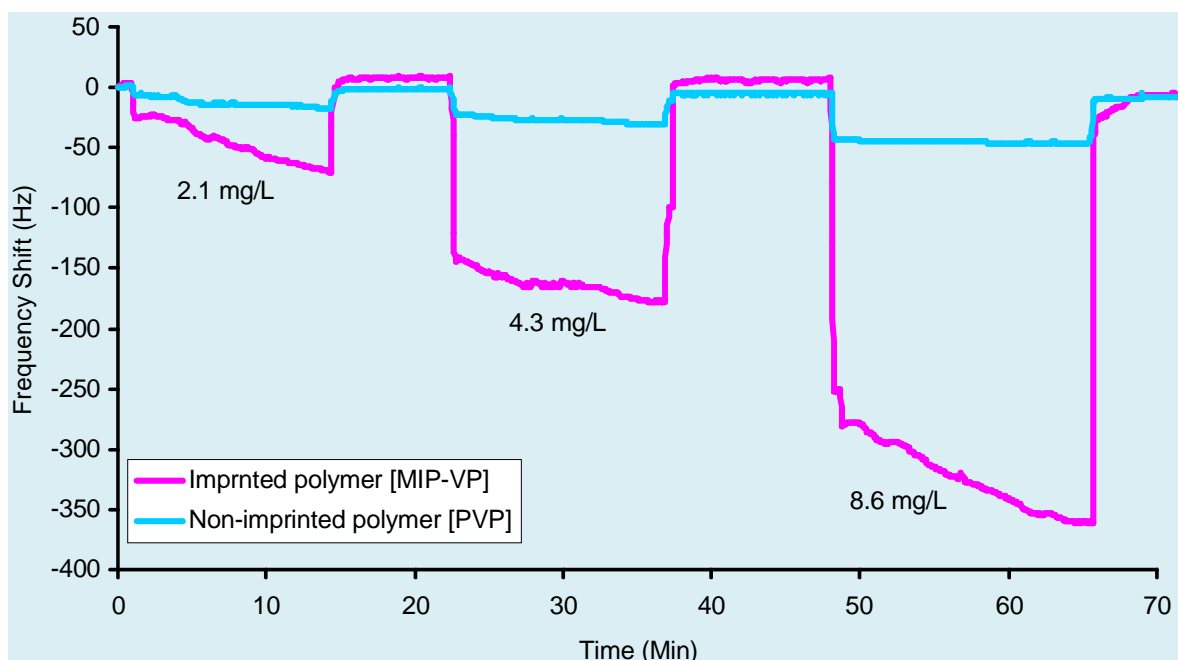


Figure 24: Frequency shift measured at 28°C for Propazine by imprinted Poly Vinyl Pyrrolidone [vinylpyrrolidone 95 mg crosslinked with Bis acrylamide 5mg and 8.5 mg Propazine as template] with layer height of 180 nm at flow rate of 0.5 mL/min.

In case of Propazine the effect is mainly due to hydrogen bonding. Therefore, it was suggested to change amount of acrylic acid to get enhance sensor effect. Propazine being more apolar, acrylic acid concentration in polymer required to be increased to improve columbic interaction. Factors like affinity of Propazine,

reversible interactions, solvent selection for washing out the template molecules were the factors considered for next polymer design.

3.1.4 Effect of Acid content of MIP-MA [Polymethacrylic acid] on Sensitivity

After investigating the sensor response in preliminary experiment with different polymers, methacrylic acid was selected for designing sensor layers for Chlorotriazines. The strong but reversible interaction between basic Chlorotriazines and methacrylic acid was the key factor for the choice of monomer. The ratio of acid to cross linker needed to be optimized for different pesticides.

For this purpose, the polymer mixtures were prepared with composition as given in **Table 6**. All polymer mixtures were synthesized taking 2.5 mg of AIBN as initiator while heating at 60°C till gel point. 10 % of atrazine by weight as template was used as template for different ratios of acid and cross linker. The pre-polymerized solutions were coated on dual electrodes QCM along with non imprinted polymeric solutions and left overnight under UV.

MAA: EGDMA	Layer height (kHz)	Net Frequency Shift (Hz)
28: 72	8	200
30: 70	10	354
33: 67	6	198
35: 65	5.2	314
40:60	5	408
46:54	6.25	546
50:50	4	180
60:40	4.2	84

Table 6: Compositions of polymethacrylic acid for optimizing ratio of monomer (methacrylic acid) to crosslinker (Ethylene glycol dimethacrylate)

Influence of acid content of the imprinted polymer over the sensor signal was investigated for 7 mg/L of Atrazine (see **Fig. 25**). Imprinted layer with 28 % of methacrylic acid gave a sensor response 200 Hz. Keeping the template amount constant i.e. 10% by weight with the increase in acid content, sensitivity of the imprinted layer improved for Atrazine. As a result of enhanced acid base interaction between the basic template molecules and polymer matrix, maximum sensor response of 546 Hz for a layer height of 250 nm was observed. Acid to cross linker ratio also played important role in stability of polymer matrix for strong incorporation of template molecules. Further increase in acid content above 46 % resulted in weak signal with small frequency shifts due to poor crosslinking in the imprinted polymer matrix. Therefore, optimized acid amount in the polymer for maximum sensitivity towards atrazine was observed in range of 40% for designing sensor coatings.

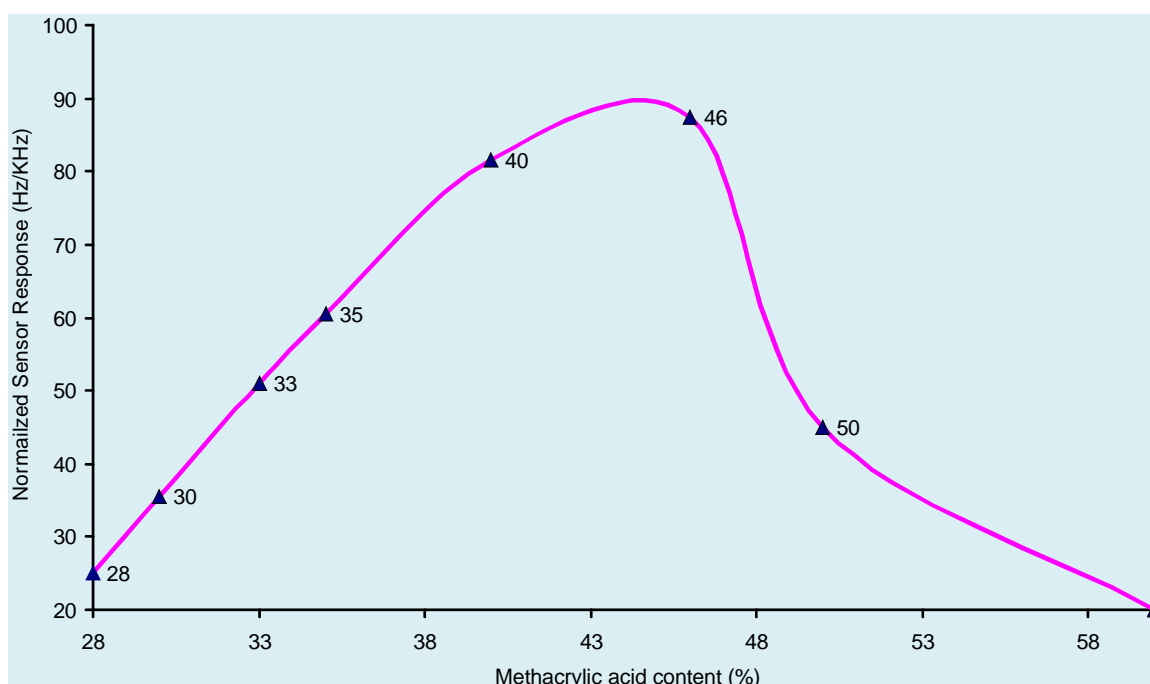


Figure 25: Effect of amount of methacrylic acid crosslinked by ethylene glycol dimethacrylate and imprinted with 10% by weight of Atrazine as template on sensor response for 7mg/L of Atrazine at 28 °C.

3.1.5 MIP-MA46 [Polymethacrylic acid]

After selection of monomer to crosslinker ratio, MA46 was synthesized following chemical composition as given in **Table 7**. After dissolution, 3.5 mg of AIBN as initiator was added and the solution was heated while stirring at 60 °C for 45 min. Following the same procedure another solution was also prepared excluding the template to be used as reference for sensor response. Similarly, the pre-polymerized solutions for were also prepared.

Monomer	Methacrylic Acid	46 mg
Cross linker	EGDMA	54 mg
Initiator	AIBN	3.5 mg
Solvent	THF	600uL
Temperature	60 °C	
Time	75 min	

Table 7: Chemical composition of MIP-MA46 [polymethacrylic acid]

In order to generate thin films in range of 220-250 nm on gold electrodes of QCM, 5 uL of pre-polymerized solutions were spin-coated at 3000rpm after 50% dilution with THF, on the 10 MHz Quartz Crystal microbalance. After coating the two gold electrodes of QCM with pre-polymerized solutions with and without template, it was left overnight under UV light in nitrogen atmosphere. For removal of the template in the polymer layer, QCM was kept in methanol depending on the solubility of related template from 30 min to 2hrs. The frequency of the electrodes was again checked with frequency analyzer to confirm the washing off the template molecules.

Solutions with a set of dilutions of Atrazine were prepared from the freshly prepared saturated solution of 7 ppm .The imprinted/non imprinted coatings for the analyte was prepared in range of 250 nm. Sensor measurements were carried out for testing the limit of detection of Atrazine in aqueous solutions. Reference channel

also responded for different analytes to some extent that can be attributed to enhanced porosity of polymer with the addition of DMF.

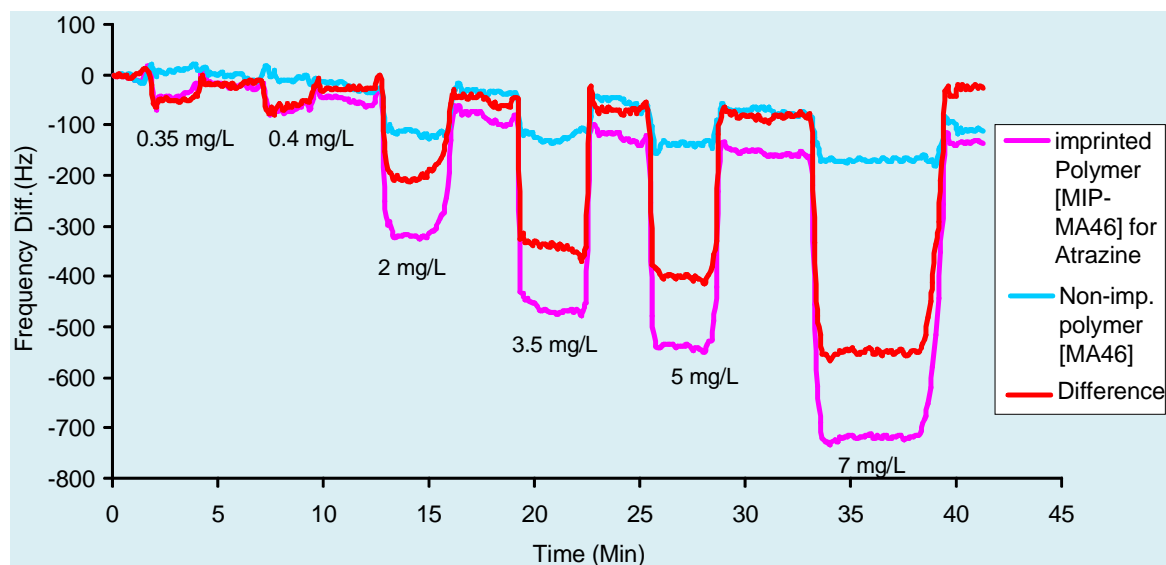


Figure 26: Sensor response of MIP-MA46 [methacrylic acid 46% crosslinked with 54% ethylene glycol dimethacrylate imprinted by 10% of Atrazine] for different concentrations of Atrazine at 28°C at flow rate of 1.5mL/min. Thickness of the imprinted and non-imprinted layers was 250 and 248nm, respectively.

Sensor responses were 35 Hz to 600 Hz respectively for Atrazine with concentrations ranging from 0.35ppm to 7 ppm. The steric effect in case of Propazine and terbuthylazine also hinders H-bonding; therefore, decreases the basicity of the amines with bulky alkyl groups with a pronounced difference of sensor effect as compared with Atrazine. **Fig. 27** presents the sensitivity towards different concentrations of Propazine as recorded by imprinted layer of MIP-MA46 methacrylic acid (46% methacrylic acid crosslinked with 54% Ethylene glycol dimethacrylate by weight) with 9% of Propazine (PRO). Sensor response was lower for Propazine by MA46 as compared imprinted layers of Atrazine, and other structural analogues. Bulky groups on both side of the triazine ring make propazine less basic. Consequently weak interactions between analyte and MIP result in smaller mass changes and lower frequency shifts.

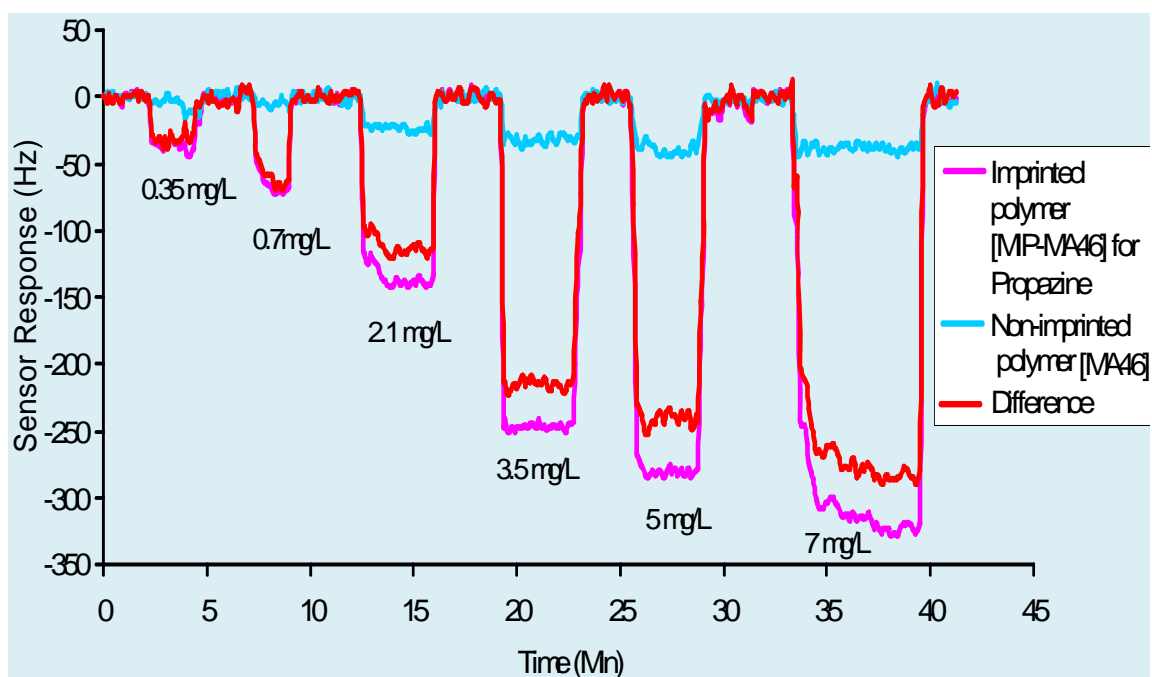


Figure 27: Sensor responses of MIP-MA46 [methacrylic acid 46% by weight crosslinked with 54% Ethylene glycol dimethacrylate] imprinted with 9% Propazine (PRO) for concentrations ranging from 0.35mg/L to 7 mg/L at 28°C. The heights of the imprinted and non-imprinted layers are 230 and 248 nm, respectively.

MIP-MA46 (methacrylic acid 46% by weight crosslinked with 54% Ethylene glycol dimethacrylate) was prepared with 8.2 % of Terbutylazine as template in pre-polymerization step. The sensitivity measurements were recorded for various concentrations of Terbutylazine (TBA) as shown in **Fig. 28**.

The difference of resonance frequency of imprinted electrode was highest for Des-isopropyl atrazine (DIA) with frequency shift of 600 Hz for 7ppm (**Fig. 29**) as compared to that for Atrazine, Terbutylazine and Propazine, respectively. Frequency shift was influenced by the relative basicity of pesticides and the strength of interaction with imprinted layer of poly methacrylic acid. Higher sensitivity of polymethacrylic acid for DEA (7ppm) was observed.

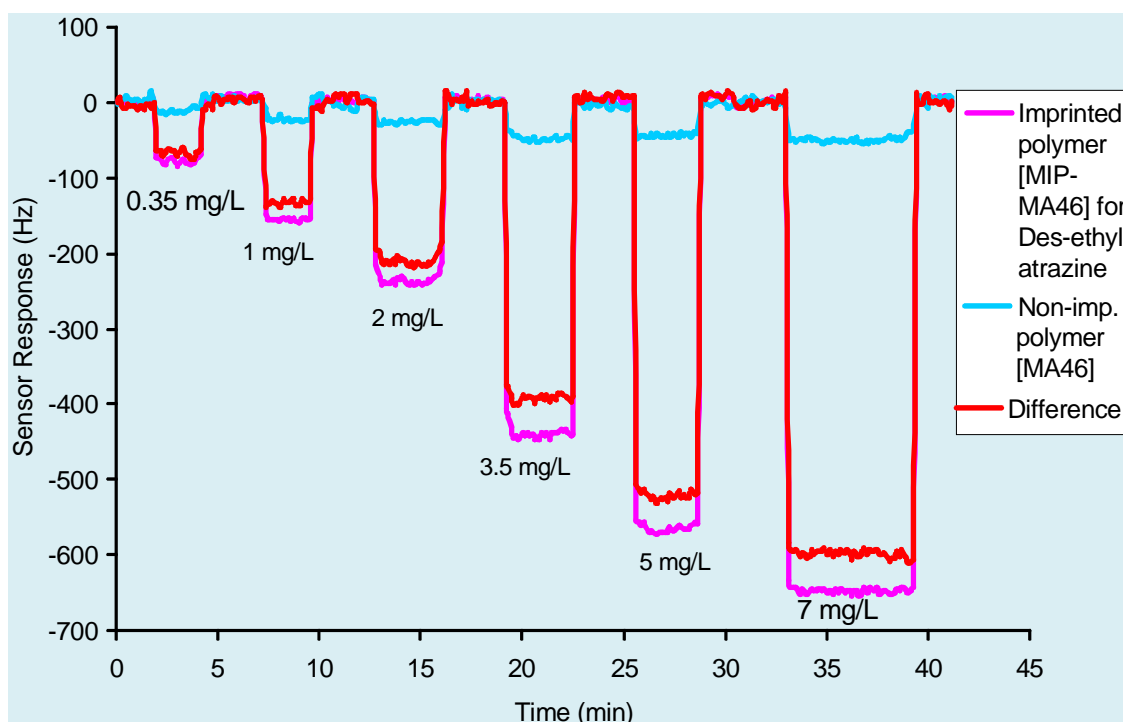


Figure 28: Sensor responses of MIP-MA46 [methacrylic acid 46% by weight crosslinked with 54% Ethylene glycol dimethacrylate] imprinted with 10 % des-ethyl atrazine (DEA) for concentrations ranging from 0.35 mg/L to 7 mg/L at 28°C. The heights of the imprinted and non-imprinted layers are 250 and 220 nm, respectively.

The accessibility of recognition sites in the imprinted layer with the passage of time increases after repeated measurements of concentrated analyte solution. Also, by the salvation effect in water, DEA as primary amine has pronounced Hydrogen bonding and strong interaction with MIP resulted in higher sensor response.

Primary amines like metabolites of Atrazine i.e. Des-isopropyl atrazine (DIA) & Des-ethyl atrazine (DEA) have pronounced basicity due to additional sites available for hydrogen bonding. On the other hand, steric effect of bulky alkyl groups in Propazine & Terbutylazine hinders the hydrogen bonding and therefore decreases their basicity.

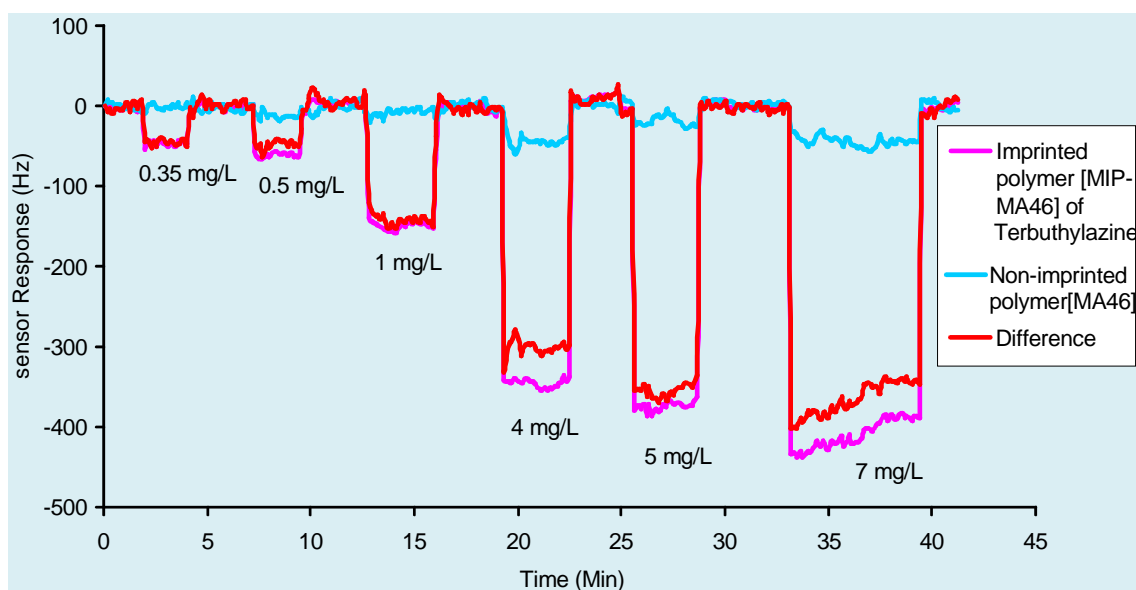


Figure 29: Sensor responses of MIP-MA46 [methacrylic acid 46% by weight crosslinked with 54% Ethylene glycol dimethacrylate] imprinted with 8.2 % terbutylazine (TBA) for concentrations ranging from 0.35 mg/L to 7 mg/L at 28°C. The heights of the imprinted and non-imprinted layers are 225 and 215nm, respectively.

3.2 Selectivity Measurements

Pesticides are widely used in agricultural areas and most often in combination. For online monitoring of Atrazine, sensor measurements were also made for selectivity. Molecular imprints are expected to show higher cross selectivity as compared to other instrumental analysis.

3.2.1 MIP-MA30 [Polymethacrylic acid]

Molecularly imprinted polymer of Atrazine containing 30 % methacrylic acid was tested for 7 ppm solution of Atrazine, its metabolites e.g. Des-ethyl atrazine (DEA), Des-ethyl-Des-isopropyl atrazine (DEDIA), Des-isopropyl atrazine (DIA) and also for other Chlorotriazines including Simazine (SIM), Propazine (PRO) and Terbutylazine (TBA). As shown in **Fig. 30**, cross selectivity with

metabolites of Atrazine was lower as compared to bulky substituent of s-triazines. Polymer matrix imprinted with Atrazine also interacted with metabolites due to excessive hydrogen bonding.

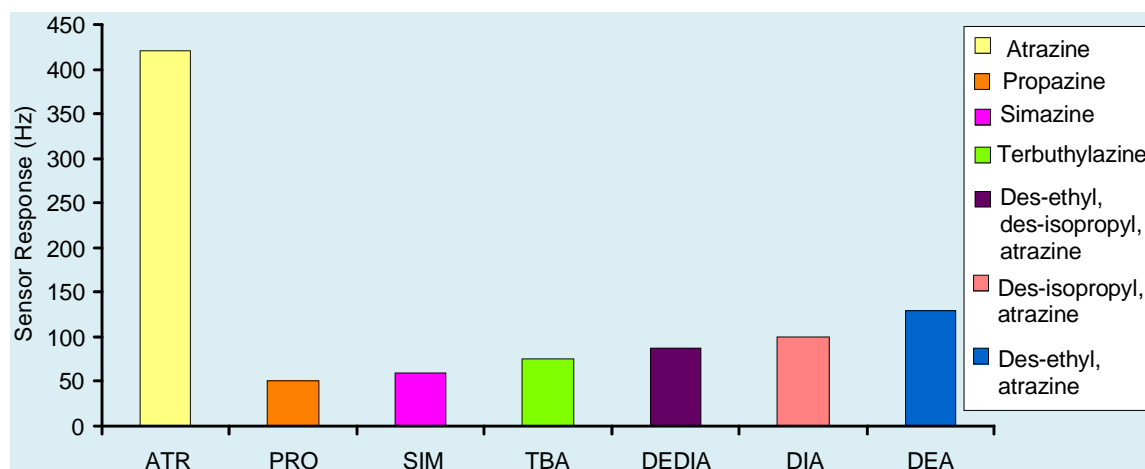


Figure 30: Selectivity of MIP-MA30 [methacrylic acid 30 % by mass crosslinked with 70 % Ethylene glycol dimethacrylate] imprinted with 10 % Atrazine (ATR) tested for, 7 ppm of Atrazine (ATR), Des-ethyl atrazine (DEA), Des-ethyl-Des-isopropyl atrazine (DEDIA), Des-isopropyl atrazine (DIA), Simazine (SIM), Terbuthylazine (TBA) and Propazine (PRO) was tested. Thickness of the imprinted and non-imprinted layers was 220 and 235 nm, respectively.

Due to high cross linking, bulky molecules of Chlorotriazines had less access to active sites in the polymer layer. Other than steric hindrance, selectivity pattern was also influenced by basicity of Chlorotriazines. As shown in **Fig. 31** molecular imprinted polymer coatings of Atrazine (ATR), Des-ethyl atrazine (DEA), Des-ethyl-Des-isopropyl atrazine (DEDIA), Des-isopropyl atrazine (DIA), Simazine (SIM), Terbuthylazine (TBA) and Propazine (PRO) with 46% methacrylic acid were analyzed for cross selectivity.

Sensor responses in each case were normalized for comparison of cross selectivity. Imprinted coating of Des-ethyl atrazine (DEA) gave a signal with almost 50% sensitivity towards ATR and TBA. Atrazine imprinted polymer showed highest selectivity for Atrazine among all other coatings. Highest sensitivity was observed in case of Des-isopropyl atrazine (DIA).

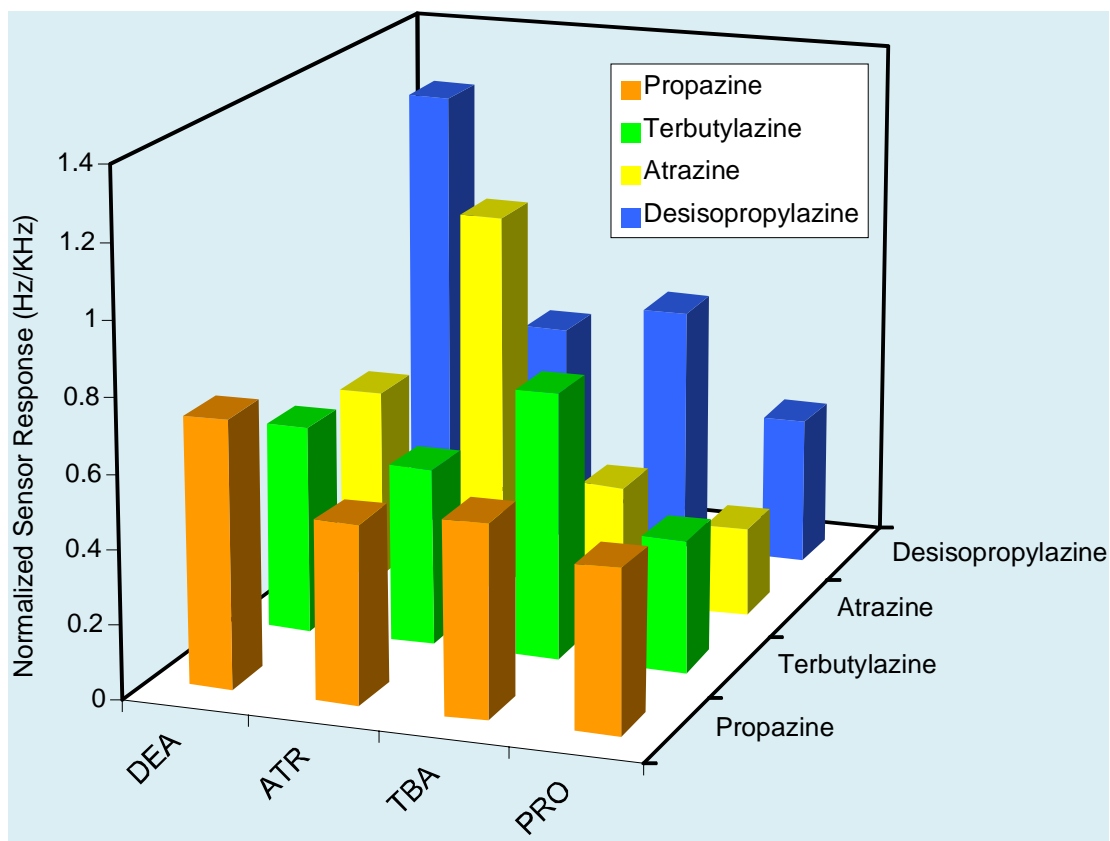


Figure 31: Cross-Selectivity responses of MIPs-MA46 [methacrylic acid 46% crosslinked with 54% ethylene glycol dimethacrylate imprinted by 10% of Atrazine] layers at 28°C, imprinted with Des-isopropyl atrazine (DIA), Atrazine (ATR), Terbutylazine (TBA) and Propazine (PRO) respectively. Frequency shifts were normalized for layer thickness and subtracted from frequency shifts of reference electrode with non-imprinted polymer in each case.

3.2.2 MIP-ME35 & ME42 MIP [Co-polymer of methacrylic acid & methyl acrylate]

To synthesize molecularly imprinted pre-polymerized solution of Atrazine (MIP-ME42), 13.5mg Atrazine was dissolved in 76mg of Methacrylic acid by diluting in 300 μ L THF in a 2 mL eppendorf vial. The mixture was centrifuged and 14mg of methyl acrylate for copolymerization and 116mg EDMA as cross linker was added to the supernatant. For pre-polymerization, 3.6mg AIBN as radical starter dissolved in 200 μ L THF was added to the clear solution and was heated at

65°C for 45min till the gel point. Following the same method another solution without Atrazine was also prepared for reference. ME33 & ME40 for ATR were also synthesized following the same procedure. The quantities of reagents for all solutions along with time required for synthesis are given in **Table 7**. Respective non-imprinted polymer solutions for reference channel were preceded in a similar way without template.

Polymer	Methacrylic acid (mg)	Methyl acrylate (mg)	EDMA (mg)	Time for synthesis (Min) at 60°C
ME33	28	7	58	65
ME42	35	7	58	70

Table 8: Chemical compositions of imprinted copolymers of (methacrylic acid and methyl acrylate) with 10% Atrazine by weight as template

The gold electrodes pair of QCM was coated with MIP-ATR solution diluted with THF (1:2) to attain a layer height of 250nm by spinning at 3200 rpm for 30 sec. Polymer layers were kept overnight under UV and afterwards dipped in pure methanol for template removal.

After drying and washing with water, frequency of quartz was checked for difference in mass load before and after coating. Frequency shifts for Atrazine and similar Chlorotriazines were determined for selectivity of Atrazine by MIP-ME35. **Fig. 32** illustrates two patterns of cross sensitivity for the metabolites of ATR and among PRO, SIM and TBA respectively.

Slightly varied signal of imprinted channel for DE, DIA and DEDIA can be attributed to the extent of availability of the lone pair of amino group attached with the triazine ring. Therefore, Des-isopropyl-Atrazine (DIA) with pronounced basicity interacted strongly with the polar matrix of ATR imprinted polymer layer. Improvement in cross selectivity for metabolites of Atrazine was observed by an average of 20% from 29 % & 50 % with MA30 and MA46, respectively.

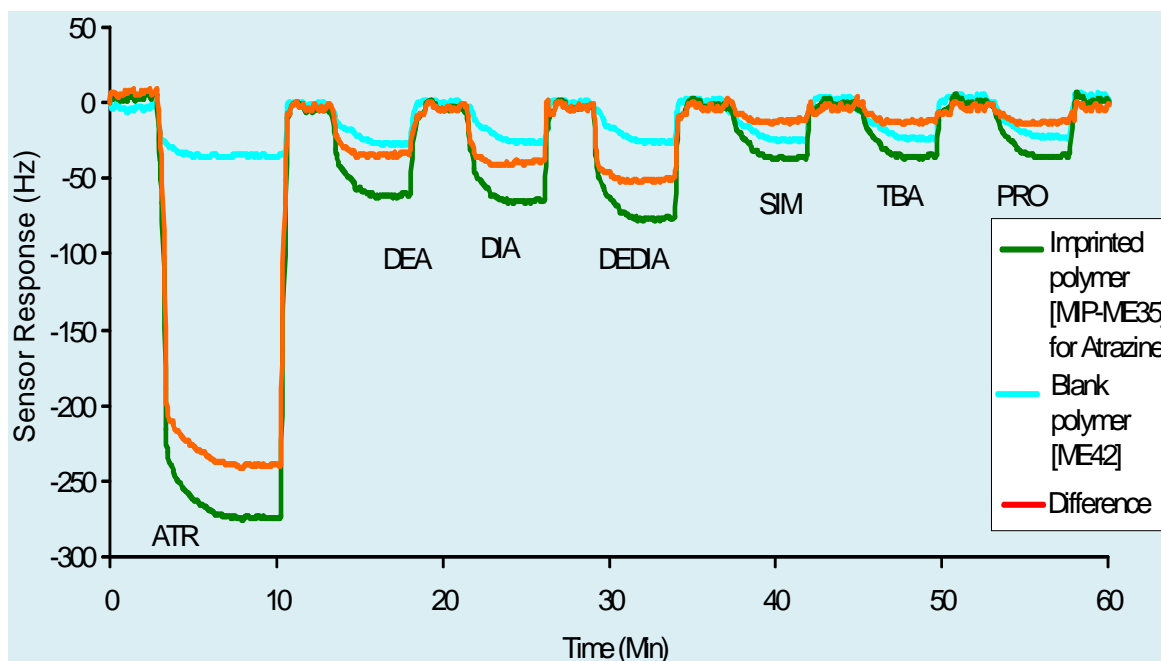


Figure 32: Selectivity analysis for Atrazine by MIP-ME35 [imprinted copolymer of 28 % methacrylic acid and 7% methacrylate by weight crosslinked with 58 % ethylene glycol dimethacrylate imprinted with 10% of Atrazine as template]. Sensor signals are shown for 7ppm of Atrazine (ATR), Des-ethyl atrazine (DEA), Des-ethyl-Des-isopropyl atrazine (DEDIA), Des-isopropyl atrazine (DIA), Simazine (SIM), Terbutylazine (TBA) and Propazine (PRO) by imprinted, non imprinted electrodes and the net shift in frequency by polymer coatings of 189 nm and 200 nm respectively.

Copolymerization of methacrylic acid with ester improved selectivity of Imprinted polymer matrix. On the basis of previous experiments, acid content of polymer was further increased for optimized detection.

As illustrated in **Fig. 33**, the sensitivity of copolymer increased towards Atrazine with the increase of acid content from 28% to 35% by weight. On the other hand, the selectivity was reduced specially against the metabolites of Atrazine. Interestingly, frequency shift for bulky molecules like Propazine, Simazine and terbuthylazine were similar. It is assumed that bulky triazine molecules selectivity is controlled by addition of methacrylate. As in both polymer compositions of MIP-

ME33 and MIP-ME42, the amount of methacrylate was kept same i.e 7 % by weight, therefore selectivity pattern of these analytes was similar.

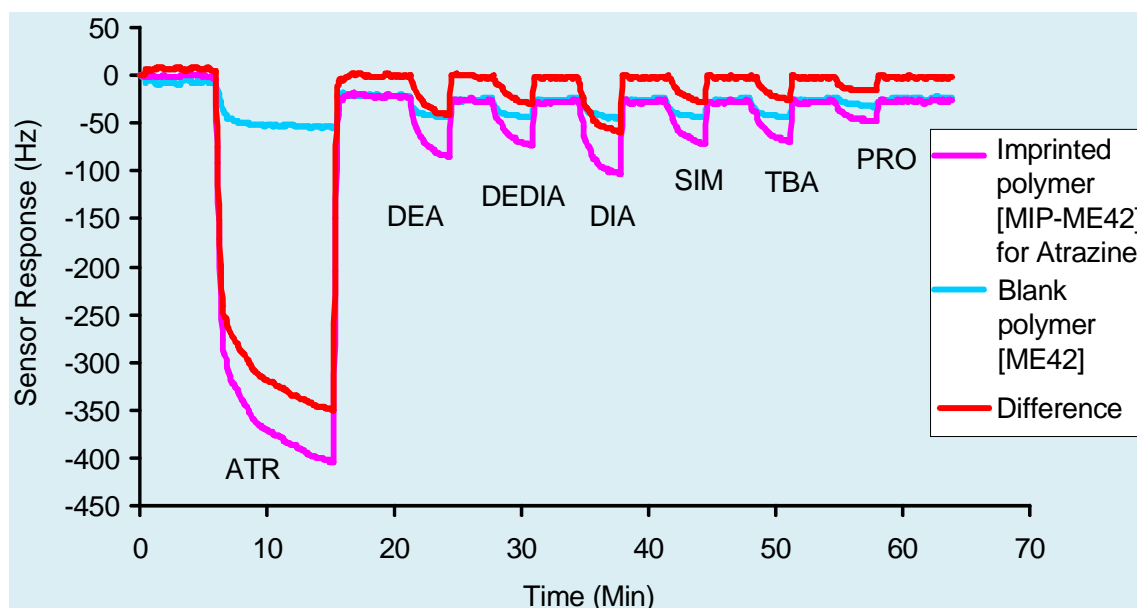


Figure 33: Sensor measurements at 28°C for cross selectivity by MIP-ME42 [imprinted copolymer of 35% methacrylic acid and 7% methacrylate crosslinked with 58% Ethylene glycol dimethacrylate by weight imprinted with 10% of Atrazine as template] with layer thickness of 185 nm for imprinted and 207nm for reference channel. 7ppm of Atrazine (ATR), Des-ethylatrazine (DEA) Des-ethyl-Des-isopropyl atrazine (DEDIA), Des-isopropyl atrazine (DIA), Simazine (SIM), Terbutylazine (TBA) and Propazine (PRO) was analyzed.

Imprinted copolymer ME42 with optimized selectivity was further tested for diluted samples of Atrazine. Starting with higher concentration, the change in frequency of imprinted layer towards aqueous solutions of Atrazine was observed (**Fig. 34 & 35**). The measurements were continued down to ppb level to detect the lowest detection limit by the imprinted polymer with excellent selectivity among all imprinted layers designed for Atrazine.

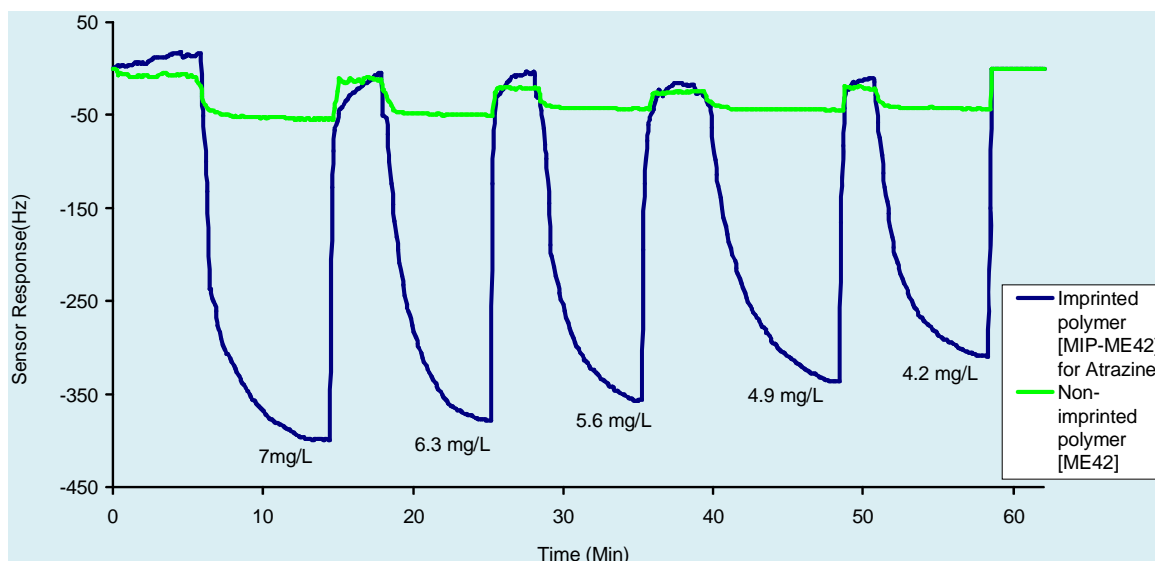


Figure 34: Sensor response of MIP-ME42 [imprinted copolymer of 35 % methacrylic acid and 7% methacrylate crosslinked with 58% Ethylene glycol dimethacrylate by weight imprinted with 10% of Atrazine as template] and non imprinted polymer film for different concentrations of Atrazine in water at 28°C. The heights of the imprinted and non-imprinted layers are 185 and 205nm, respectively.

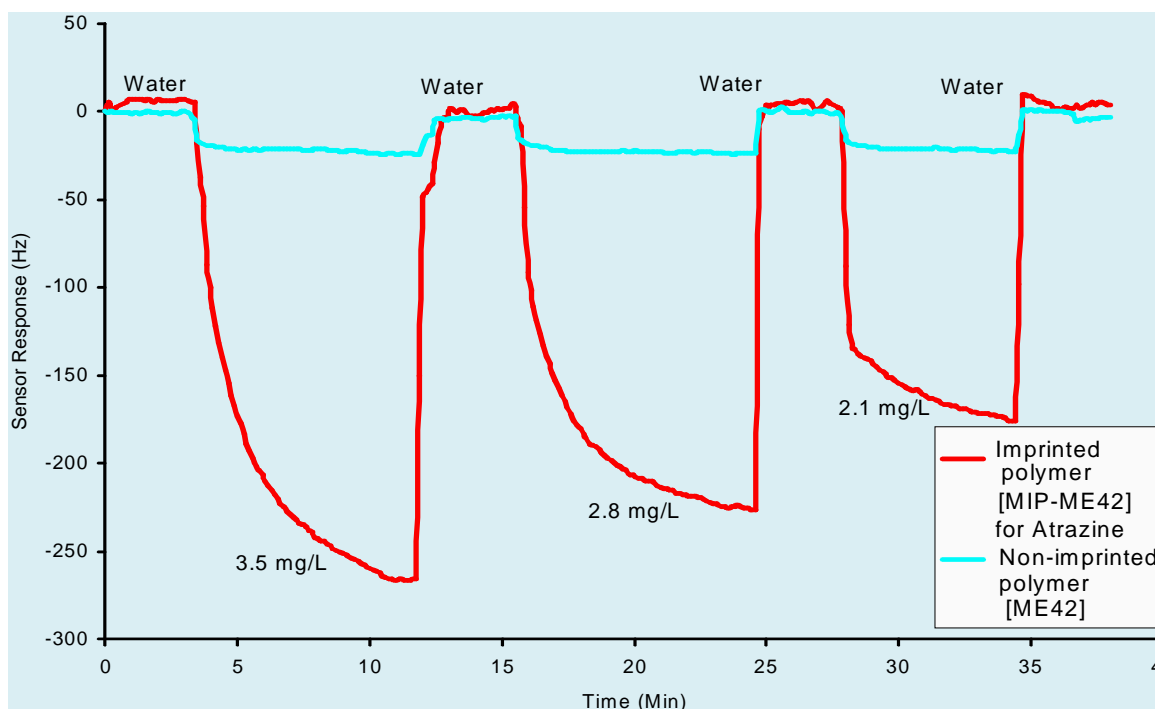


Figure 35: Sensitivity of MIP-ME42 [35 % methacrylic acid & 7% methacrylate crosslinked with 58 % Ethylene glycol dimethacrylate by weight imprinted with 10% of Atrazine as template] and non imprinted polymer film for different concentrations of Atrazine in water at 28°C. The heights of the imprinted and non-imprinted layers are 185 and 205nm, respectively.

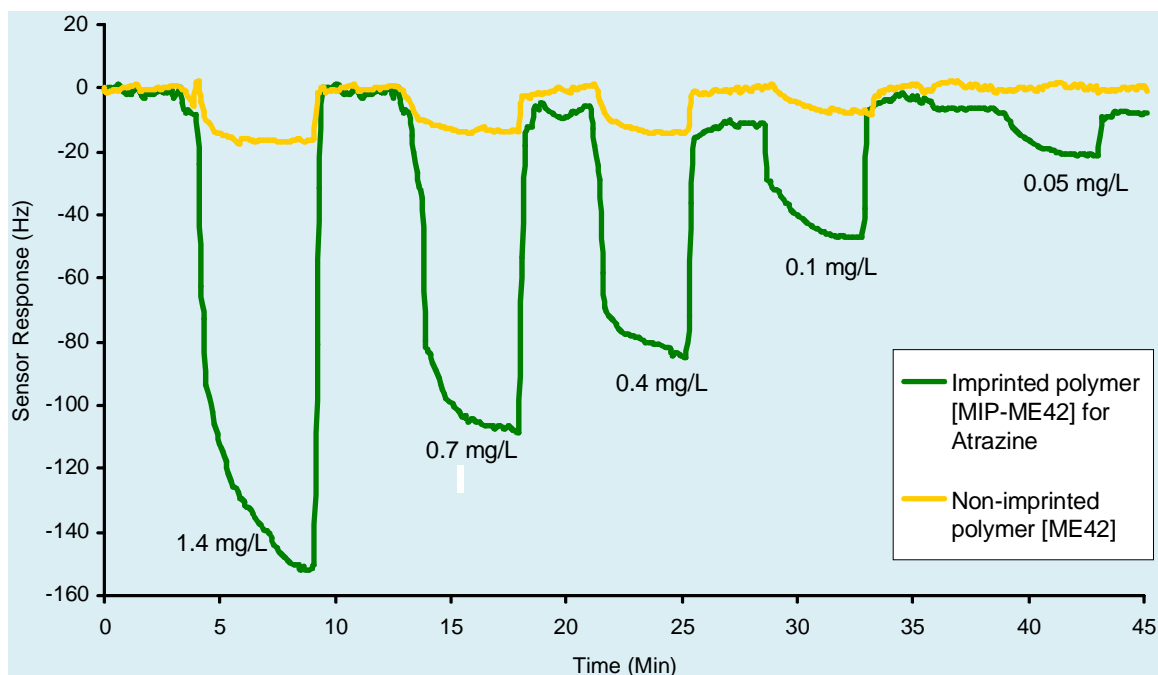


Figure 36: Sensor response of MIP-ME42 [imprinted copolymer of 35% methacrylic acid and 7% methacrylate by weight crosslinked with 58% Ethylene glycol dimethacrylate imprinted with 10% of Atrazine as template] and non imprinted polymer film for different concentrations of Atrazine in water at 28°C. The heights of the imprinted and non-imprinted layers are 185 and 205nm, respectively.

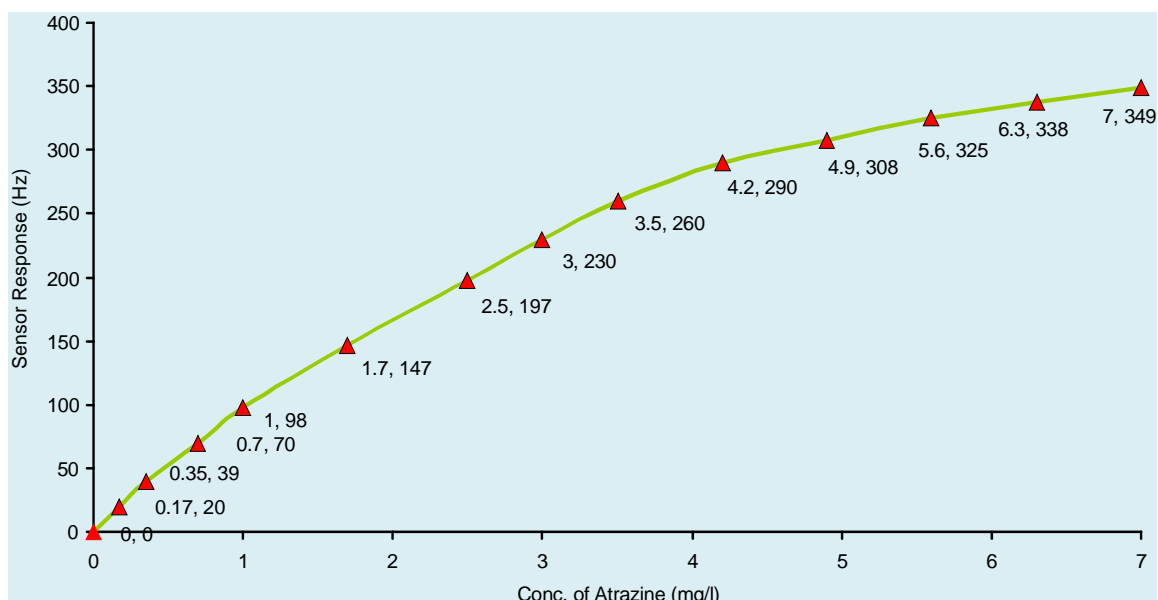


Figure 37: Effect of concentration of Atrazine on Frequency Shift measured at 28°C by MIP-ME42 layer of 185nm at flow rate of 1.5mL/min.

As given in **Fig. 36-37** the lowest detectable concentration was 50 ppb where signal to noise ratio was ≥ 3 . Sensor coating was used for repeated measurements for checking stability and reproducibility of analytical results.

After analysis, imprinted electrode of QCM was also investigated for surface roughness by Atomic Force microscope. **Fig. 38** shows image obtained by AFM. The thickness of sensor layer was also checked by frequency analyzer after analysis and no damage to the thin film was observed.

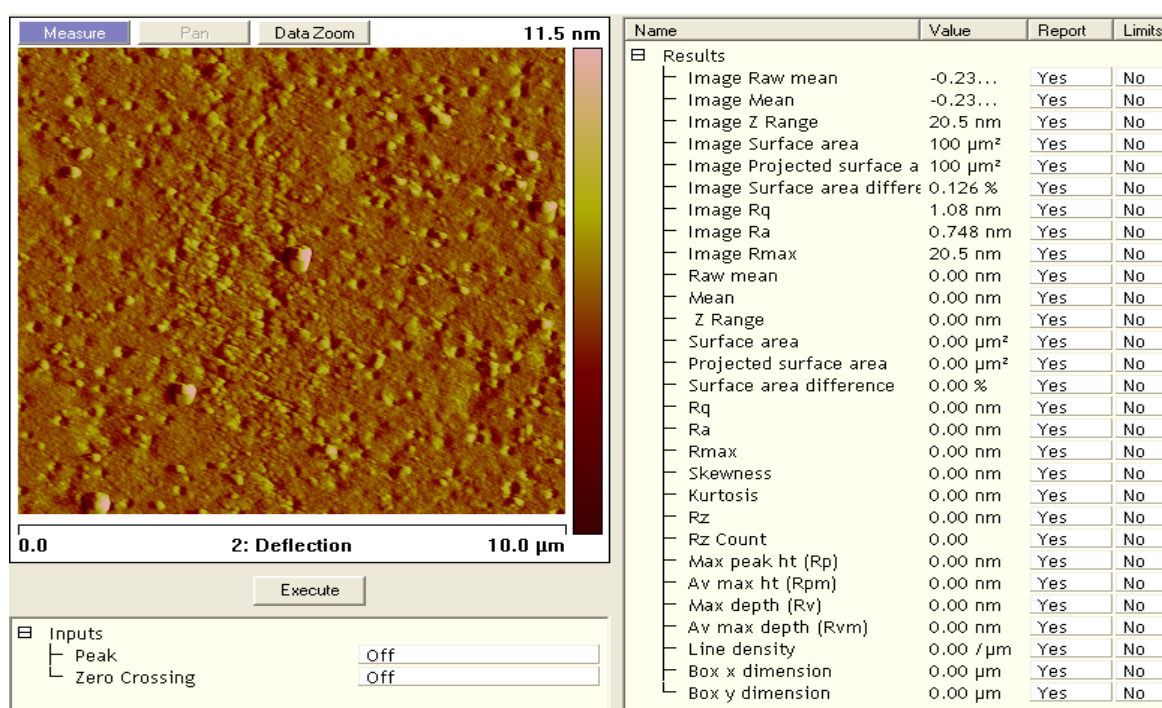


Figure 38: AFM Scan of 10µL scan size in contact mode surface study of imprinted polymer layer MIP-ME42 after sensor measurements [imprinted copolymer of 35% methacrylic acid and 7% methacrylate by weight crosslinked with 58% ethylene glycol dimethacrylate imprinted with 10% of Atrazine as template]

3.3 Temperature Effects on Sensor Response

Fluctuations in temperature may cause fluctuations in frequency of QCM. Due to less solubility of analytes at low temperatures, freshly prepared solutions were used for sensor measurements. To improve sensor signals, all the

measurements were made at 28°C. Furthermore, temperature variations during the analysis were minimized by keeping the liquids in thermostat.

3.4 Effect of Methanol on MIP Layers for Template Removal

Fig. 39 illustrates a comparison of the time required in template removal for different molecularly imprinted polymer coating of Atrazine. Depending on nature of imprinted polymer, removal of Atrazine was different in each case. Reference polymer MA46 showed very small difference loss of layer during washing.

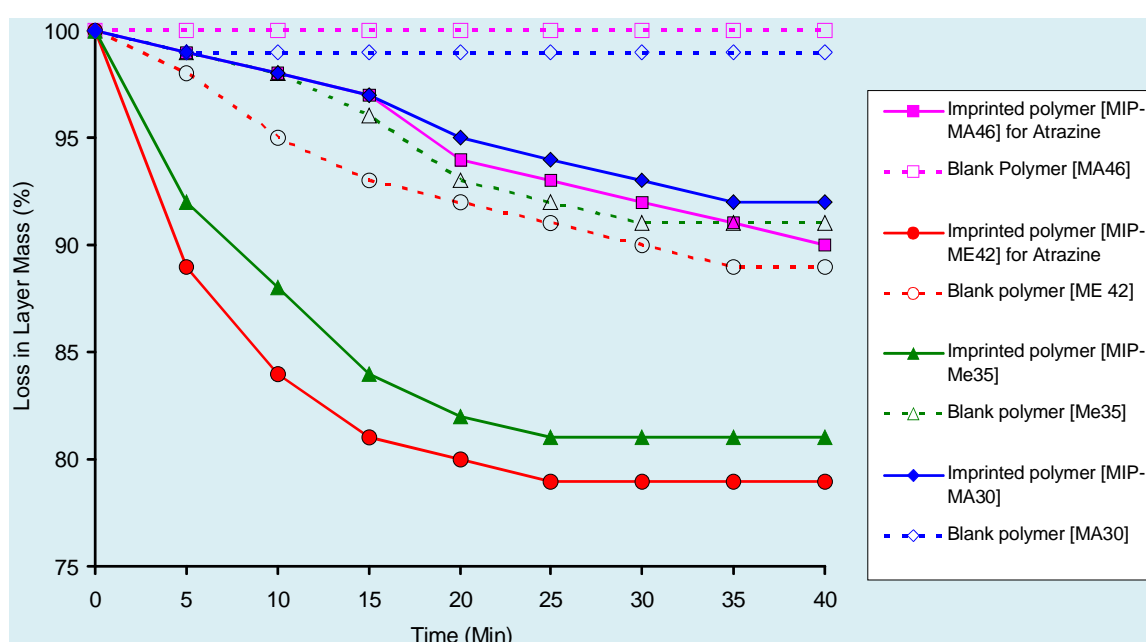


Figure 39: Effect of methanol on mass of synthetic imprinted and reference coatings for removal of Atrazine including MIPs-MA46 [methacrylic acid 46% crosslinked with 54% ethylene glycol dimethacrylate imprinted by 10% of Atrazine], MIPs-MA30 [methacrylic acid 30% crosslinked with 70% ethylene glycol dimethacrylate imprinted by 10% of Atrazine], MIP-ME33 [imprinted copolymer of 28% methacrylic acid and 5% methacrylate crosslinked with 58% ethylene glycol dimethacrylate by weight imprinted with 10% of Atrazine as template] & MIP-ME42 [imprinted copolymer of 35% methacrylic acid and 7% methacrylate crosslinked with 58% Ethylene glycol dimethacrylate imprinted by weight with 10% of Atrazine as template].

While, maximum removal of template was observed in the imprinted polymer ME42. From this data, improved sensitivity was expected from ME42 with greater number of recognition sites available for analyte.

3.5 Comparison of Sensor Response of MIP Layers

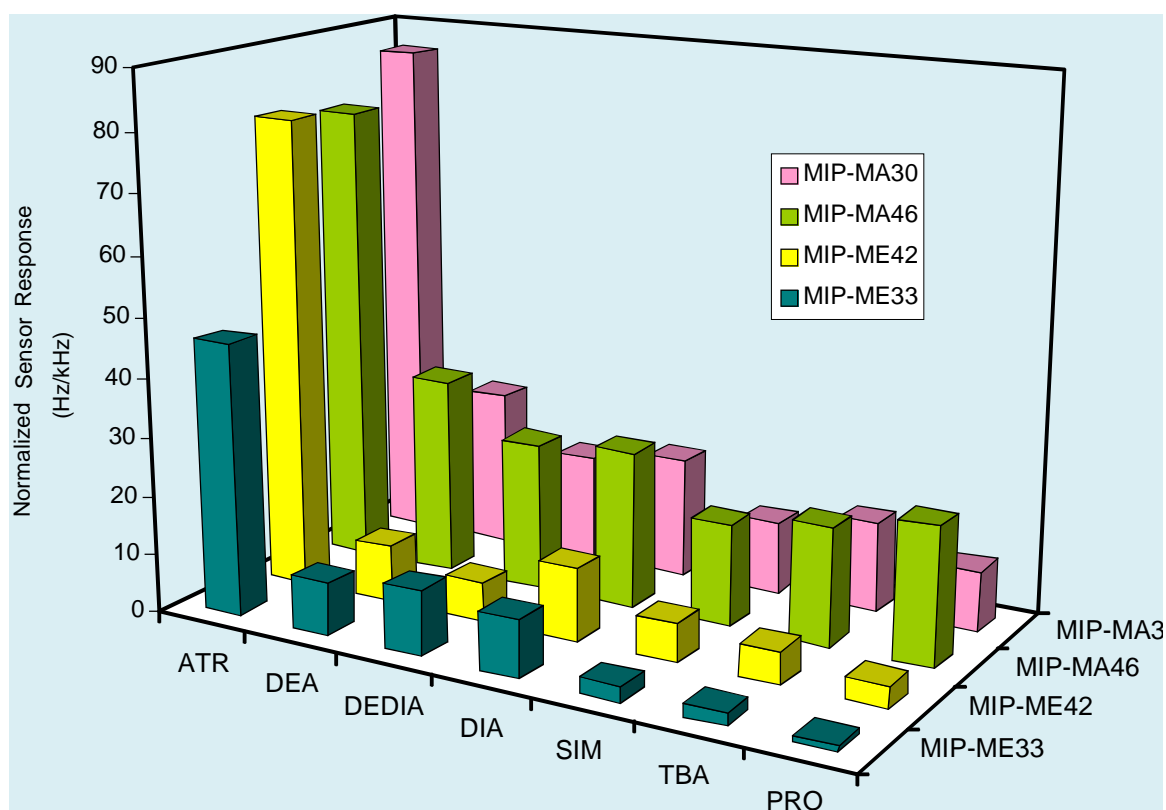


Figure 40: Cross selectivity comparison of MIPs-MA30 [methacrylic acid 30% crosslinked with 70% ethylene glycol dimethacrylate imprinted by 10% of Atrazine], MIPs-MA46 [methacrylic acid 46% crosslinked with 54% ethylene glycol dimethacrylate imprinted by weight and 10% of Atrazine as template], MIP-ME42 [imprinted copolymer of 35% methacrylic acid and 7 % methacrylate crosslinked with 58% ethylene glycol dimethacrylate by weight imprinted with 10% of Atrazine as template], MIP-ME35 [imprinted copolymer of 28% methacrylic acid and 5% methacrylate crosslinked with 58 % ethylene glycol dimethacrylate by weight imprinted and 10% of Atrazine as template].

As illustrated in **Fig. 40**, sensor design for Atrazine imprinted polymer is found sensitive for ATR with LOD 0.05 mg/L. Selectivity of the imprinted layer is enhanced by optimized polarity of the matrix for Atrazine. The metabolites of Atrazine (ATR), Des-ethyl atrazine (DEA), Des-isopropyl atrazine (DIA) and Des-ethyl-des-isopropyl atrazine (DEDIA) with enhanced polarity respond to Atrazine imprinted layer more than Simazine (SIM), Propazine (PRO) & Terbutylazine (TBA). Sensor response is found fully reversible and the robust sensitive layer may work efficiently for a time period of more than a year.

Chapter 4

DETECTION WITH MOLECULARLY IMPRINTED NANOPARTICLES

In recent decades, nanotechnology has evolved at a very fast pace due to the desire to fabricate materials with novel or improved characteristics. Among such materials, use of highly sophisticated nanoscale particles “Nanoparticles” (NPs) has gained significant interest in the field of research particularly in life sciences and analytical chemistry with myriad of applications³⁴. Intrinsic feature of these particles is their individual behavior as three dimensional surfaces, imparting exceptional chemical, physical and biological properties to nanoscale materials.

4.1 Nanoparticles as Chemical Sensor Coatings

With the parallel advancement of analytical tools, nanoparticles open up a novel world with enormous implication of developing chemical sensors in areas of clinical diagnosis, pharmaceutical, biological (proteins etc), pesticides, drugs, industrial wastes, pollutants, explosives gases, industrial process and quality control etc³⁵⁻³⁶. The number of publications regarding the applications of nano particles for sensors generation is increasing every year ranging from few publications (ten years back) to hundreds these years.

Nanoparticles offer increased surface area giving better sensitivity, LOD and selectivity as compared to that of the MIPs used for sensing specific templates. Thus, making nanoparticles highly suitable for QCM based gravimetric chemical sensors with small area for sensitive coatings³⁷. The nanoparticles with smaller size, offer minimum surface roughness, lower viscosity and hence less damping of QCM. The quality of frequency signal with respect to noise is thereby expected to improve by

nanoparticles as sensor materials. On the other hand, larger surface area of nanoparticles increases accessibility of analyte molecules deeper into the particles film, resulting in greater mass load and consequently higher sensitivity. Moreover, NPs' surface functionality can be easily modified to achieve selective sample detection. Therefore, by increasing the interaction sites on QCM surface, sensitivity of the sensor can be further enhanced.

For this purpose, synthesis of nanoparticles was carried out to replace synthetic antibodies of imprinted polymer layers by imprinted nanoparticles. From the finding that synthetic antibody MIP-M42 exhibited stronger and specific affinity to Atrazine; NPs of the same were generated to check sensor performance.

4.2 Synthesis & Extraction of Imprinted Particles

Imprinted nanoparticles were synthesized by precipitation polymerization⁴² in two simple steps. First the pre-polymerized cocktail of imprinted copolymer of methacrylic acid and methacrylate was prepared. The mixture of monomers methacrylic acid and methyl acrylate was pre-polymerized as in previous experiments (See **Table 8**) following the composition of MIP-ME42 [35% methacrylic acid and 7 % methacrylate crosslinked with 58% ethylene glycol dimethacrylate by weight imprinted with 10% of Atrazine as template]. The solution was kept under constant stirring and was taken out of the water bath just before reaching the gel point. In the second step, the imprinted nanoparticles were extracted in a solvent by precipitation. For this purpose, the pre-polymerized solution was brought into a solvent in which the polymer was insoluble (ACN) under fast stirring. The size of the particles depends on degree of cross linking, time, temperature and volume of pre-polymerized solution added to the solvent. Keeping all the factors constant, except the amount of polymer gel added to the solvent, particles were precipitated in three solutions using round bottom flask (10mL) for generating particles of different sizes.

Solution A:

In a 10mL round bottom flask with 6mL of acetonitrile (ACN) drop-wise 60 μ L

of imprinted ME42 pre-polymerized solution was added, using 20 μ L eppendorf pipette while stirring at maximum speed of 4000 rpm.

Solution B:

Repeating the same procedure another solution was prepared with slow addition of 30 μ L of pre-polymerized solution in 6 mL of acetonitrile.

Solution C:

In another flask (10mL), 15 μ L of pre-polymerized solution was mixed slowly to 6 mL of ACN. All the solutions were kept under rigorous stirring with maximum speed for 30 hrs. After removing the solutions from stirring plate, sedimentation of particles occurred with milky appearance.

Nanoparticles obtained as sediments were centrifuged at 4400 rpm for 5 minutes and the supernatant was removed. The pallet of particles was dispersed in acetone for characterization using atomic force microscope.

4.3 Atomic Force Microscope Studies

In order to scan the purified nanoparticles under AFM, glass slides were used as substrates with a size of 2 x 2 cm after cleaning with acetone. The particles in acetone were filtered through a 1.2 μ m syringe to remove larger particles or agglomerates i.e.; the clusters of smaller particles. Diluted solutions were spin coated on glass pieces at a speed of 1200 rpm for 20 sec.

AFM images of the dried slides for nanoparticles from solution A, B and C, were taken in contact mode with Silicon Nitride tip. As depicted in the **Fig. 41** the particles taken from of solution A were observed narrowly distributed in size of few hundred nanometers.

Fig. 42 presents 3-D image of the imprinted particles scanned in contact mode. In **Fig. 43**) another AFM scan of 1mg of imprinted nanoparticles in 50 mL of acetone was recorded. The particles were narrowly distributed and required further dilution.

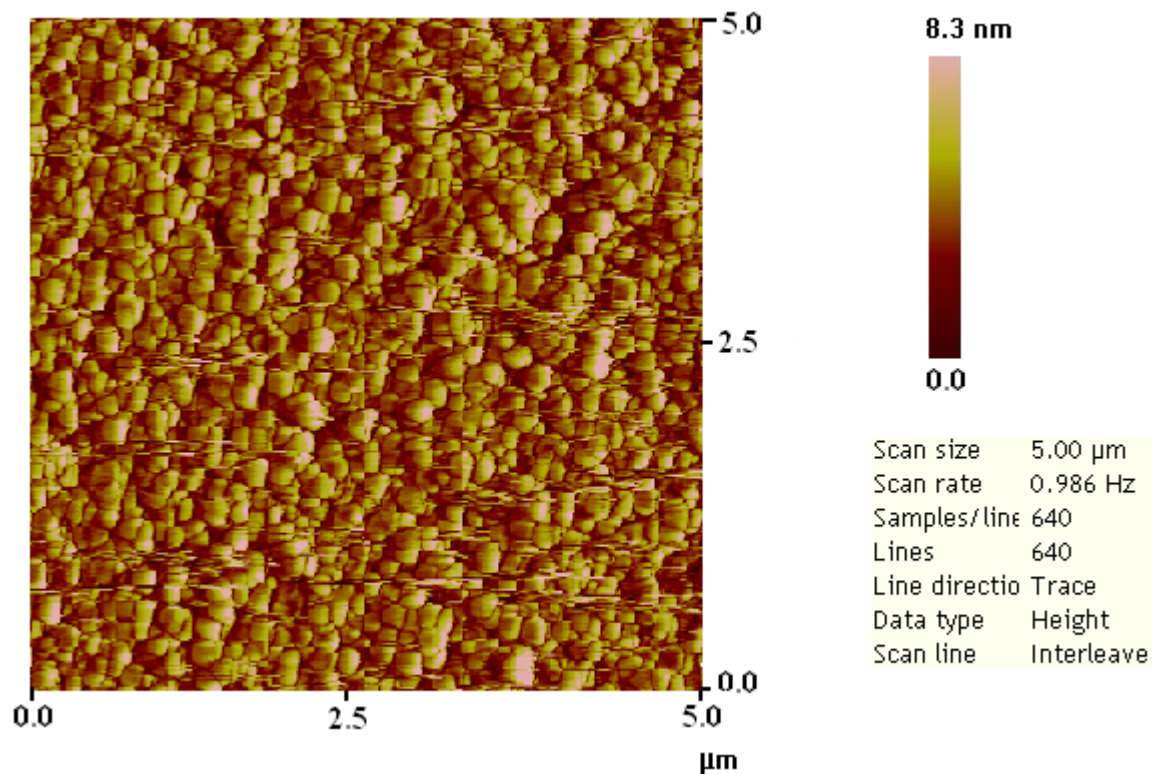


Figure 41: AFM scan (in contact mode with Silicon Nitride tip) of 1mg of molecularly imprinted nanoparticles precipitated from MIP-ME42 [imprinted copolymer of 35 % methacrylic acid and 7% methacrylate crosslinked with 58 % ethylene glycol dimethacrylate by weight imprinted with 10% of atrazine as template] in 10mL of Acetone.

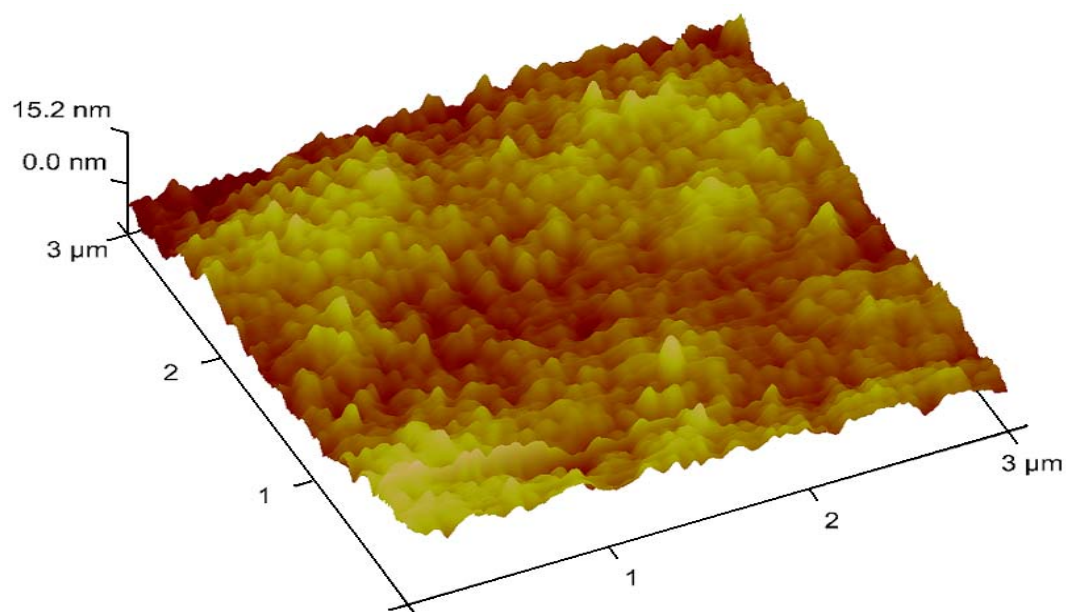


Figure 42: Three dimensional AFM image narrowly distributed imprinted nanoparticles (1mg) in 10 mL of acetone.

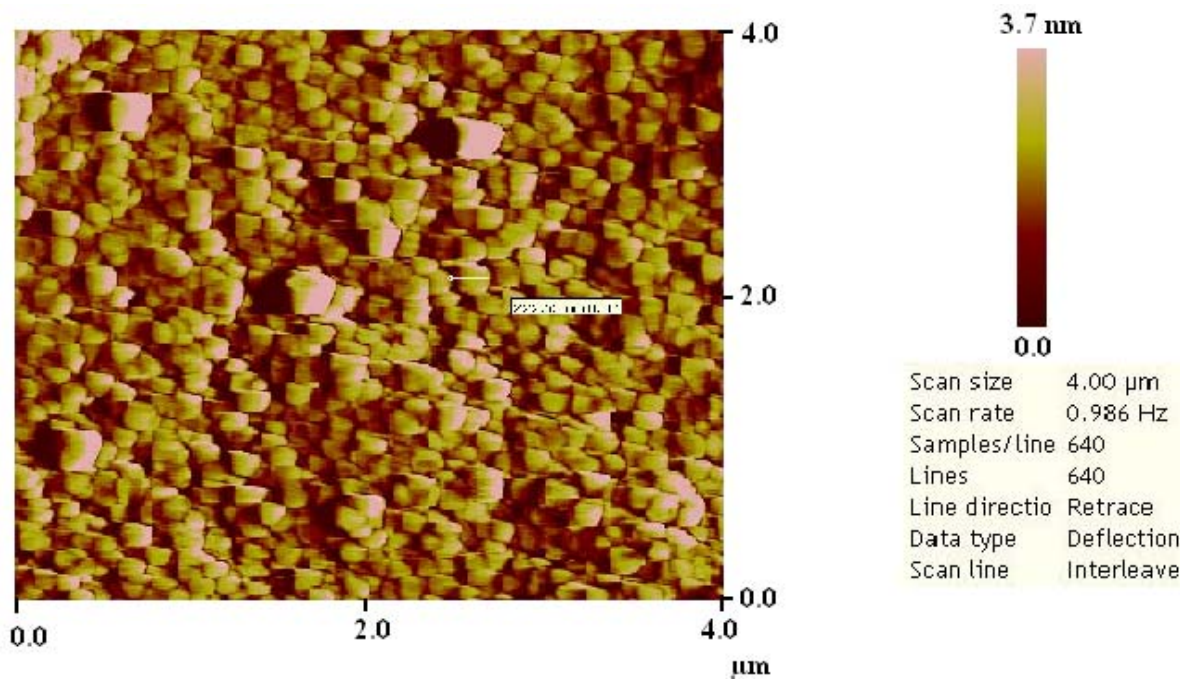


Figure 43: AFM image (in contact mode with Silicon Nitride tip) of narrowly distributed nanoparticles with a concentration of 1 mg in 20 mL of Acetone. The maximum size of the particle was in range of 200-220 nm.

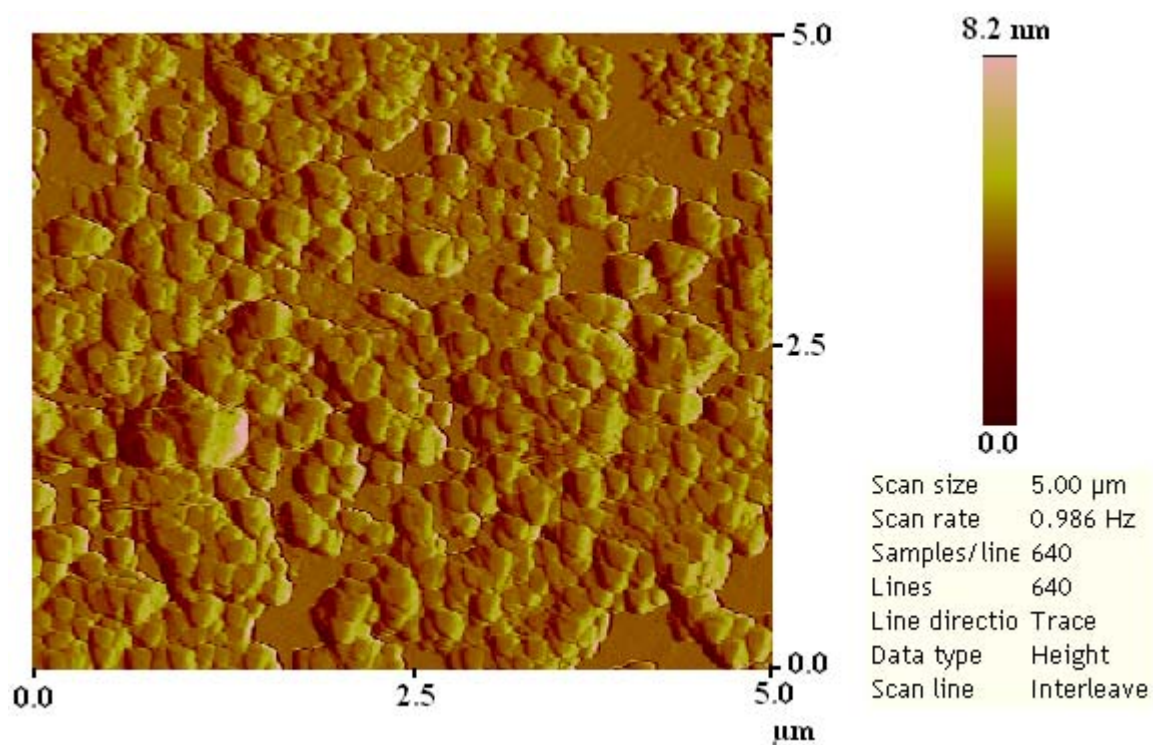


Figure 44: AFM image taken in contact mode of molecularly imprinted nanoparticles (1mg) diluted in 50 mL of Acetone.

As illustrated in **Fig. 44**, imprinted nanoparticles solution with a dilution of 1 mg particles in 50 mL of acetone were scanned. The distribution of particles was improved but agglomerates of particles were still obvious. Therefore, the solution was further diluted with 1mg of particles in 200 mL of acetone. A homogeneous distribution of the nanoparticles was attained as shown in the AFM image (**Fig. 45**).

From the AFM images, nanoparticles were visualized with excellent morphology but their performance as sensor coating could only be tested by template removal to make the active sites free for reincorporation of analyte molecules.

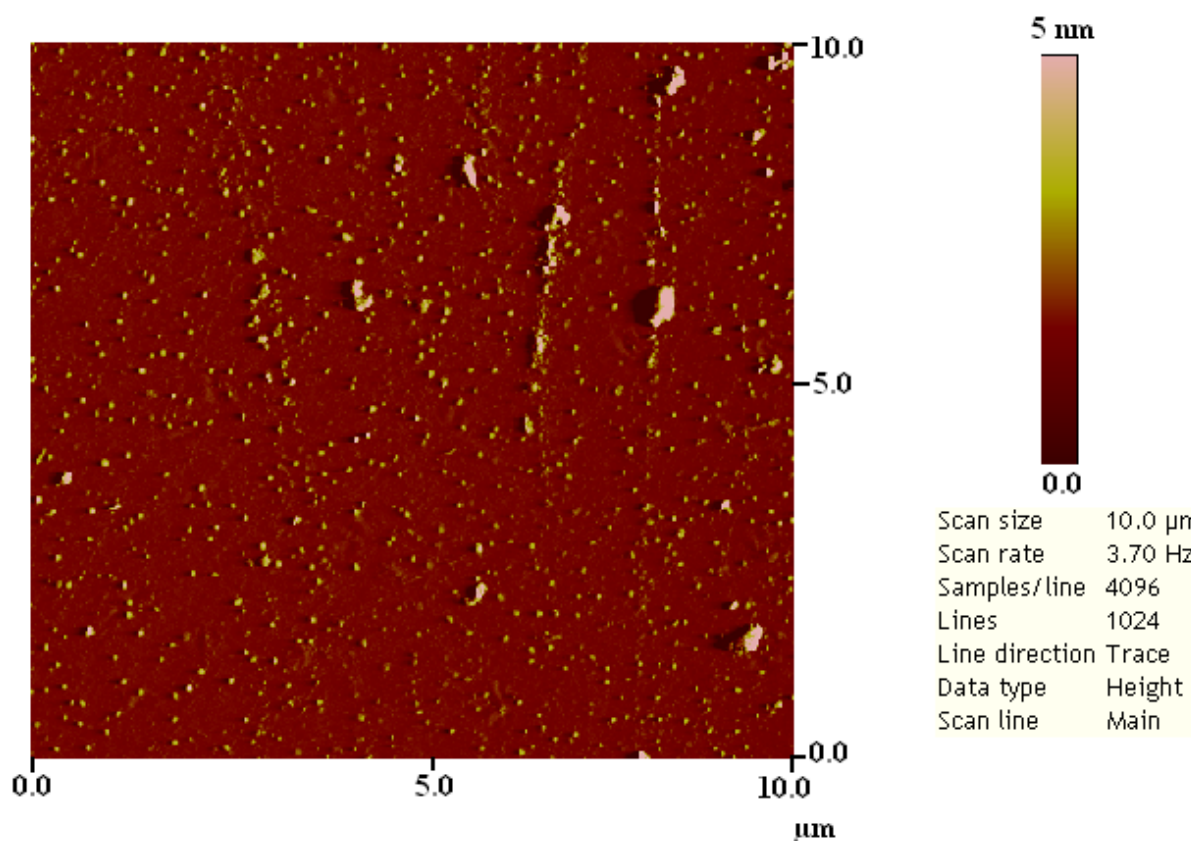


Figure 45: AFM image recorded (in contact mode with Silicon Nitride tip), of Imprinted nanoparticles (1mg) diluted in 200 mL of acetone with excellent distribution ranging from 55-81 nm in size.

4.4 Template Removal

The suspension of Nanoparticles in acetone was washed for template removal prior to coating on quartz. First, nanoparticles were centrifuged at 4400 rpm for 5 min. The supernatant was removed and the pallet was bloated in methanol to remove imprinted molecules. After ultrasonic treatment for 30 sec, the whole washing procedure was repeated twice to fully remove the template.

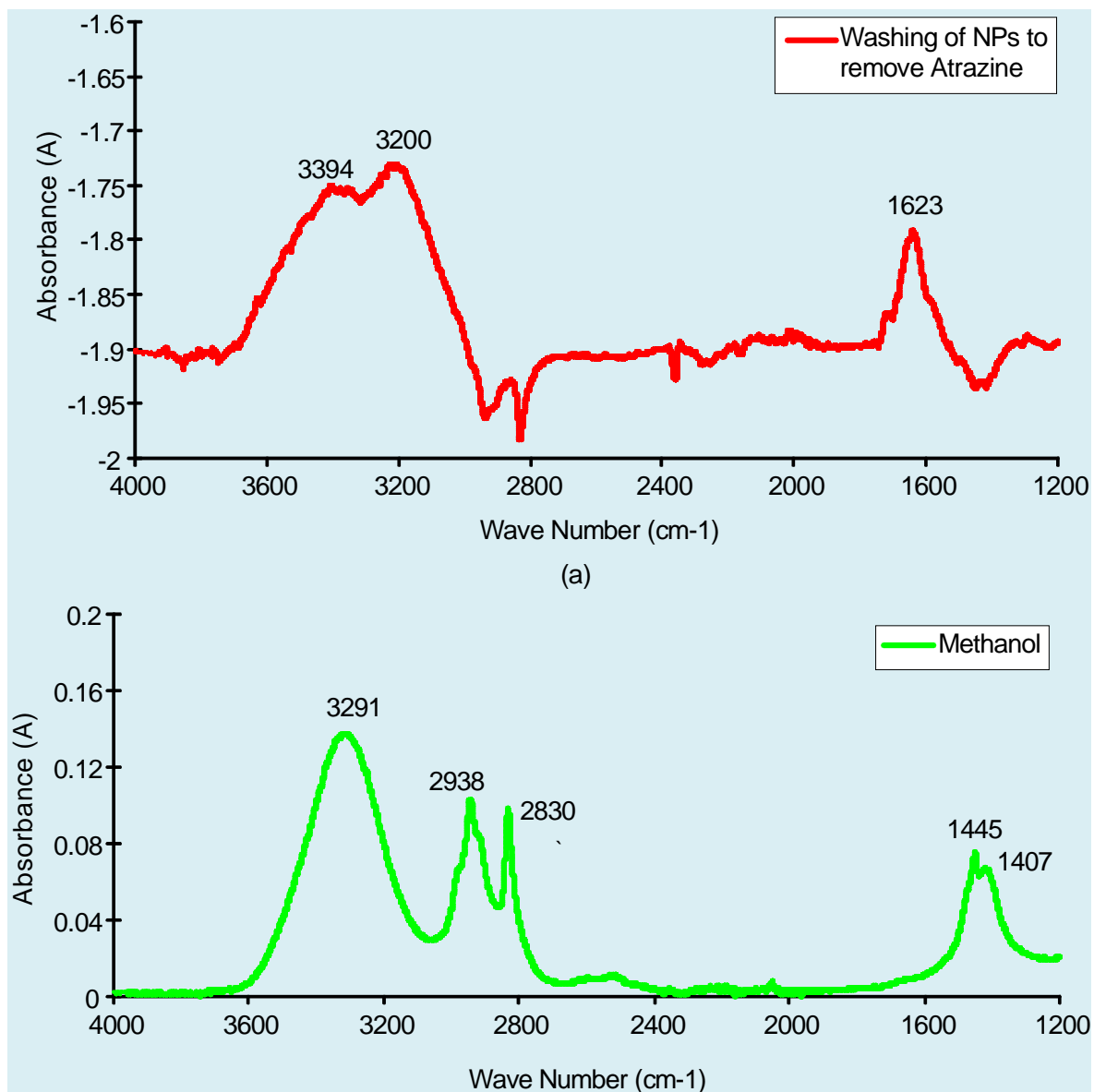


Figure 46: FTIR Spectra of washings of Nanoparticles in methanol for removal of Atrazine used as template and of methanol as reference. Peaks at 3394cm^{-1} and 1623cm^{-1} are observed for $-\text{NH}$ group and aromatic carbon of the triazine ring indicating presence of Atrazine in the solvent.

An FTIR spectrum (Fig. 46) of methanol washings was taken to confirm extraction of imprint molecules from imprinted particles. Presence of Atrazine in methanol washing was confirmed from -NH peak at 3190 cm^{-1} . A broad peak at 3397 cm^{-1} represents -OH group of methanol.

4.5 Immobilization of Imprinted Nanoparticles on QCM

Immobilization of imprinted nanoparticles and generation of homogeneous layer on QCM was a tedious job due to lack of adhesion of particles directly with the gold surface. After removing the template, methanol was evaporated off and 2mg of particles were diluted in 1mL of THF to immobilize them on gold electrode of quartz substrate. First an attempt was made to distribute the particles by spin coating 5 μ L of particles solution on a pre-coated polymer layer of non-imprinted ME42 having a thickness of 80 nm. The polymer layer was pre-coated to provide the particles better adhesion to the surface. After keeping the quartz overnight under the UV, the particles were agglomerated and white crystals appeared on the electrode surface.

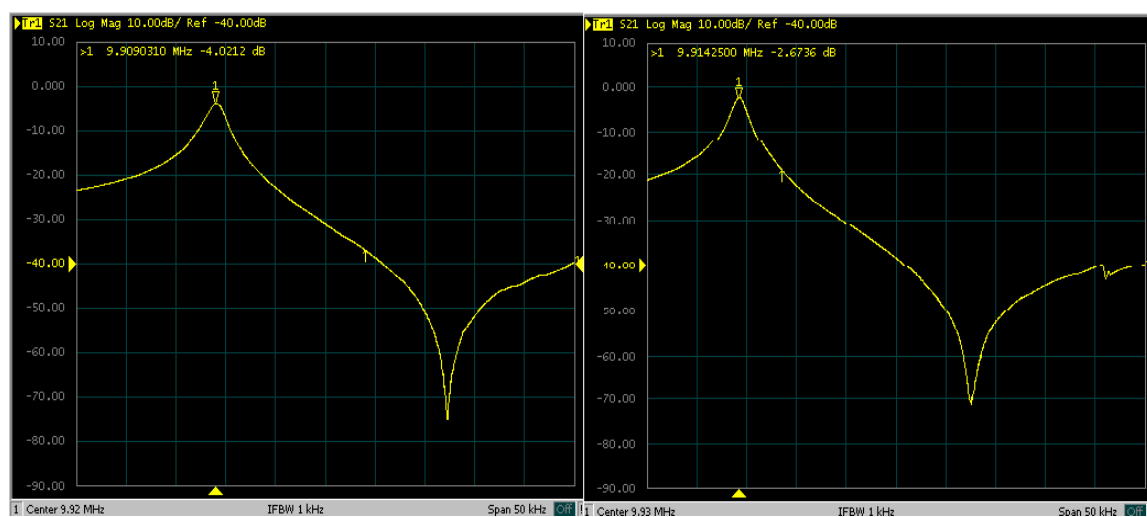


Figure 47: Screen image of damping spectra of QCM before and after coating nanoparticles.

To distribute the particles homogeneously on the quartz surface, 100 μ L of non-imprinted polymer solution (ME42) was added to 400 μ L of nanoparticle solution

(2 mg/mL) in THF. The mixture was stirred and spin coated at 2100 rpm on gold electrode of QCM.

The reference electrode was spin coated at 1200 rpm by non-imprinted ME42 to compensate the non specific sensor effects e.g. temperature fluctuations during the sensor measurement. The layers were left for hardening at room temperature overnight

Coated electrodes were checked for layer thickness by calculating frequency shifts of respective electrodes before and after coating the layers. **Fig 47 & 48** show image and graph of damping spectra of the electrode with imprinted particles taken at a frequency span of 50 kHz.

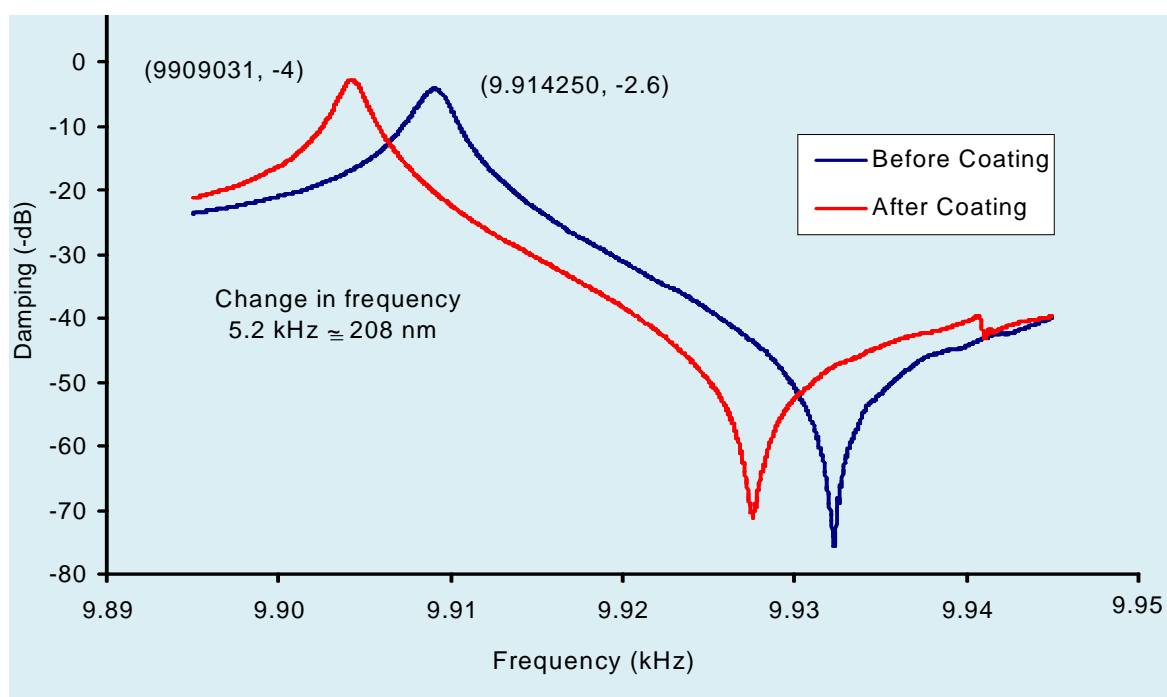


Figure 48: Damping spectra of QCM before and after coating imprinted nanoparticles recorded at frequency span of 50 kHz. Decrease in the resonance frequency was 5.219 kHz indicating mass load of 208 nm thick layers of nanoparticles extracted from MIP-ME42 [imprinted copolymer of 35 % methacrylic acid and 7% methacrylate crosslinked with 58 % Ethylene glycol dimethacrylate imprinted by weight with 10% of Atrazine as template].

Further the layer homogeneity and surface roughness was checked by AFM. As shown in the AFM image of imprinted particles with a layer height of 208

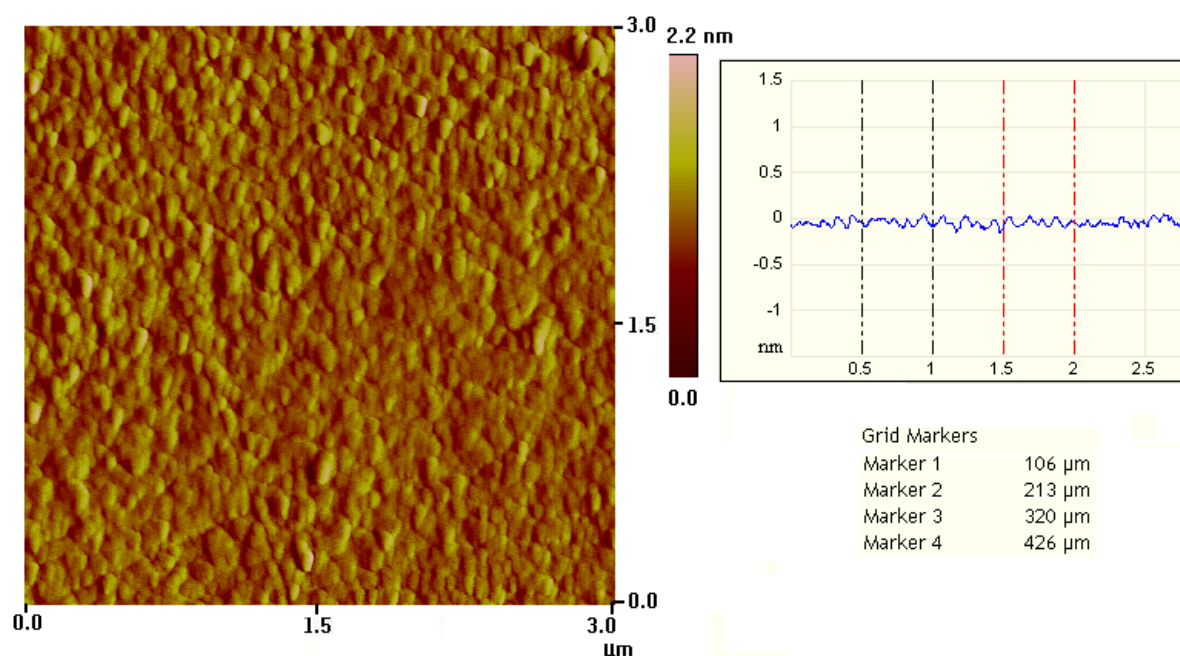


Figure 49: AFM image showing deflection of Silicon Nitride tip while scanning in contact mode the Imprinted particles as coated on gold electrode of quartz substrate.

4.6 Sensor Measurements

To evaluate recognition properties of imprinted nanoparticles, QCM was fixed into measuring cell for gravimetric analysis. Sensitivity of the imprinted NPs for Atrazine was analyzed using non imprinted layer of ME42 as reference. **Fig. 50** shows image of running measurement in Winsens XP while preliminary testing of imprinted NPs coating. Aqueous solution of Atrazine (2 mg/L) was flowed through the cell at a rate of 1.5mL per minute while keeping the temperature constant at 28 °C. As illustrated in image, excellent curve of frequency shift was observed by imprinted layer of particles with a thickness of 208 nm.



Figure 50: Image of running measurement in WINSSENS XP for sensitivity response of imprinted nanoparticles layer (208nm) and reference polymer ME42 coatings (225 nm) as recorded by WINSSENS XP software. The curve in second window presents the net sensor response. The size of imprinted nanoparticles used in layer was 45-81 nm.

4.7 Size and Distribution of Imprinted Nanoparticles

The optimization of synthetic methodology, choice of suitable size and distribution of nanoparticles may improve sensor responses. Keeping in view this fact, nanoparticles with varied sizes and distribution were tested as sensor coatings. The nanoparticles precipitated in Solution A, B and C varied in sizes. It was observed that the size of nanoparticles was proportional to amount of pre-polymerized solution added slowly to rigorously stirred solvent. Atomic force images of particles from Solution A, B and C were diluted to 1 mg in 200 mL of acetone and scanned for comparison. Scans as given in **Fig. 51-56** illustrated different sizes of particles from each solution. Particles size was found to be in range of 100-170 nm in solution A. Particles with size of 90-140 nm were obtained by Solution B. While Solution C precipitated out nanoparticles with a size range of 45nm-81nm.

The size of the nanoparticles was visualized by scanning with AFM in contact mode

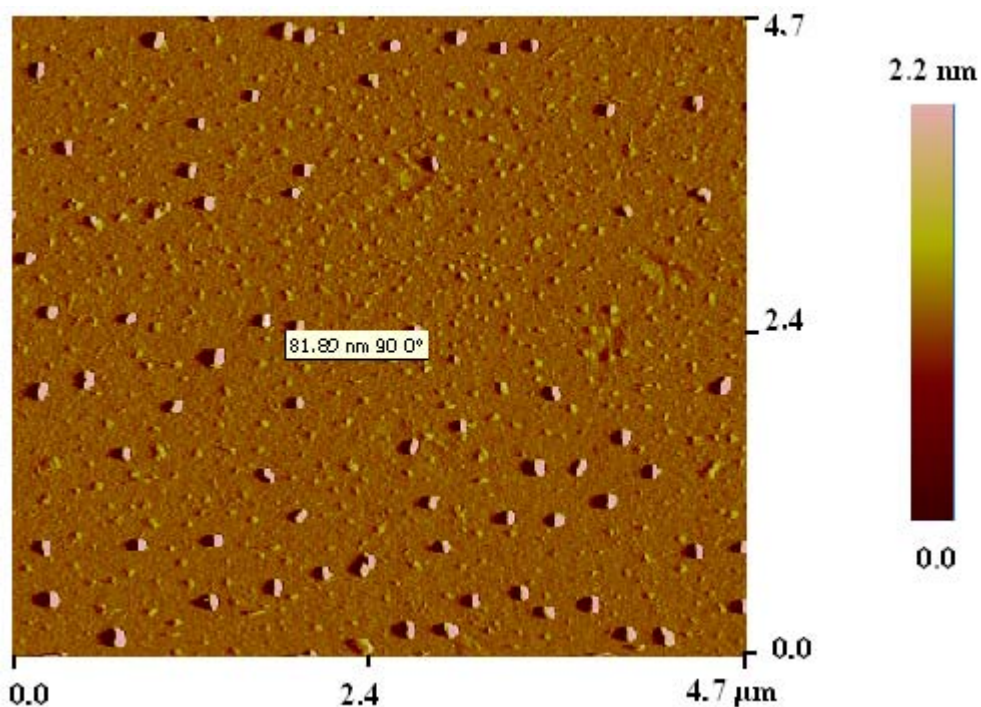


Figure 51: Size of Imprinted Nanoparticles 45-81 nm as illustrated in AFM image (recorded in contact mode with Silicon Nitride tip), of particles precipitated from solution C (15 μL of MIP-ME42 in 6 mL of Acetonitrile)

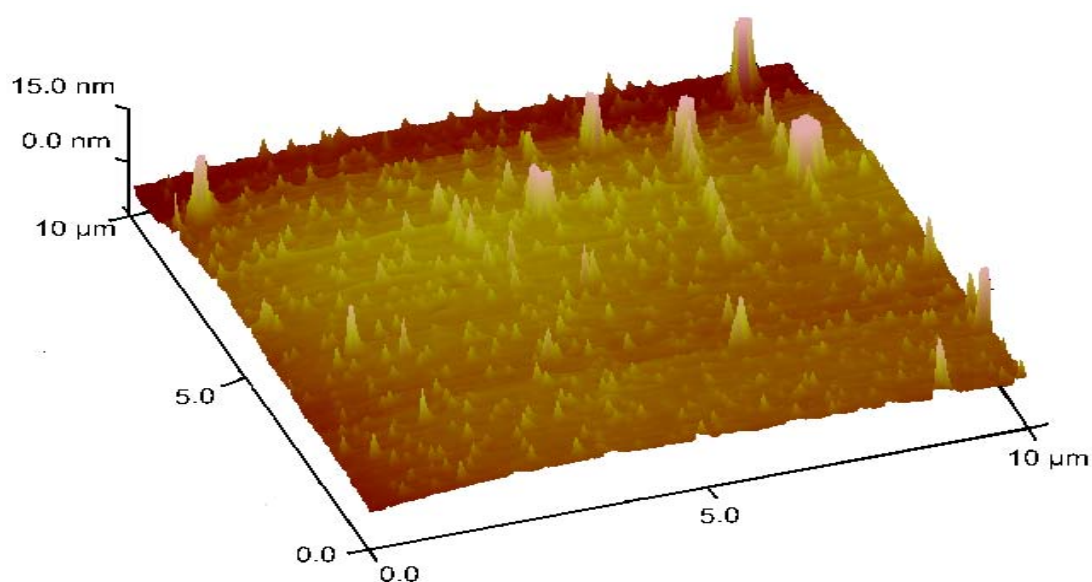


Figure 52: AFM image (in contact mode with Silicon Nitride tip), of imprinted Nanoparticles in 3-D with size range of 45-81 nm precipitated by solution B (15μL of MIP-ME42 in 6 mL of Acetonitrile)

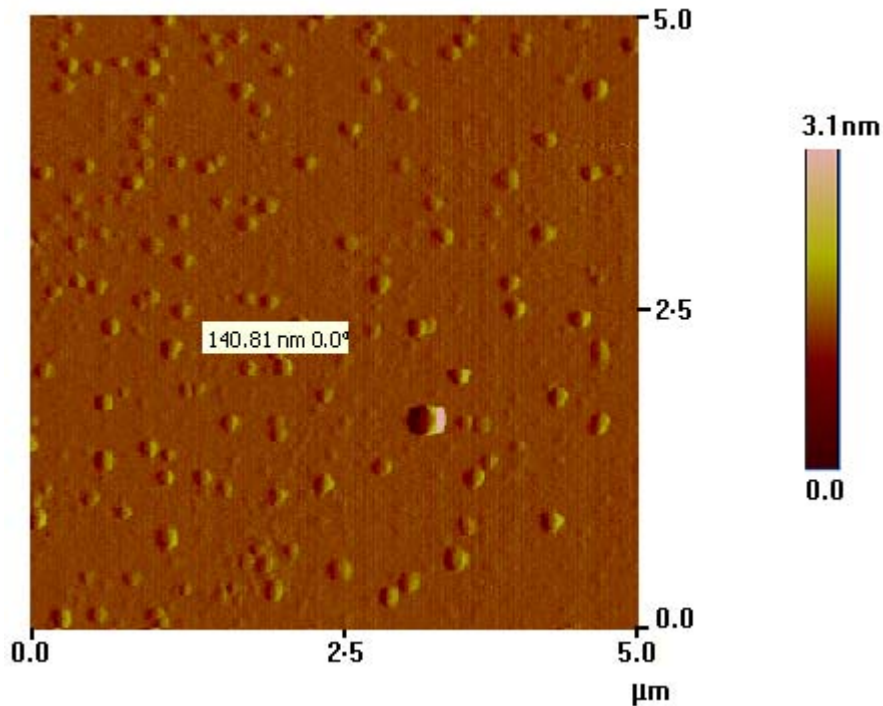


Figure 53: Size of Imprinted Nanoparticles 90-140 nm as shown in AFM image (taken in contact mode with Silicon Nitride tip with Silicon Nitride tip) of particles precipitated from solution B (30 μL of MIP-ME42 in 6 mL of Acetonitrile)

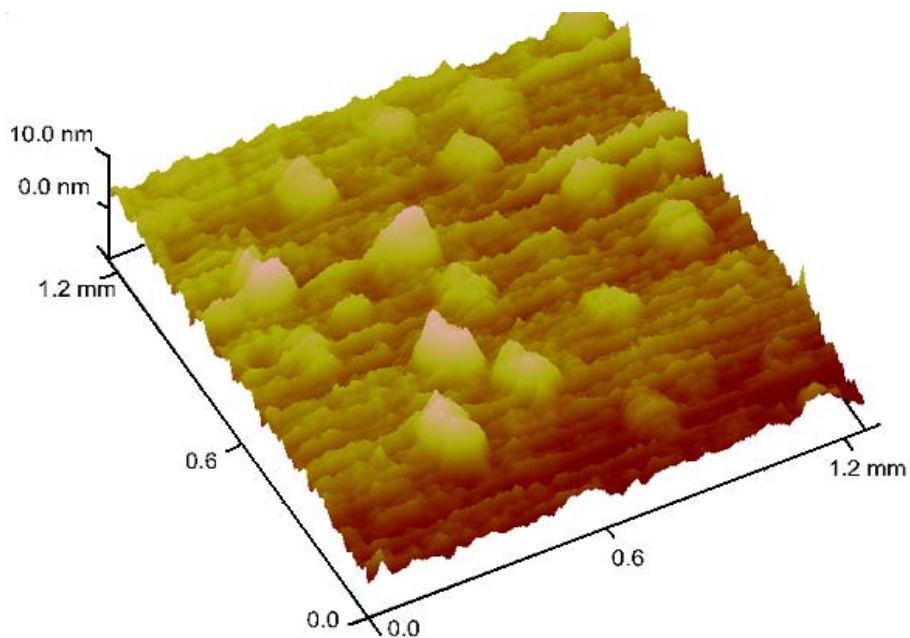


Figure 54: AFM image (in contact mode with Silicon Nitride tip), of imprinted Nanoparticles in 3-D with size range of 90-140 nm precipitated by solution B (30 μL of MIP-ME42 in 6 mL of Acetonitrile)

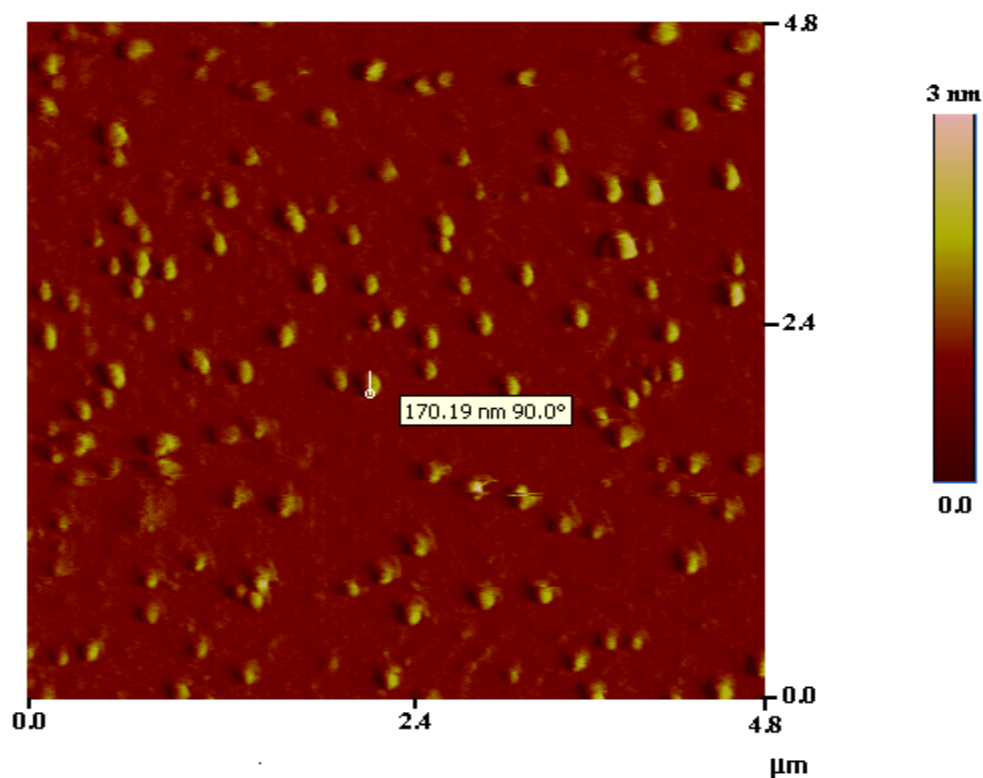


Figure 55: Size of Imprinted Nanoparticles 100-170 nm as shown in AFM image (taken in contact mode with Silicon Nitride tip with Silicon Nitride tip) of particles precipitated from solution A (60 μL of MIP-ME42 in 6 mL of Acetonitrile)

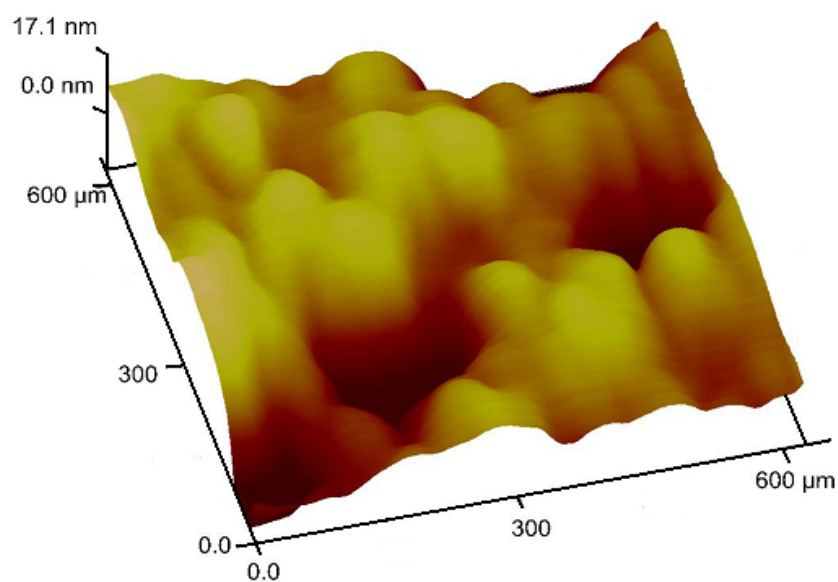


Figure 56 AFM image (recorded in contact mode with Silicon Nitride tip), of Imprinted Nanoparticles with size range of 100-170 nm precipitated from Solution A (60 μL of MIP-ME42 in 6 mL of Acetonitrile)

4.8 Effect of Size of Nanoparticles on Sensor Response

Mass sensitive measurements were performed to determine the size effect on sensitivity of the particles for Atrazine. Three dual electrodes quartz each coated by solution A, B and C of the imprinted nanoparticles and the non-imprinted polymer M42 were mounted into the flow cell for separate measurement. To maintain the solubility of solutions, the temperature of liquids being pumped into cell was kept at 28 °C by a thermostat.

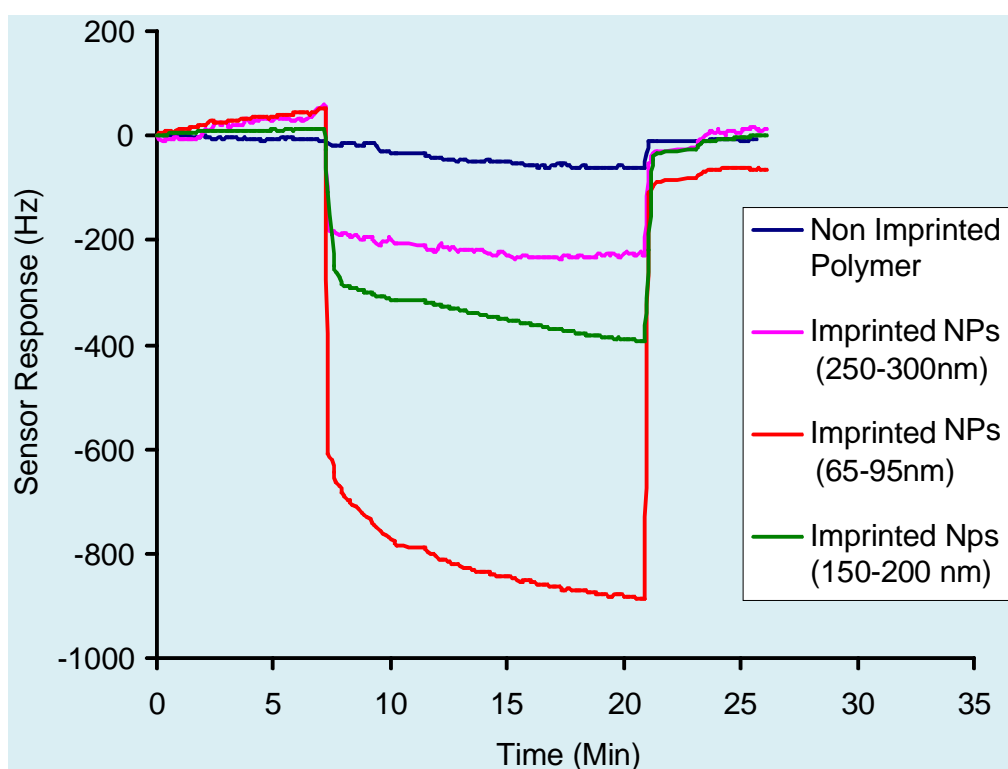


Figure 57: Sensor response recorded at 28°C with Nanoparticles of different sizes for 7mg/L of Atrazine.

The sensitivity curves by imprinted particles of various sizes as obtained from three individual measurements are combined for comparison. As illustrated in **Fig.57**, sensitivity of imprinted nanoparticles with a size range of 45-81nm gave a net sensor response of 840 Hz. However, frequency shift in case of bigger particles with size range of 150-200 nm was 200 Hz. The imprinted particles with the size varying from 250-300 nm showed a sensor signal of 360 Hz. The enhanced mass effect with smaller size of imprinted particles is caused by greater number of active sites with

increased number of particles. Also with smaller size, analyte molecules are diffused to a higher extent within imprinted layer. Gradual decrease in mass with time indicates incorporation of Atrazine molecules into imprinted particles via diffusion. On the other hand removal of template molecules from the imprinted layer was also found rapid in each case.

4.9 Sensitivity Measurements

Considering the efficient response of imprinted particles for Atrazine with size ranging in 45-81 nm, the sensor coating of the same was exposed to further dilutions. At 0.7 ppm of Atrazine, molecules were incorporated into the sensor layers producing a mass load of 96 Hz (**Fig. 58**).

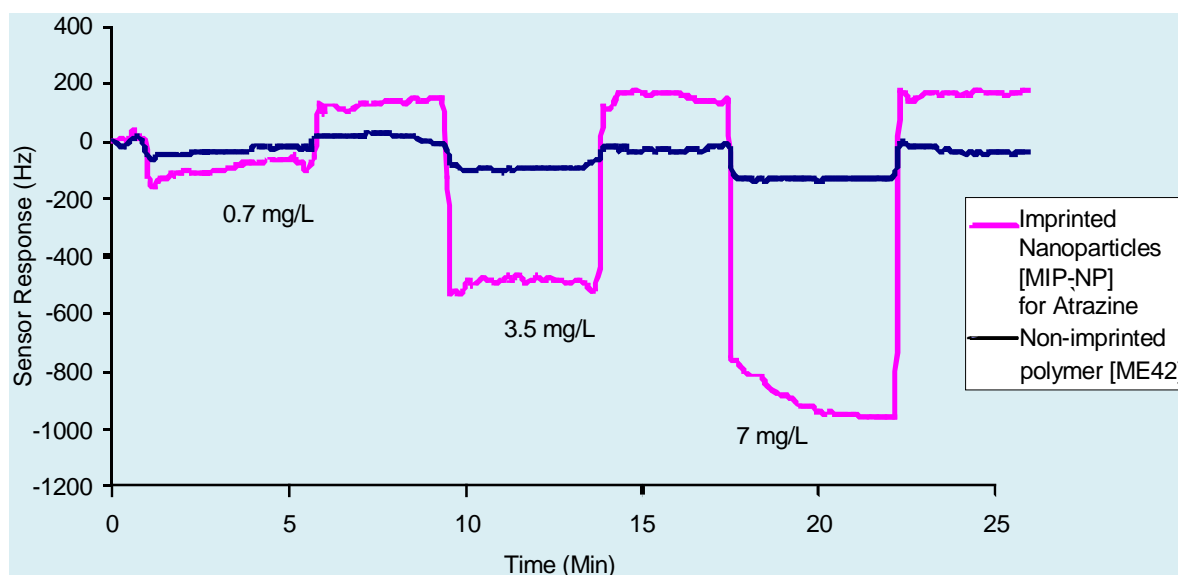


Figure 58: Measurement of sensitivity of imprinted nanoparticles 28°C with flow rate of 1.5mL/min for different concentrations of Atrazine in water by imprinted nanoparticles of size 45-81nm precipitated from MIP-ME42 [imprinted copolymer of 35 % methacrylic acid and 7% methacrylate crosslinked with 58 % Ethylene glycol dimethacrylate by weight imprinted with 10% of Atrazine as template] with layer height of 168nm and reference layer of non-imprinted polymer ME42 with layer height of 180nm.

Those molecules which found strong interaction were not removed in the following washing step. But as the new measurement is started, by repeated washing,

original frequency of imprinted electrode is recovered. At higher concentration of 3.5 mg/mL with a sensitivity of 400 Hz, signal to noise ratio was improved. By switching to even higher concentration of 7 mg/L, an excellent sensor response was regenerated increasing gradually to 900 Hz. While, the reference polymer also showed some mass effect of 60 Hz. On changing the phase to water an increase in frequency greater than the initial frequency of imprinted electrode was observed. Such change may happen because of loss of layer mass. As it was only observed in the beginning of measurement. It might be possible that the analyte molecules were not removed fully in measurement made earlier at maximum concentration.

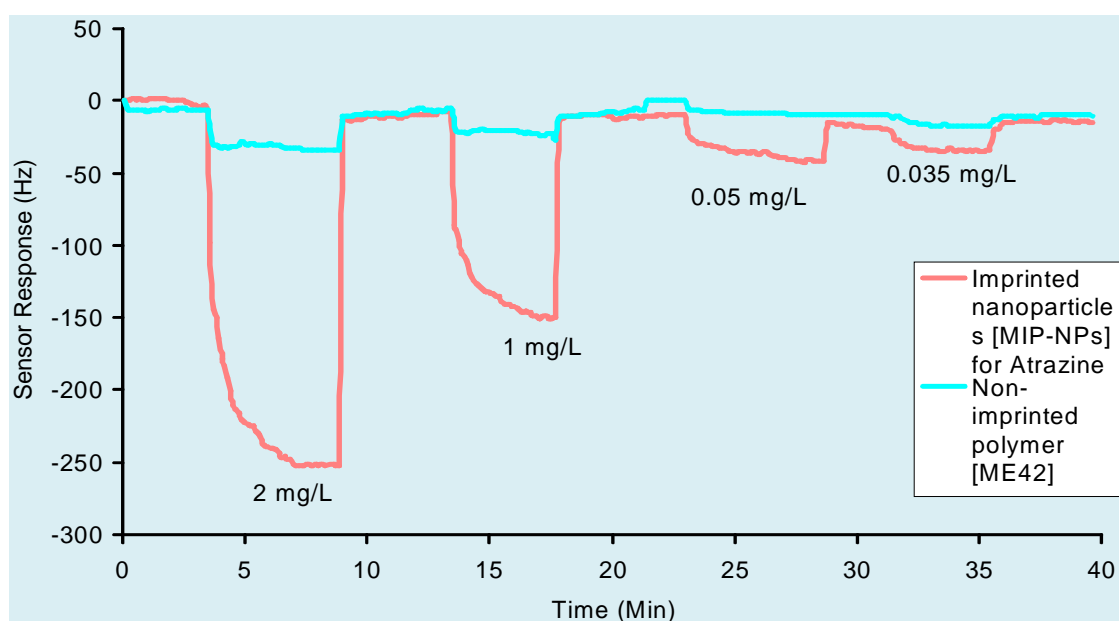


Figure 59: Sensor response recorded at 28°C with flow rate of 1.5 mL/min for different concentrations aqueous solution of Atrazine by imprinted nanoparticles of size 45-81nm precipitated from MIP-ME42 [imprinted copolymer of 35% methacrylic acid and 7 % methacrylate by weight crosslinked with 58% Ethylene glycol dimethacrylate imprinted with 10% of Atrazine as template] with layer height of 208 nm and reference layer of non-imprinted polymer ME42 with layer height of 220 nm.

Layer height of imprinted particles and non imprinted polymer was 208 & 220 nm, respectively. The binding strength on the imprinted coating of electrode varies in different areas. As given in **Fig.60**, the lowest detection limit was observed to be 35 ppb where signal to noise ratio was ≥ 3 .

The sensor responses of imprinted nanoparticles against different concentrations of atrazine ranging from 0.035 to 7 mg/L was linear as illustrated in **Fig.59**.

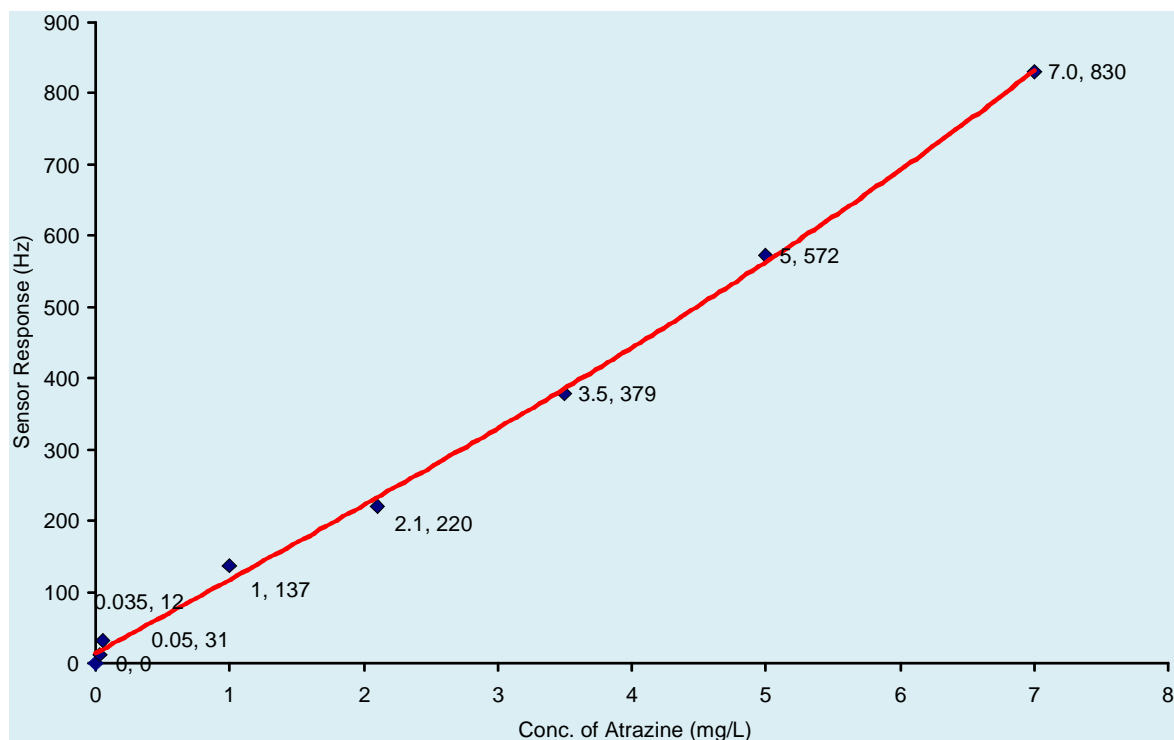


Figure 60: Sensitivity of imprinted nanoparticles 28°C for different concentrations of Atrazine in water, by imprinted nanoparticles of size 45-81nm precipitated from MIP-ME42 [imprinted copolymer of 35 % methacrylic acid and 7 % methacrylate by weight crosslinked with 58 % Ethylene glycol dimethacrylate imprinted with 10% of Atrazine as template] with layer height of 208 nm and reference layer of non-imprinted polymer ME42 with layer height of 220 nm.

In **Fig. 61**, the normalized sensor response of imprinted particles was compared with imprinted polymer layer recorded for concentrations of Atrazine. The sensitivity signal for 7mg/L by imprinted particles was found nearly 3 times higher than imprinted polymer layers.

Sensitivity of particles for lower concentration was possible down to 0.035mg/L (S/N ratio ≥ 3) as compared to imprinted polymer for which the LOD was 0.05 mg/L.

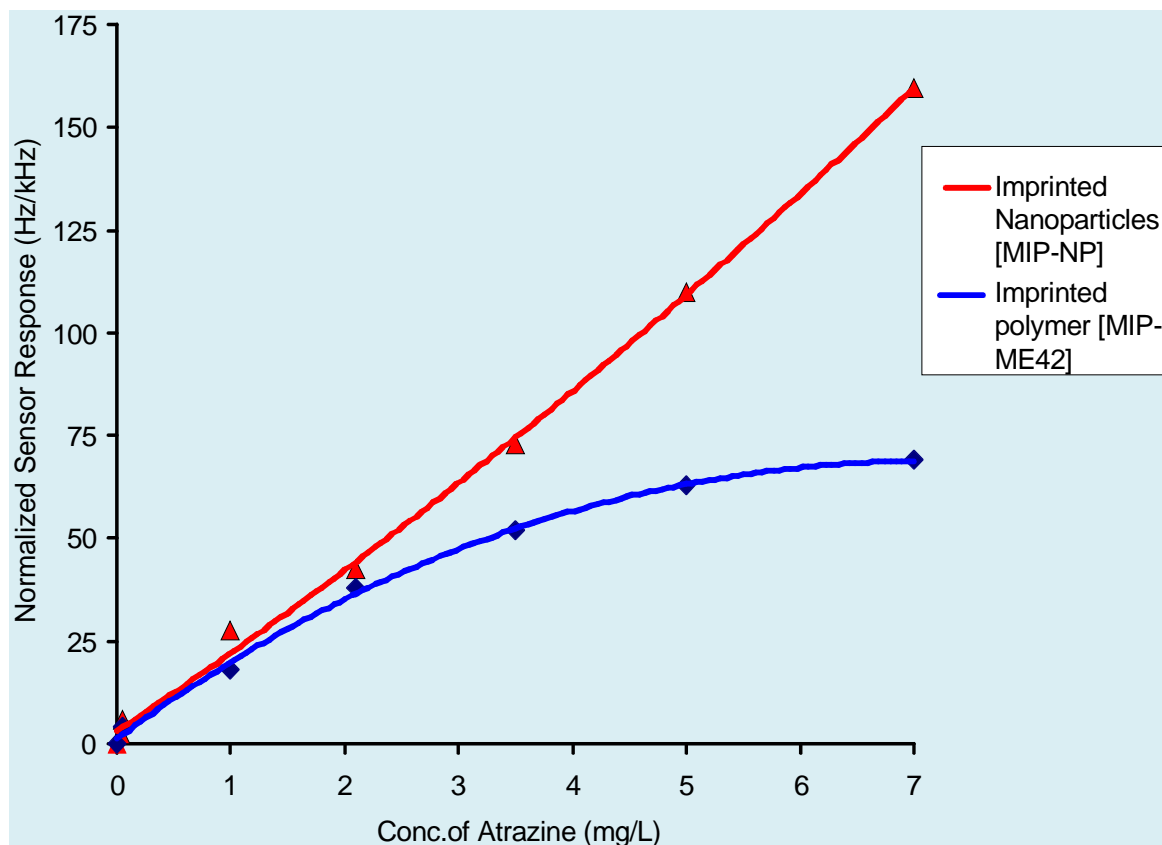


Figure 61: Comparison of normalized Frequency shifts recorded at 28°C by imprinted polymer MIP-ME42 [35 % methacrylic acid and 7% methacrylate crosslinked with 58 % ethylene glycol dimethacrylate by weight imprinted with 10% of Atrazine as template] and imprinted nanoparticles precipitated from MIP-ME42 for various concentrations of Atrazine at flow rate of 1.5mL/min

4.10 Selectivity Measurements

The selectivity of the imprinted nanoparticles for Atrazine was investigated for sensor layer of 208 nm with particle size of 45-81nm.

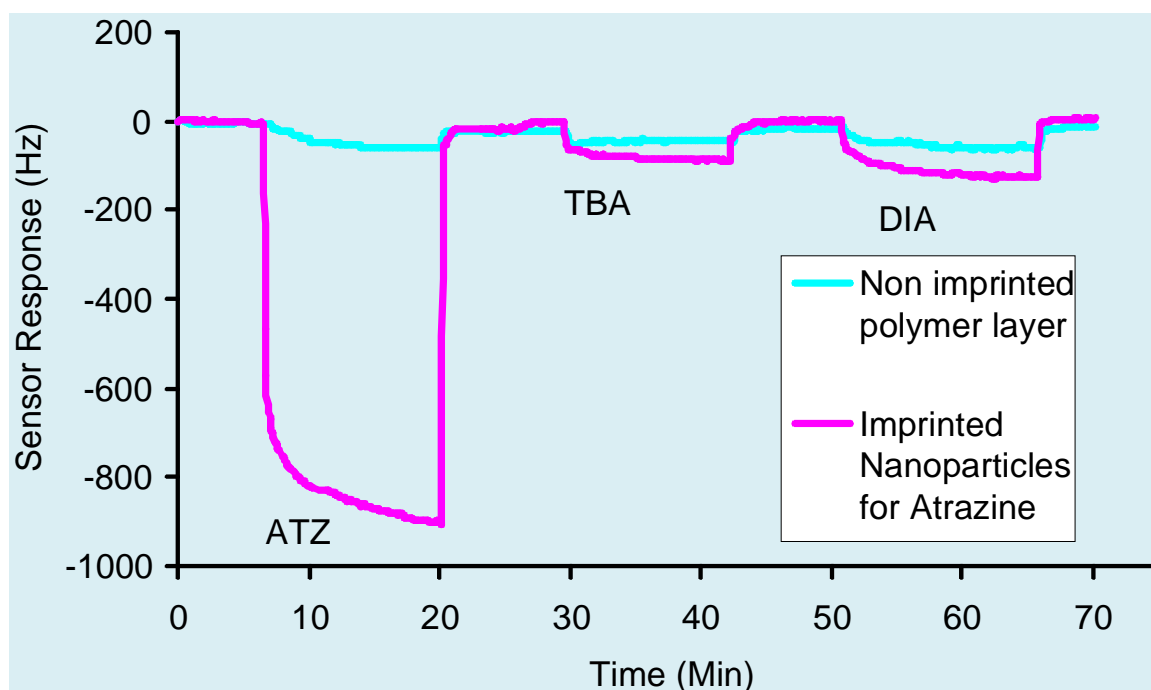


Figure 62: Selectivity measurement for Atrazine at 28°C with flow rate of 1.5mL/min for (7mg/L) Atrazine by imprinted nanoparticles of size 45-81nm precipitated from MIP-ME42 [imprinted copolymer of 35 % methacrylic acid and 7% methacrylate crosslinked with 58% Ethylene glycol dimethacrylate by weight imprinted with 10% of Atrazine as template] against 7mg/L of Terbutylazine

As described earlier, in previous experiments two patterns of sensor responses were observed among 6 analytes being used for cross selectivity analysis (see **fig. 62-63**). Terbutylazine (TBA) and Desisopropylazine (DIA) were analyzed for cross selectivity tests. Where, TBA presented bulky molecules of s-triazine family and DIA among metabolites of Atrazine causing higher mass effect than the rest. The frequency shifts for both analytes were smaller than for Atrazine by roughly a factor of 9, proving the imprinted particles highly selective for Atrazine.

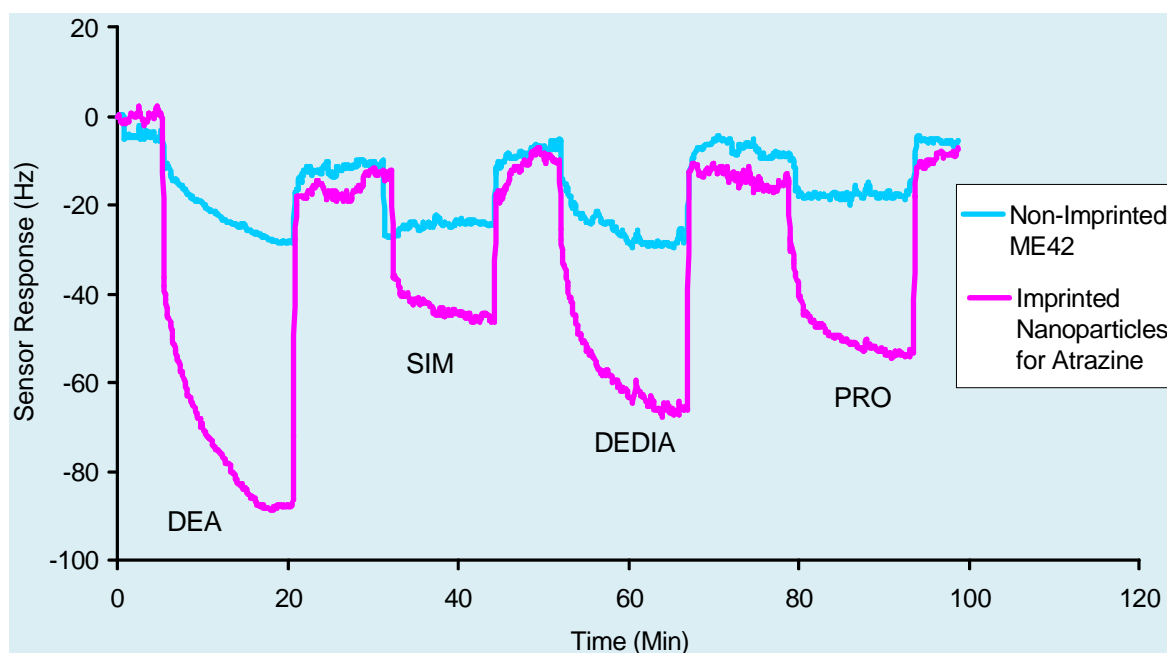


Figure 63: Selectivity measurement for Atrazine at 28°C with flow rate of 1.5mL/min for (7ug/l) Atrazine by imprinted nanoparticles of size 45-81nm precipitated from MIP-ME42 [imprinted copolymer of 35 % methacrylic acid and 7% methacrylate by weight crosslinked with 58 % Ethylene glycol dimethacrylate imprinted with 10% of Atrazine as template] against 7mg/L of Des-ethyl atrazine (DEA), Simazine (SIM), Des-ethyl- des isopropyl atrazine (DEDIA) and Propazine (PRO).

Fig.64 illustrates a comparison of sensor responses for relative selectivity patterns of imprinted nanoparticles with previously tested synthetic antibodies of ME-MIP42. It is observed that individual signals for Des-isopropyl atrazine (DIA) were higher in both cases comparative to Terbutylazine (TBA) by imprinted coatings for ATR. This can be attributed to similar basicity of DIA and imprint molecules of ATR. On the other hand, bulky molecules of Terbutylazine (TBA) as well as Propazine (PRO) and Simazine (SIM) are assumed to find least access to imprinted cavities of sensor coatings

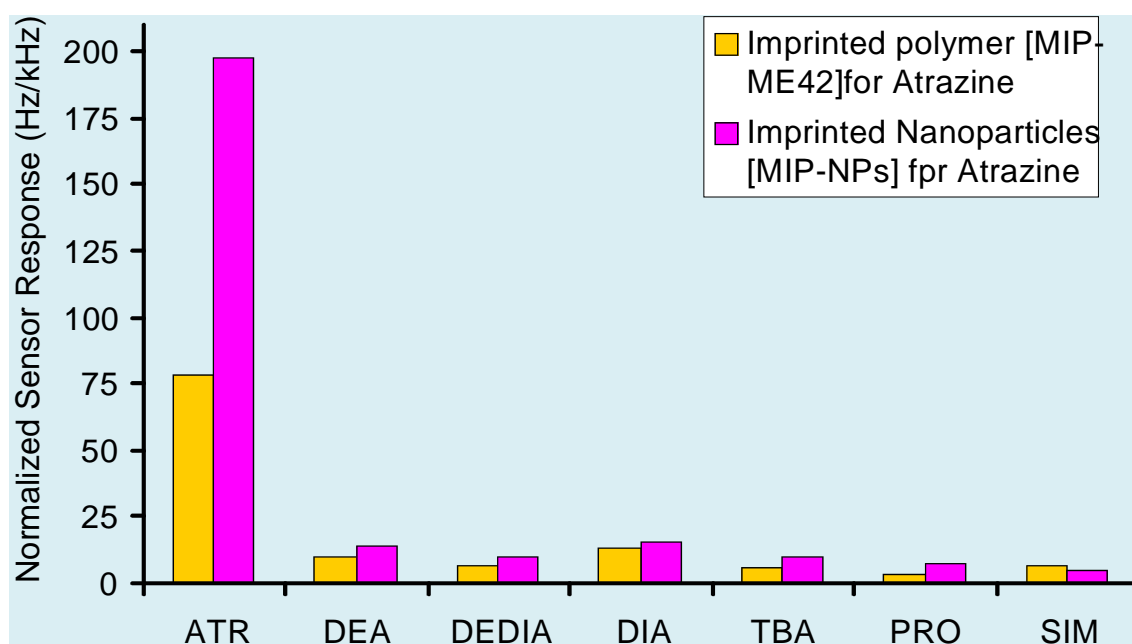


Figure 64: Mass sensitive sensor signals for selectivity of molecularly imprinted synthetic antibodies for Atrazine (ATR) against Des-ethyl atrazine (DIA), Des-ethyl-isopropyl atrazine (DEDIA), Des-isopropyl atrazine (DIA), Terbutylazine (TBA), Propazine (PRO) and Simazine (SIM).

4.11 Surface roughness of Imprinted NPs Layer

Coated layers of Nanoparticles were examined under Atomic force microscope for surface roughness and cracks after chemical analysis. As shown in **Fig. 65 & 66**, the layer was found homogeneous and was stable after sensor measurements. The height of the layer was also confirmed through frequency analyzer. No damage or mass loss of particles was observed during the repeated measurements.

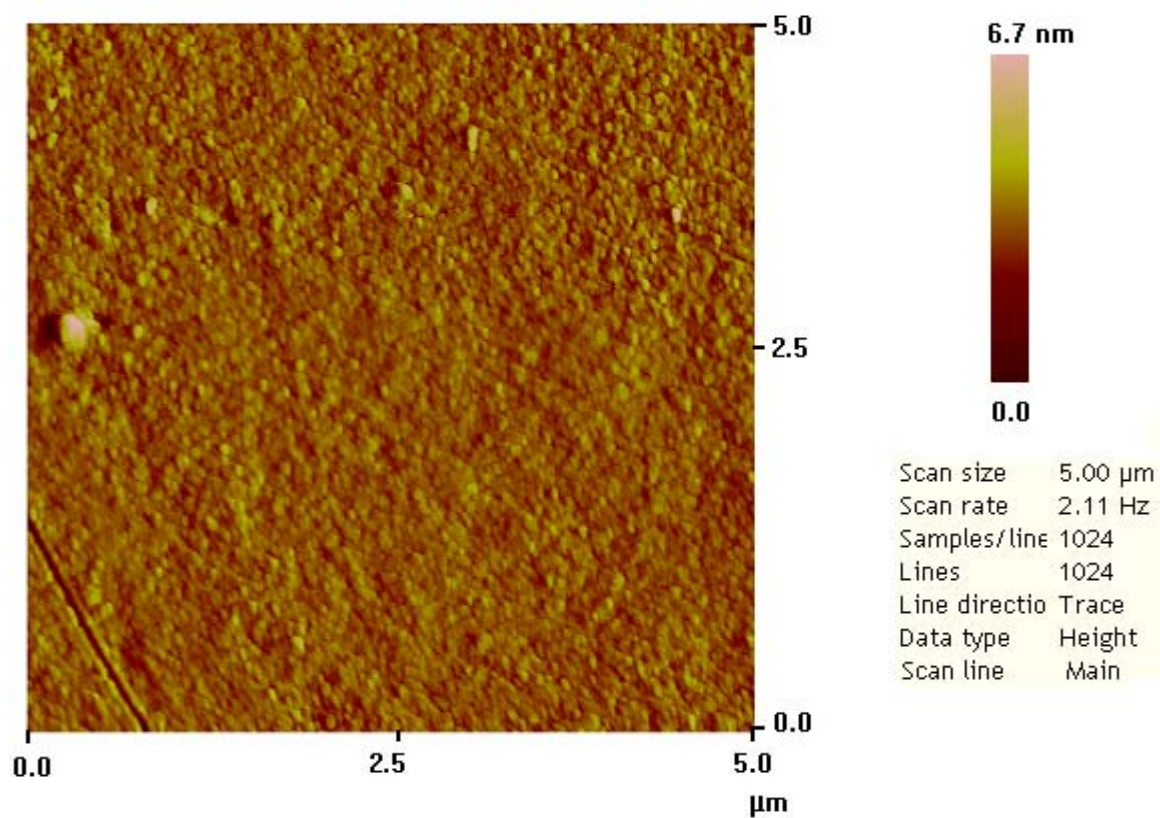


Figure 65: AFM image taken in contact mode showing surface of electrode coated with imprinted NPs used for sensor measurement.

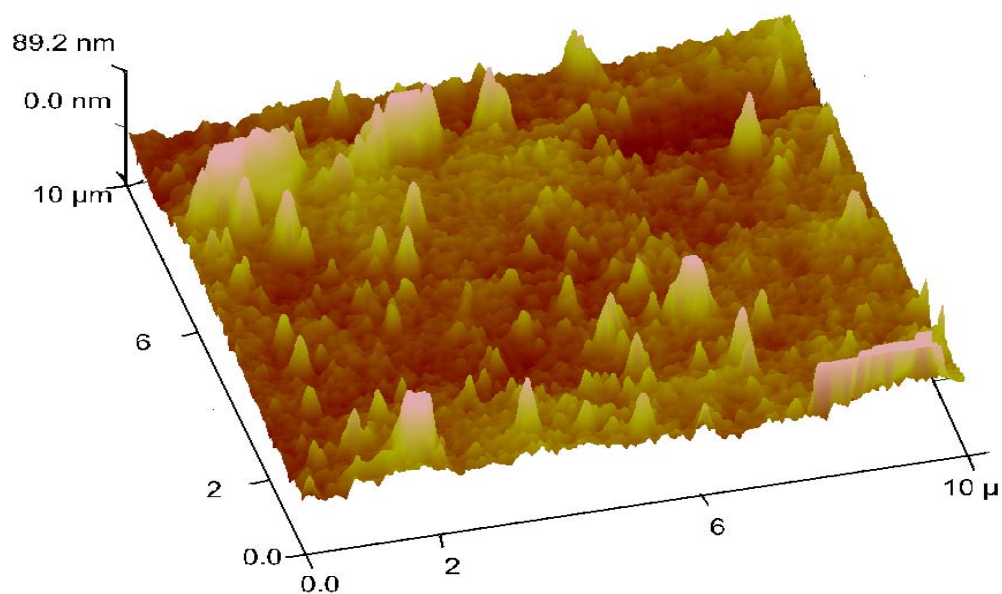


Figure 66 : A three dimensional view of the sensor layer of imprinted

Chapter 5

QCM BASED SENSOR WITH NATURAL ANTIBODY

Natural antibodies are commonly used in clinical diagnostics and research analysis for a wide variety of antigens³⁸. To determine the efficiency of the synthetic antibodies of Atrazine, the study of sensor response by the natural antibody is interesting. For this purpose natural antibody of Atrazine was tested for screening pesticide solutions using gold surface of QCM for transduction.

Natural antibody for Atrazine is commercially available and is used for routine analysis of also environmental samples in immunosensors³⁹⁻⁴⁰. Although natural antibody is very expensive but its application in developing analytical tools for pesticides detection has been significant for environmental protection. Natural antibody used in present work was extracted from egg yolk.

5.1 Piezo Acoustic Devices & Measurement Set-Up

As described in previous experiments, the quartz disc (10 MHz, AT-cut, 15.5 mm diameter) were coated with gold following the same procedure. All the measurements were performed without the reference electrode.

For coating the natural antibody over the electrode surface, the strategy was to inject it directly on bare electrodes within the measuring cell. The binding of the layer with gold electrode was monitored by observing frequency of electrodes before and after coating the layer.

5.2 Sensitivity Measurements

Immobilization of natural antibody on gold electrodes was performed within measuring cell through injection mode using a 200 μ L Gilson pipette. Initially, the cell was flushed twice with 200 μ L of water before continuing the measurement.

Frequency of non-imprinted electrodes was checked in liquid phase. After attaining equilibrium, water in the cell was replaced by fresh solution of natural antibody. To avoid bubbles on electrode surface, injection of liquid was made slowly while in halting measuring software. By exposing quartz surface with natural antibody a rapid frequency drop was observed due to increase of mass on the electrode, following Sauerbrey's equation. (See Fig 67)

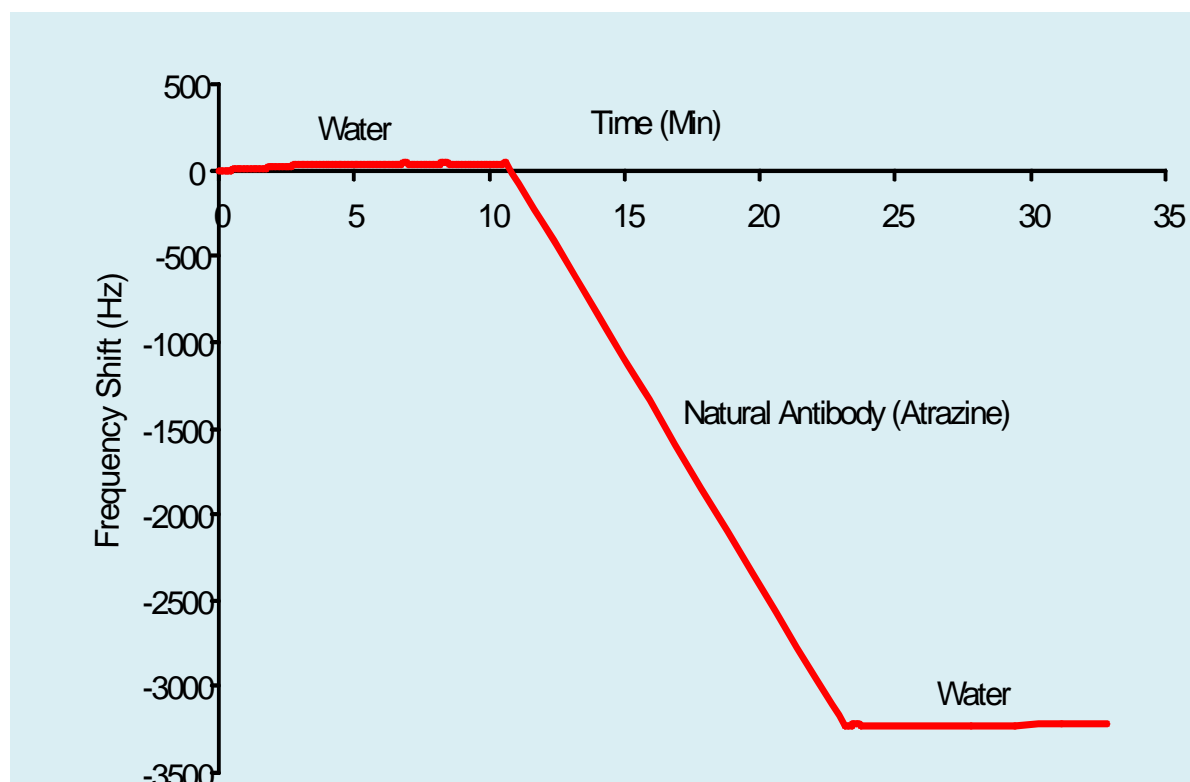


Figure 67: Immobilization of Natural Antibody (Atrazine) within measuring cell after attaining equilibrium in water pumped at 1.5mL/min by injecting and sucking back antibody solution with 200 μ L Gilson pipette, generating a layer of 128nm as illustrated by frequency shift of 3.2 kHz.

Natural antibody was expected to adhere with the gold surface due to high affinity of thiol groups to the gold. As illustrated in Fig. 63, the adsorption of natural antibody on the gold electrode resulted into a frequency shift of 3.2 KHz. The solution of natural antibody was sucked out within 13minutes and water was pumped into the measuring cell at a flow rate of 1.5 mL per min.

After attaining the equilibrium in water phase, the sample solutions of Atrazine with known concentrations were analyzed. Decrease in frequency of the measuring channel by 235 Hz was observed for 7ppm of Atrazine. Frequency drop was abrupt and then gradually became constant in nearly 10 min. Complete removal of analyte also took sometime and was not rapid as illustrated in **Fig. 68**.

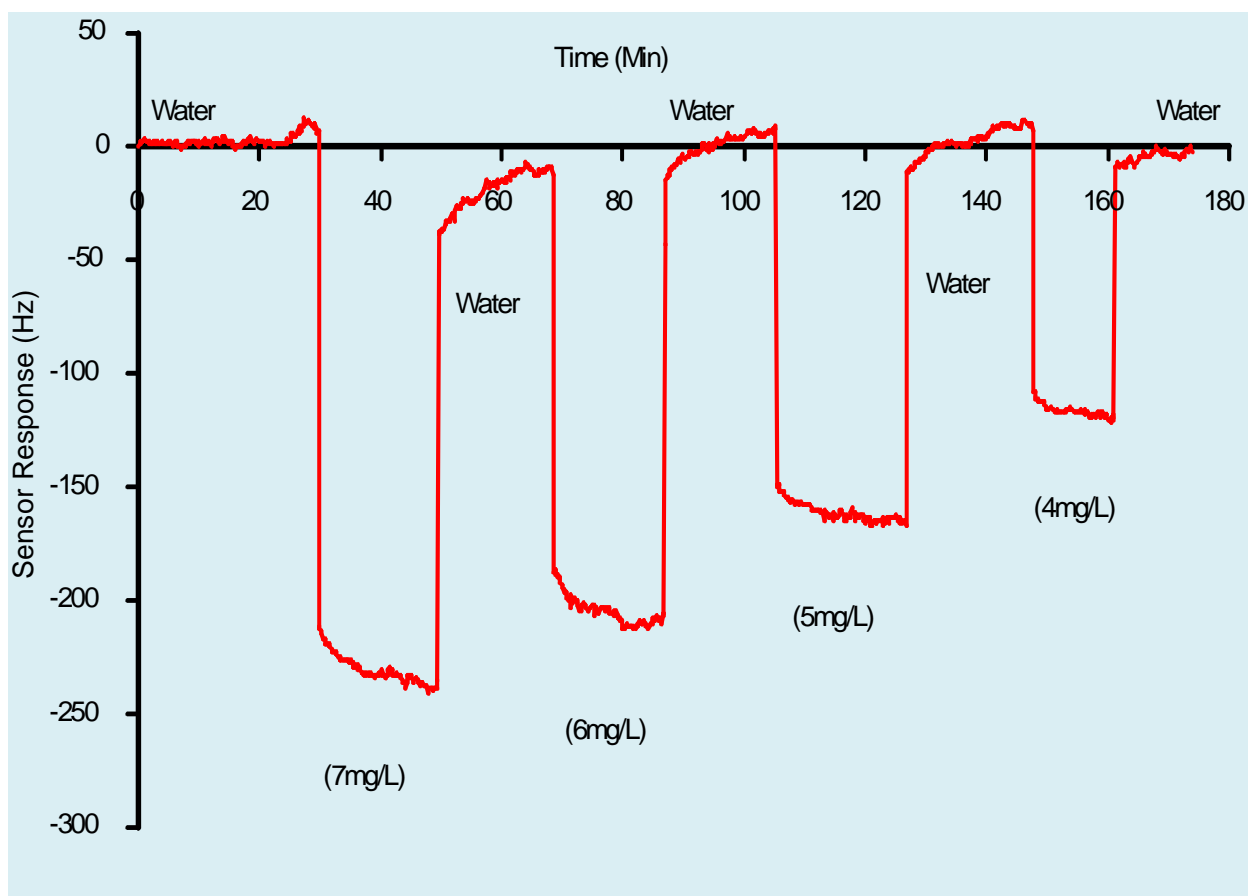


Figure 68: Sensor Response by natural antibody (Atrazine) having layer thickness of 128 nm at room temperature for concentrations starting from 7ppm down to 4ppm of Atrazine solution in water pumped at constant flow rate of 1.5 mL/min.

Furthermore, lower concentrations of Atrazine were analyzed for sensitivity to measure limit of detection. As illustrated in **Fig. 69**, sensor responded to 0.5ppm with a smallest shift of frequency of 12 Hz.

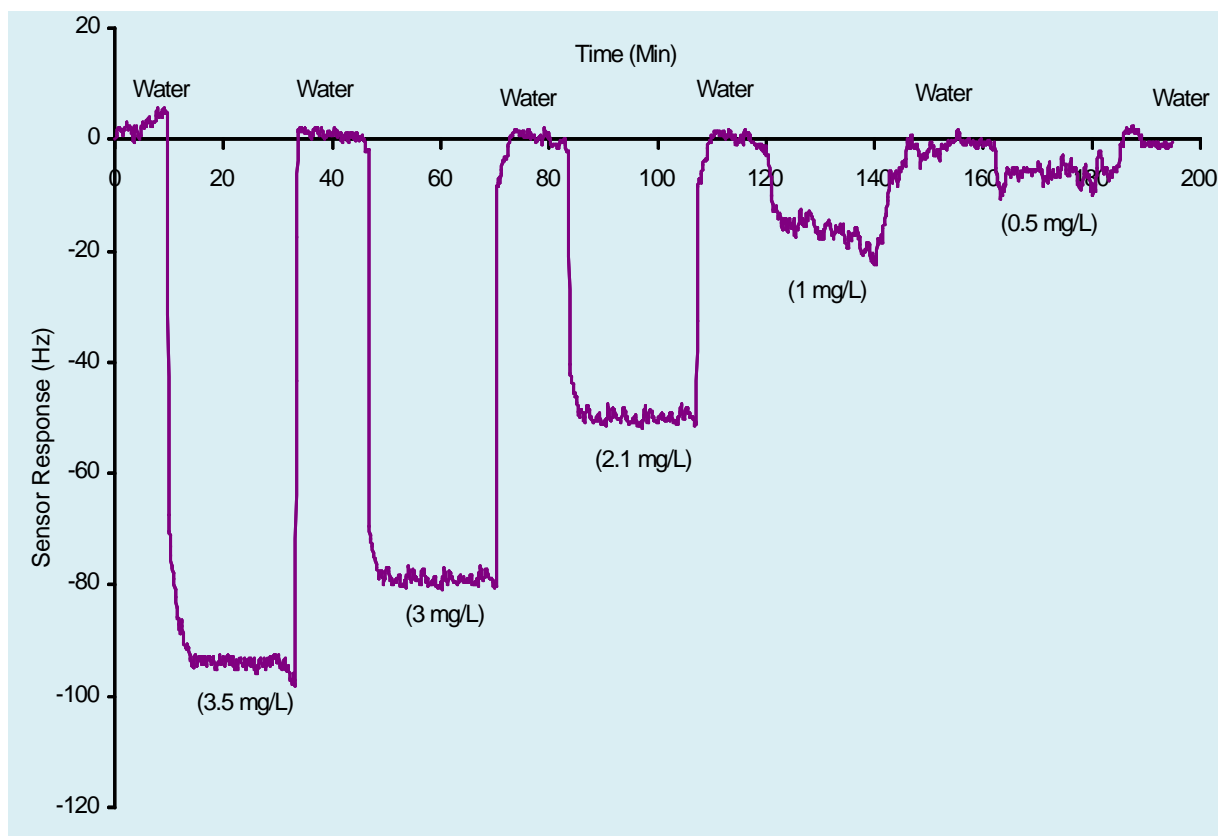


Figure 69: Sensitivity of Natural antibody at room temperature with a layer thickness of 128nm for Atrazine solutions with concentrations from 3.5ppm down to 0.5ppm reaching signal to noise ratio ≥ 3 .

In **Fig. 70**, respective frequency shift measured against different dilutions of Atrazine in water are plotted. It gives a typical sensor curve where signal rises linearly in the beginning with increase in concentration tends to be non linear. The highest signal was recorded for 7 mg/L of Atrazine solution with a frequency shift of 235 Hz while the limit of detection of Atrazine in water by natural antibody was 0.5 mg/L with signal to noise ratio ≥ 3 .

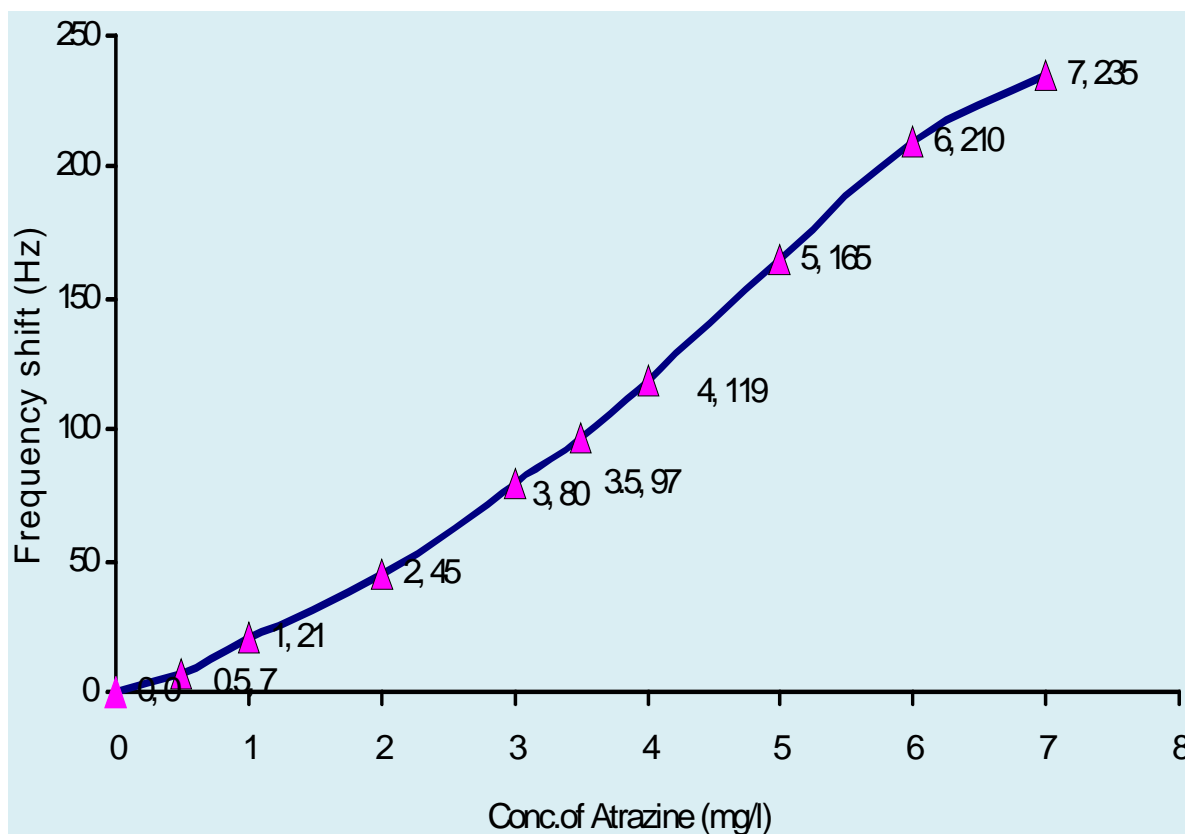


Figure 70: Sensitivity of natural antibody layer of 128 nm towards different concentration of Atrazine in water pumped at 1.5 mL/min, ranging from 0.5mg/L to 7mg/L at room temperature.

5.3 Selectivity Measurements

As given in **Fig. 71**, the cross sensitivities for metabolites of Atrazine e.g. des-ethyl atrazine, des-isopropyl atrazine and des-ethyl-des-isopropyl atrazine was observed to be negative. Furthermore, the selectivity of the natural antibody (atrazine) was tested for other structural analogues of Atrazine.

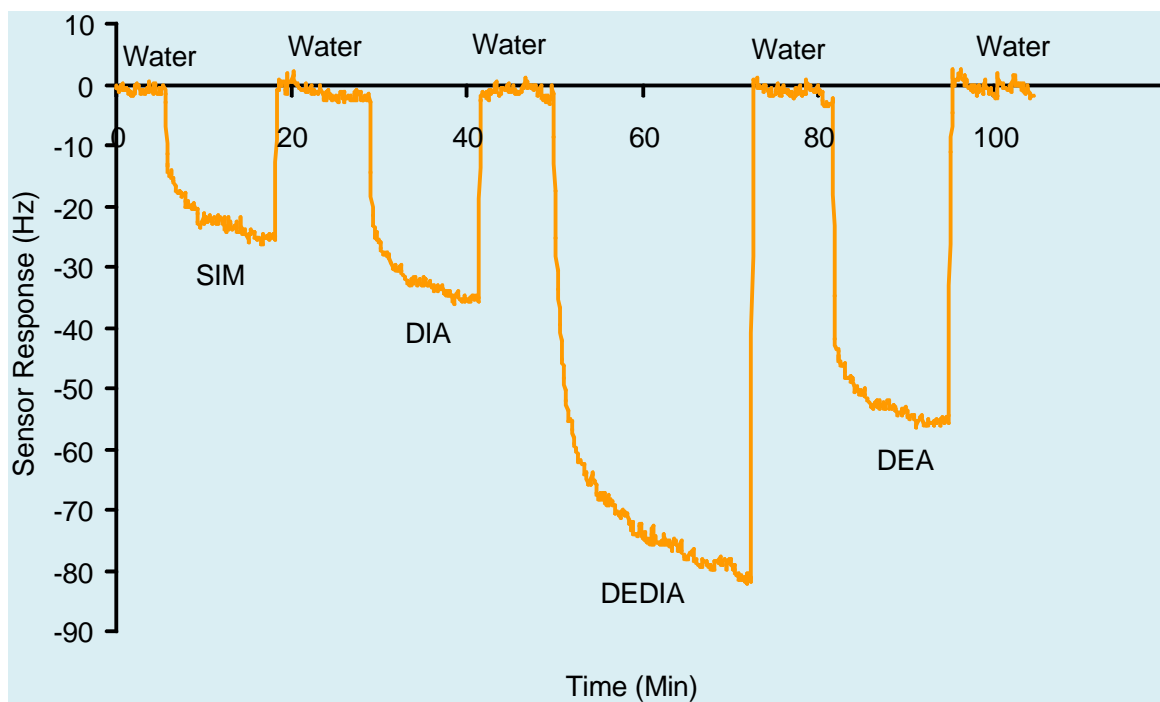


Figure 71: Cross sensitivity measurement curves by Natural antibody Atrazine layer (128nm) for Ter-buthylazine (TBA) 7mg/L, Propoxur (PROP) 7 mg/L, Propazine (PRO) 7 mg/L at room temperature in flow mode at the rate of 1.5 mL/min.

The sensor response of the natural antibody was recorded for bulky molecules like Terbutylazine, Propoxur and Propazine. **Fig. 72** shows chemical structure of Propoxur commonly used as insecticide. Though structurally different, its presence in contaminated ground water makes its important analyte for testing cross sensitivity for Atrazine.

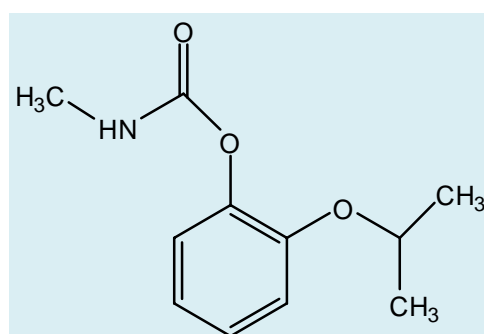


Figure 72: Chemical structure of Propoxur (Carbamate Insecticide)

Frequency shifts for cross sensitivity were observed close to that exhibited by imprinted synthetic antibodies for Atrazine (**Fig.73**). The drift in baseline of starting frequency was noticed with time which could be due to some loss of mass by repeated measurements with natural antibody.

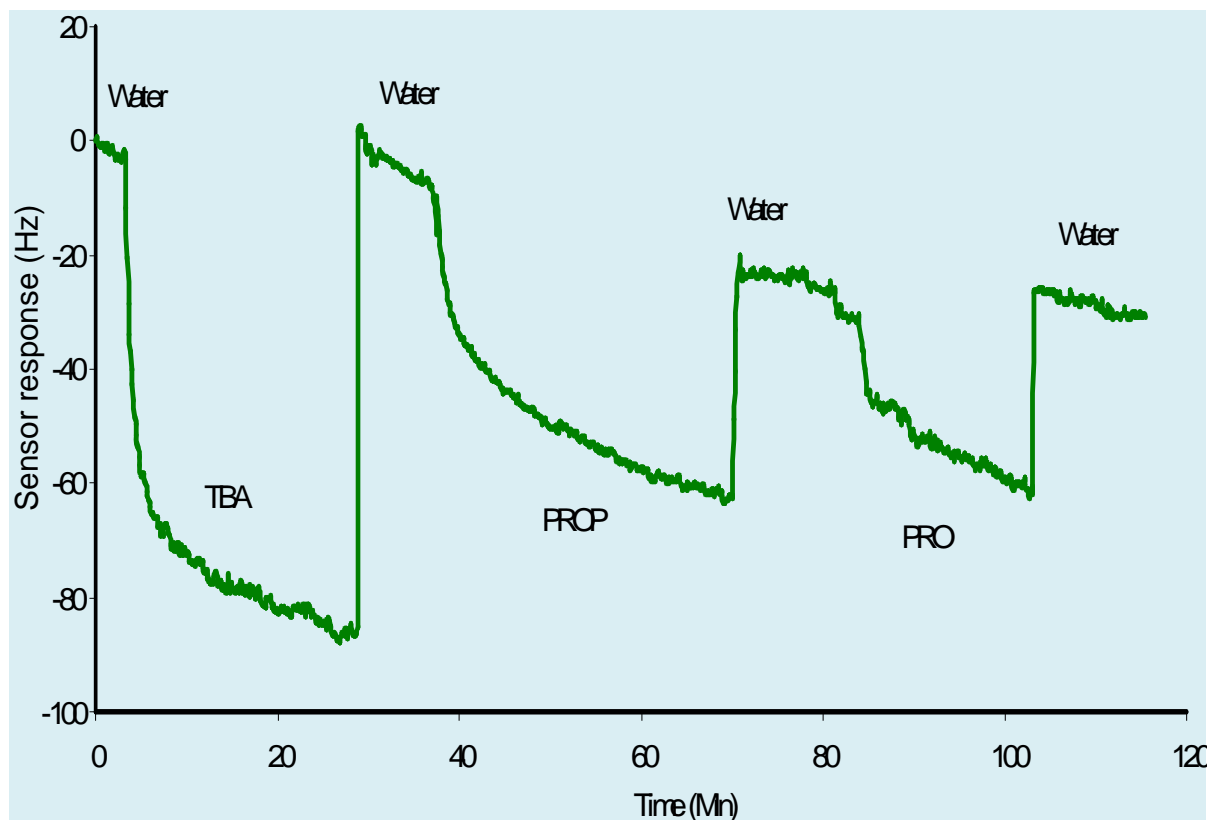


Figure 73: Cross sensitivity measurement curves by Natural antibody Atrazine layer (128 nm) for Terbuthylazine (TBA) 7 mg/L, Propoxur (PROP) 7mg/L, Propazine (PRO) 7 mg/L at room temperature in flow mode at the rate of 1.5 mL/min.

5.4 AFM Studies of Sensor Surface

The surface of quartz was studied under atomic force microscope after measurements to examine sensor coating of natural antibody by contact mode of atomic force microscope. The thickness of coated antibody was confirmed in dry phase by a scratch. (See Fig. 74).

As the frequency of gold electrode fluctuates in dry and liquid phase; actual thickness of the coated layer could be examined with AFM scanning.

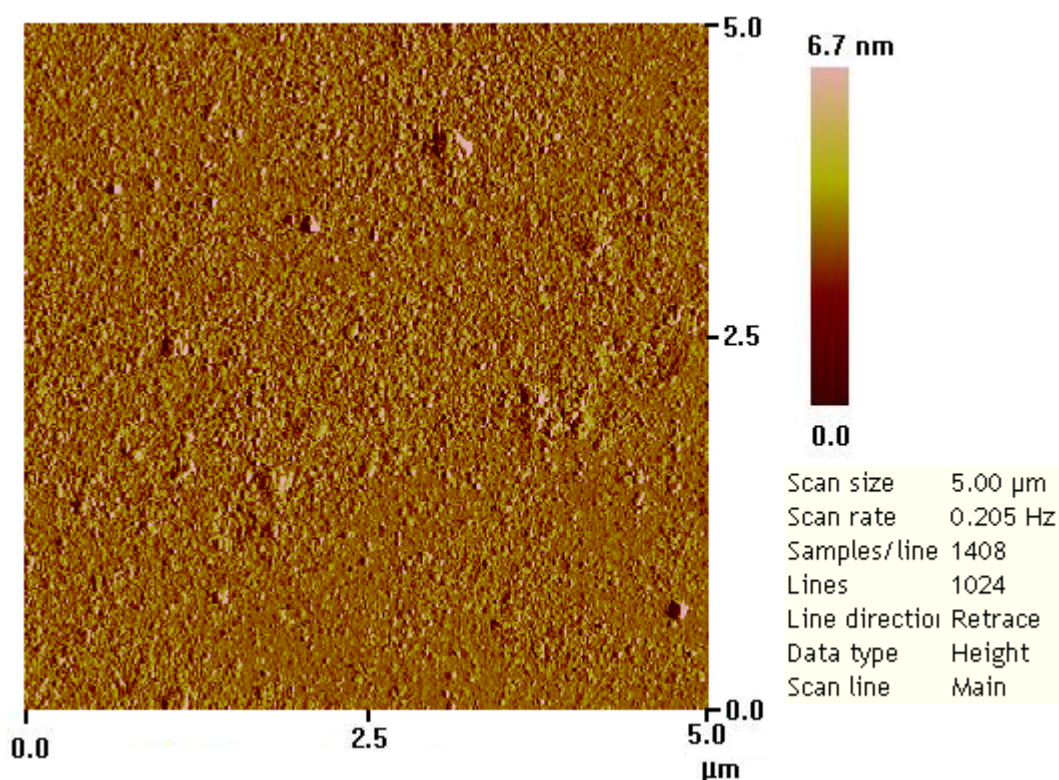


Figure 74: Surface scan in contact mode by AFM of sensor layer on gold electrode of QCM comprising natural antibody of Atrazine

A sharp cut was drawn on the surface of the layer with the help of a paper-cutter and analyzed under the microscope. The AFM image in **Fig.75** shows elevation profile of the scratch made in sensor layer. In the liquid phase the frequency of gold electrode before and after coating thin film varied by a shift of 3.2 kHz. As theoretically 1 kHz frequency shift is caused by a layer thickness of 40 nm.

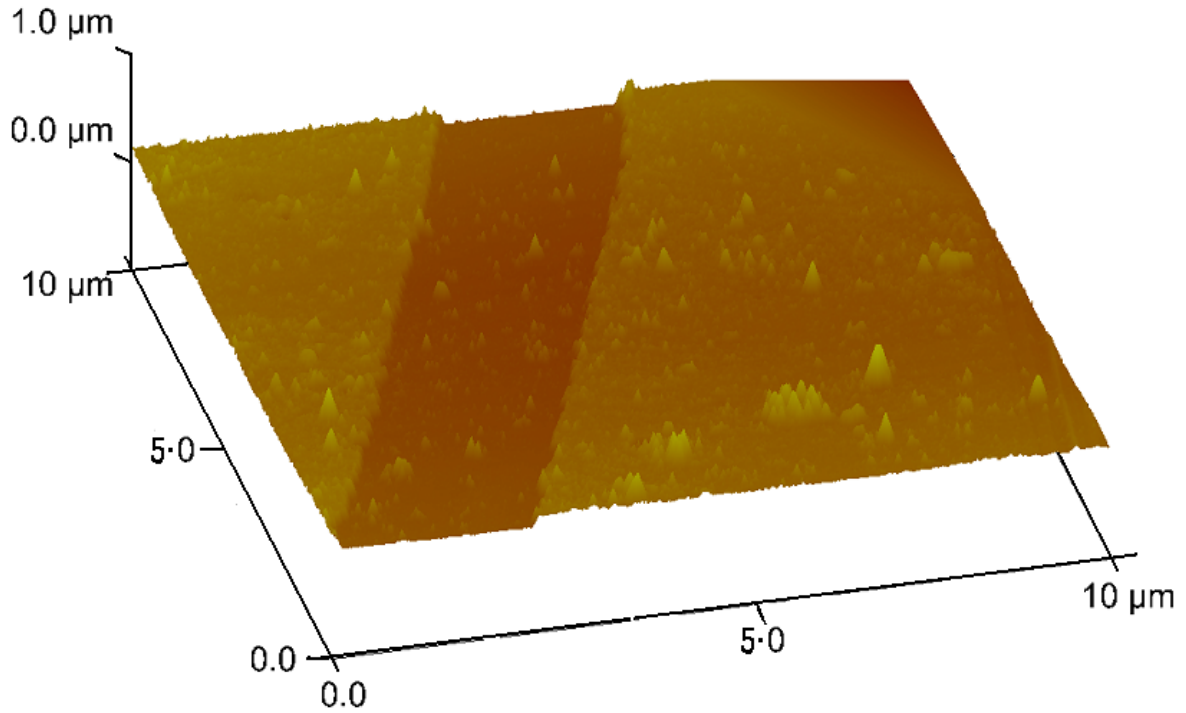


Figure 75: AFM image in contact mode scanning scratch in the sensor layer of natural antibody of Atrazine for investigating layer height

On this basis, the height of antibody layer was 128nm. From the scratch method, the height was nearly same i.e. ~117 nm for the used layer as illustrated in **Fig.76.**

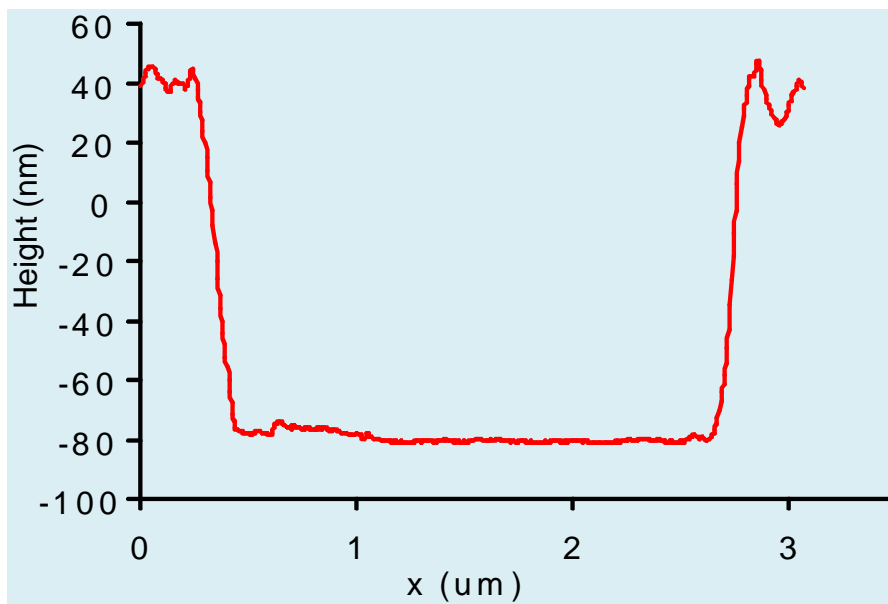


Figure 76: Cross section of thin film of natural antibody on gold electrode of QCM after sensor measurement to investigate mechanical loss of the layer.

CONCLUSIONS

QCM based chemical sensors comprising synthetic antibodies in form of imprinted layers and imprinted particles were successfully designed for detection of pesticides specifically for Atrazine and related structural analogues of Triazines family. Artificial antibodies showed excellent sensitivity for atrazine with more than two fold sensitivity as compared to that of natural antibody. Sensor responses by artificial and natural antibodies with varied thickness for different dilutions of Atrazine are presented in **Table 10**.

Atrazine Conc. in water (mg/L)	Imprinted NPs 5.2 kHz (Hz)	Imprinted ME42 4.4 kHz (Hz)	Imprinted M46 5.4 kHz (Hz)	Natural Antibody 3.2 kHz (Hz)
0.5	67	55	59	7
1.0	125	132	110	21
2.0	220	190	185	45
3.5	379	260	276	97
5.0	572	315	365	165
7.0	830	349	420	235

Table 10: Frequency shifts by synthetic and Antibodies for different concentrations of Atrazine (ATR) at varied thickness of sensor layers

As illustrated in **Fig. 77** synthesized sensor layers are compared to check performance and efficiency of synthetic antibodies with natural antibody for chemical sensitivity towards atrazine. The graph is plotted by normalizing the layer height as the sensitivity of thin films of chemical sensor varies with thickness. Imprinted nanoparticles extracted from polymer MIP-ME42 (comprising copolymer of methacrylic acid (35%) and methyl acrylate (7%) cross-linked with ethylene glycol

dimethacrylate (58 %) by weight & 10% Atrazine as template) demonstrated outstanding sensor responses among all sensitive layers. The maximum limit of detection for atrazine was 35 ppb by imprinted nanoparticles along with highest sensor response for 7 ppm of the analyte. Highest sensitivity offered by particles is attributed to their larger surface area as well as polarity of copolymer with optimized imprinted polymer network providing greater docking points for atrazine molecules. The sensor responses by synthetic layers were also fast attaining stability within 5-10 minute.

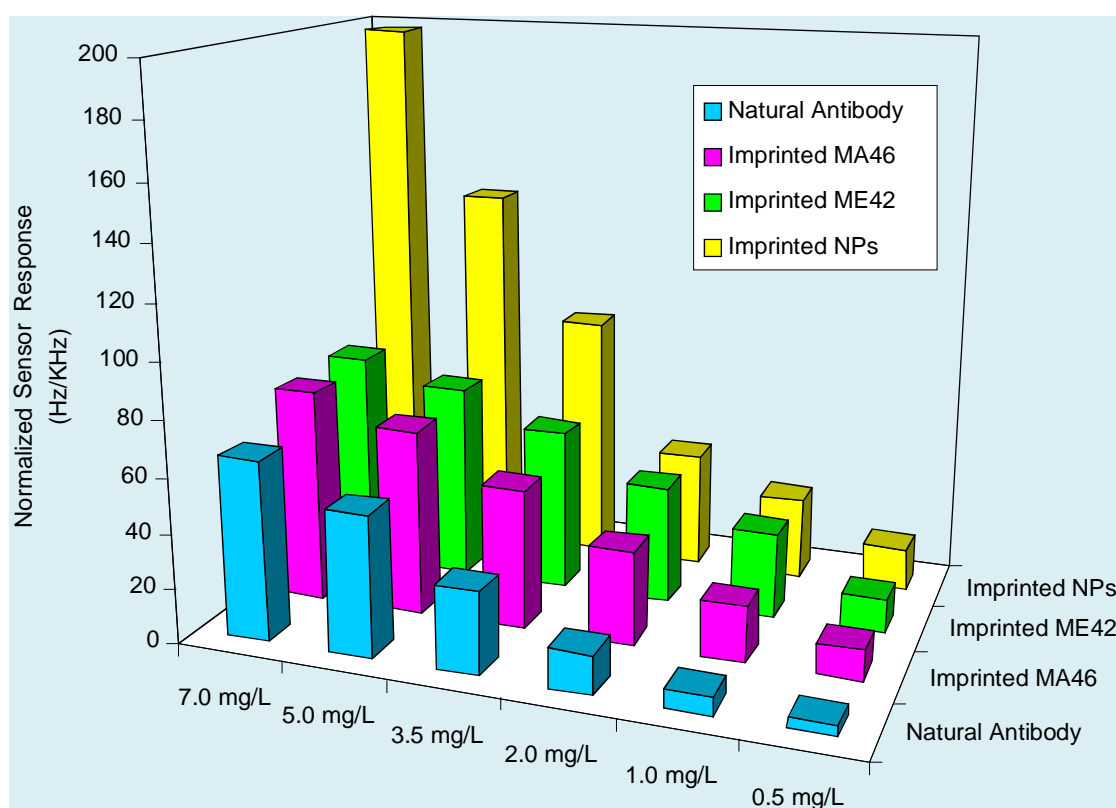


Figure 77: Normalized sensitivity signals of synthetic and natural antibodies for atrazine solutions in water ranging from 0.5 mg/L to 7mg/L at room temperature. Synthetic antibodies include Imprinted MA46 [methacrylic acid (46 %) crosslinked with (54 %) ethylene glycol dimethacrylate with 10% Atrazine], Imprinted ME42 [copolymer of methacrylic acid (35 %) and methylacrylate (7 %) crosslinked with ethylene glycol dimethacrylate 58 % by weight & 10% Atrazine], and Imprinted (NPs) nanoparticles (size: 65-85nm) extracted from MIP-ME42.

Sensor responses of synthetic and natural antibodies with varied thickness for selectivity of Atrazine against its metabolites and other structural analogues e.g. des-ethyl atrazine (DEA), des-ethyl-des-isopropyl atrazine (DEDIA), Des-isopropyl atrazine (DIA), Terbutylazine (TBA), Propazine (PRO), and Simazine (SIM) are depicted in **Table -11** .

Sensor Response (Hz) of				
Sensor Layer /Height	Imprinted NPs/ 5.2 kHz	Imprinted ME42/ 4.4 kHz	Imprinted MA46/ 5.4 kHz	Natural Antibody/ 3.2 kHz
Analytes (7 mg/L) at 28 °C				
Atrazine (ATR)	830	345	420	235
Des-ethyl atrazine (DEA)	59	42	181	55
Des-ethyl-des-isopropyl atrazine (DEDIA)	40	29	135	80
Des-isopropyl-atrazine (DIA)	66	59	143	35
Terbutylazine (TBA)	42	26	108	85
Propazine (PRO)	31	16	126	34
Simazine (SIM)	38	29	93	26

Table 11: Data of Frequency shifts for different chlorotriazines cross selectivity measurements by synthetic and natural antibody (Atrazine) of varied thickness.

Among all sensitive layers, MIP-ME42 [copolymer of methacrylic acid (35 %) and methylacrylate (7 %) crosslinked with ethylene glycol dimethacrylate 58% by weight imprinted with 10 % of Atrazine] and imprinted nanoparticles showed pronounced selectivity being 4-5 times and 14 to 50 times, respectively towards Atrazine.

As manifested in the **Fig. 78**, the selectivity of MIP-MA46 [methacrylic acid (46 %) crosslinked with (54 %) ethylene glycol dimethacrylate with 10% Atrazine] and natural antibody was relatively low being only 2 to 5 times & 3 to 9 times greater for Atrazine against other triazine analogues.

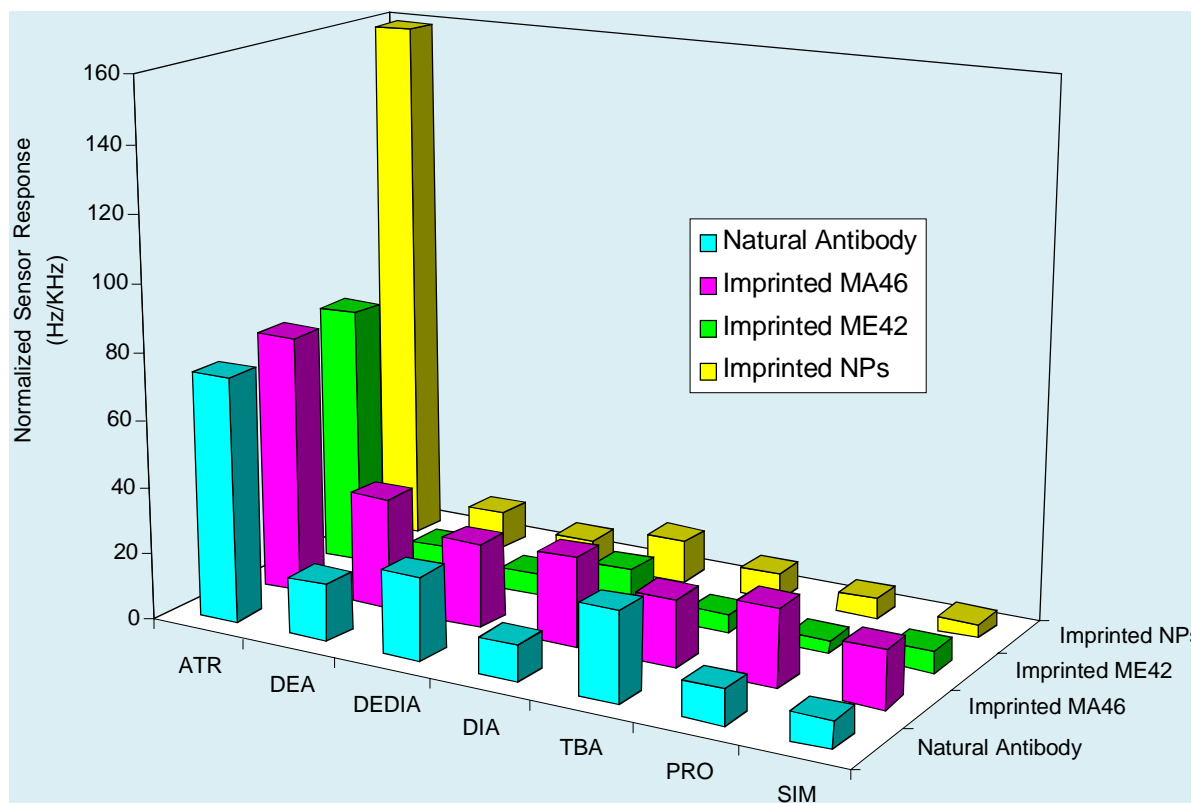


Figure 78: Selectivity of synthetic and natural antibodies for atrazine solutions in water for Atrazine (ATR) and its structural analogues des-ethyl atrazine (DEA), des-ethyl-des-isopropyl atrazine (DEDIA), Des-isopropyl atrazine (DIA), Terbutylazine (TBA), Propazine (PRO), and Simazine (SIM) at 28°C. Synthetic antibodies include Imprinted MA46 [methacrylic acid (46%) crosslinked with (54%) ethylene glycol dimethacrylate with 10% Atrazine] Imprinted ME42 [copolymer of methacrylic acid (35%) and methylacrylate (7%) crosslinked with ethylene glycol dimethacrylate 58% by weight], and (NPs) nanoparticles (size: 65-85nm) extracted from imprinted ME42.

The reproducibility and stability of synthetic antibody was consistence over a period of one year. Also, the expenditure of sensor coatings with synthetic antibodies was very less as compared to natural antibody. In conclusion, such synthetic antibodies can replace natural antibody for detection of a large number of contaminants in water, thereby making chemical sensor technology a versatile tool for environmental protection.

ABSTRACT

A large variety of insecticides and herbicides are applied in Europe and other parts of the world. These compounds differ strongly in respect to their functionality and polarity. Well known are persistent halogenated hydrocarbons (e.g. members of Chlorotrazine family) which are also found in soil causing serious risk to environment by contaminating underground water.

Instrumental analysis has proven to be an efficient strategy to detect all kinds of compounds which are generated by synthetic activities. In the course of time it gets more important to perform an “on-line” monitoring to reduce costs.

Self-organization of monomers around a template species leads to highly selective molecular imprints in the nanometer- and sub-nanometer range. The purpose of this dissertation is to apply this phenomenon for designing artificial receptors for online detection of Chlorotriazines. Initially, imprinted polymers containing both hydrophilic and hydrophobic side chains from acrylate-/methacrylate monomers were designed for Atrazine. Structural analogues of atrazine share the basic heterocyclic structure of triazine. Adjusting acid to cross linker ratio as well as introducing acrylate ester as copolymer resulted in optimal non-covalent interaction with the rather hydrophobic core of the Atrazine molecule and the amino groups. Deposited on QCM, molecularly imprinted copolymer of methacrylic acid and methacrylate crosslinked with ethylene glycol dimethacrylate led to fully reversible sensor responses with of 50 ppb for Atrazine. The polymer layer was also selective with 4-5 times higher sensor signal against its metabolites des-ethyl atrazine (DEA), des-isopropyl-atrazine (DIA) and des-ethyl-des-isopropyl-atrazine (DEDIA) and structural analogues e.g. Simazine (SIM), Propazine (PRO) and Terbutylazine (TBA).

Furthermore, transforming imprinted polymer copolymer of methacrylic acid and methylacrylate into nanoparticles enhanced capturing potential of the sensor

layers. Sensitivity for Atrazine was enhanced three fold as well as 14-50 times higher frequency shifts against its metabolites and structural analogues were recorded.

Finally, the sensor characteristics of synthetic receptors were compared with natural antibody of Atrazine. Sensitivity of imprinted nanoparticles towards Atrazine was 2.6 times higher than natural antibody of Atrazine. The selectivity of natural antibody was also comparatively low being only 3 to 9 times greater frequency shifts for Atrazine against other triazine analogues. The detection limit by synthetic receptors (MIP-NP) was excellent (35 ppb) compared to that of natural antibody (500 ppb) due to their larger surface area providing greater docking points for analyte molecules. In short, overall efficiency of the synthetic antibody was appreciable with high reproducibility and stability. Also, the cost of synthetic sensor layers was very low as compared to the natural antibody, suggesting the synthetic antibodies replaceable with natural ones as chemical sensor coatings for online monitoring of pesticides.

ABSTRACT

In Europa und anderen Teilen der Welt wird eine große Zahl an Insekten- und Pflanzenschutzmitteln verwendet. Diese unterscheiden sich bezüglich ihrer Funktionalität und Polarität sehr stark voneinander. Gut bekannt sind langlebige halogenierte Kohlenwasserstoffe (z.B.: Gruppe der Chlorotriazine), die auch im Erdboden gefunden werden und durch die Kontamination des Grundwassers ein ernst zu nehmendes Umweltrisiko darstellen.

Die Instrumentelle Analytik hat sich als eine sehr effiziente Strategie erwiesen, alle Arten von synthetisch hergestellten Schädlingsbekämpfungsmitteln zu detektieren. Da die Zeit einen immer beträchtlicher werdenden Kostenfaktor darstellt, wird die Strategie der „On- Line- Überwachung“ zur Kostenreduktion immer wichtiger.

Die Selbstorganisation von Monomeren um ein Templatgerüst führt zu hoch selektiven molekularen Prägungen im Nanometer- und Subnanometer Bereich. Ziel dieser Dissertation ist die Anwendung dieses Phänomens zur Herstellung von künstlichen Rezeptoren, um mit ihnen Chlorotriazine online zu detektieren. Im ersten Schritt werden geprägte Polymere hergestellt, die aus hydrophilen und hydrophoben Seitenketten von Acrylat / Methacrylat Monomeren bestehen, um mit ihnen Atrazin zu detektieren. Strukturanaloga des Atrazin beinhalten die heterozyklische Struktur von Triazin. Um optimale nichtkovalente Interaktionen zwischen der eher hydrophoben Leitstruktur des Atrazins und den Aminogruppen zu erhalten, wird sowohl das Monomerverhältnis zwischen Säure und Quervernetzer gerändert, als auch ein geeigneter Acrylatester als Kopolymer zugesetzt. Das auf einen Quarzsensor aufgebrachtes Copolymer, bestehend aus Methacrylsäure und Ethylenglykoldimethacrylat, führt zu einer vollständig reversiblen Atrazin-

Sensorantwort mit 50 ppb als Detektionslimit. Die große Selektivität dieses Sensors zeigte sich durch ein 4-5 fach so großes Sensorsignal von Atrazin sowohl gegenüber dessen Metaboliten, Des- Ethyl- Atrazin (DEA), Des- Isopropyl- Atrazin (DIA), und Des- Ethyl- Des- Isopropyl- Atrazin (DEDIA), als auch gegenüber Strukturanaloga z. B. Simazin (SIM), Propazin (PRO), und Terbutylazin (TBA).

Darüber hinaus wird das Sättigungsverhalten der Sensorschicht bestehend aus geprägtem Copolymer durch den Übergang zu Nanopartikeln beträchtlich erhöht, was sowohl eine 3 mal größeren Sensitivität zu Atrazin, als auch in einer 14-50 fach höheren Frequenzänderungen gegenüber dessen Metaboliten und Strukturanaloga bedingt.

Schließlich wurde das Sensorverhalten der künstlichen Rezeptoren mit den natürlichen Antikörpern für Atrazin verglichen. Die Empfindlichkeit der künstlichen Atrazin- Rezeptoren waren 2,6 fach höher, als deren natürliche Antikörper. Die Kreuzempfindlichkeit für natürliche Atrazin- Antikörper fiel mit dem 3 bis 9 fach höheren Atrazin- Signal vergleichsweise niedrig aus. Das Detektionslimit für synthetisch hergestellte Rezeptoren war mit 35 ppb dem Detektionslimit für natürliche Antikörper 500 ppb weit überlegen, da aufgrund der größeren Oberfläche mehr Interaktionsstellen für das Analytmolekül angeboten werden. Kurz gesagt, die Reproduzierbarkeit und Stabilität der künstlichen Antikörper war ausgezeichnet. Als weiteren Aspekt sind die Kosten für synthetisch hergestellte Sensorschichten im Vergleich zu natürlichen Antikörper sehr gering, was man bedenken soll, wenn man synthetische Antikörper oder natürliche Antikörper zur "online" Überwachung einsetzt.

LIST OF FIGURES

Figure 1: Classification of Pesticides	1
Figure 2: Chemical Structures of Chlorotriazine Herbicides; Atrazine (ATR), b. Simazine (SIM), c. Propazine (PRO). d.Terbuthylazine (TBA), e. Des-ethyl-isopropyl atrazine (DEDIA), f. Des-iso propyl atrazine (DIA), g. Des-ethyl atrazine	1
Figure 3: The metabolic pathways for Atrazine (ATR) in sorghum through N-dealkylation, hydrolytic dehalogenation, or nucleophilic displacement. Solid lines present major pathways and dashed lines show minor pathways of formation of Metabolites like des-ethyl atrazine (DEA), des-isopropyl atrazine (DIA) and des-ethyl des-isopropyl atrazine (DEDIA).....	1
Figure 4: Scheme illustrates pathway of pesticides during the course of time from field to underground water.	1
Figure 5: Schematic set up for Sensor Measurements	1
Figure 6: Generation of electric potential in QCM	1
Figure 7: Schematic illustration of the MIP preparation for Sensor Layer on Gold electrode of QCM.	1
Figure 8: Schematic sketch of ATR	1
Figure 9: Working principle of AFM.....	1
Figure 10: Screen image of AFM scan with “Nanoscale” software while probing imprinted nanoparticles film in contact mode	29
Figure 11: Photographs of silk-screen sieves showing dual-electrode structure printed for coating front and back sides of electrodes on QCM.....	1

Figure 12: Network Analyzer generating damping and phase spectra for gold electrode of QCM.	1
Figure 13: Chemical Sensor set up in running mode.	1
Figure 14: Chemical structures of reagents used for polymer synthesis.....	1
Figure 15: Graphic presentation of increase in frequency of electrodes due to loss in layer height (shown in percent) due to different solvents applied to remove (10%) Atrazine used as template. Imprinted and non imprinted layers each of 12 kHz composed of copolymer [35% of methylacrylic acid & 7% of methylacrylate cross-linked with 58% ethylene glycol dimethacrylate by weight].	1
Figure 16: Damping spectra of QCM electrode taken at 50 kHz span, before and after washing with methanol, coated with MIP-ME42 [35% of methylacrylic acid & 7% of methylacrylate cross-linked with 58% ethylene glycol dimethacrylate by weight and 10% Atrazine as template]. Difference in the resonance frequencies was 2.68 kHz (a). Image of spectra by network analyzer (b). Graphic presentation.....	1
Figure 17: Damping spectra of QCM electrode taken at 50 kHz span before and after washing with methanol coated with non imprinted polymer ME42 [35% of methylacrylic acid & 7% of methylacrylate cross-linked with 58% ethylene glycol dimethacrylate by weight] layer with Methanol. Difference in the resonance frequencies was 343 Hz. (a) Image of spectra by network analyzer, (b). Graphic presentation.....	1
Figure 18: ATR-IR Spectra of copolymer [methacrylic acid (35%) & methylacrylate (7 %) cross-linked with ethylene glycol dimethacrylate (58%) by weight] to analyze removal of Atrazine (10 %) as template. Two absorption bands for –NH (at 3270 cm ⁻¹) amino group of Atrazine and or the aliphatic –CH (at 3000cm ⁻¹) of methacrylic acid are observed. After washing with methanol, imprinted polymer peak for amino group disappeared indicating removal of Atrazine.....	1

Figure 19: Sensor response of imprinted polymer MA30 [methacrylic acid 30% with 70% ethylene glycol dimetacrylate by weight crosslinked with 10% Atrazine as template] & Non-imprinted polymer MA30 at 28°C with flow rate of 1.5mL/min. The respective layer heights for the imprinted and non-imprinted layers are 480 nm and 375nm. 1

Figure 20: Difference of frequency shift from sensitivity responses of imprinted polymer MIP-MA30 [methacrylic acid 30% crosslinked with 70% ethylene glycol dimethacrylate by weight and 10% Atrazine as template] and non imprinted layer MA30 with thickness of 480 nm and 375 nm, respectively. The analysis was carried out at 28°C for different concentrations of Atrazine ranging from 0.35mg/L to 5 mg/L in water at flow rate of 1.5 mL/min..... 1

Figure 21: Sensitivity of imprinted polymer MA30 [methacrylic acid 30% crosslinked with 70% ethylene glycol dimethacrylate by weight and 8.5 % Propazine as template] after washing out template with Acetic acid & Methanol mixture (1:4), at 28°C with a layer height of 210 nm and 217nm of imprinted and non imprinted layers, respectively. Propazine solution (8.6ppm & 4.33ppm) was pumped at a flow rate of 1.5 mL/min. 1

Figure 22: Sensitivity of imprinted polymer MA30 [methacrylic acid 30% by mass crosslinked by 70% ethylene glycol by weight and 8.5 % Propazine as template with addition of 100uL toluene] at 28°C. The layer thickness of imprinted and reference channel was 220 nm and 212 nm, respectively. 1

Figure 23: Washing of QCM by water at 28 °C with flow rate 0.5 mL/min coated with imprinted layer of polyurethane [197 mg Bisphenol A, 100 mg of 4,4methylene diphenyldiisocyanate and Pholoroglucinol 22 mg with propazine as template 9mg]. The layer thickness of imprinted and non-imprinted channel before washing was 5.6 kHz and 5.5 kHz, respectively. 1

Figure 24: Frequency shift measured at 28°C for Propazine by imprinted Poly Vinyl Pyrrolidone [vinylpyrrolidone 95 mg crosslinked with Bis acrylamide 5mg and 8.5 mg Propazine as template] with layer height of 180 nm at flow rate of 0.5 mL/min. ... 1

Figure 25: Effect of amount of methacrylic acid crosslinked by ethylene glycol dimethacrylate and imprinted with 10% by weight of Atrazine as template on sensor response for 7mg/L of Atrazine at 28 °C. 1

Figure 26: Sensor response of MIP-MA46 [methacrylic acid 46% crosslinked with 54% ethylene glycol dimethacrylate imprinted by 10% of Atrazine] for different concentrations of Atrazine at 28°C at flow rate of 1.5mL/min. Thickness of the imprinted and non-imprinted layers was 250 and 248nm, respectively. 52

Figure 27: Sensor responses of MIP-MA46 [methacrylic acid 46% by weight crosslinked with 54% Ethylene glycol dimethacrylate] imprinted with 9% Propazine (PRO) for concentrations ranging from 0.35mg/L to 7 mg/L at 28°C. The heights of the imprinted and non-imprinted layers are 230 and 248 nm, respectively. 1

Figure 28: Sensor responses of MIP-MA46 [methacrylic acid 46% by weight crosslinked with 54% Ethylene glycol dimethacrylate] imprinted with 10 % des-ethyl atrazine (DEA) for concentrations ranging from 0.35 mg/L to 7 mg/L at 28°C. The heights of the imprinted and non-imprinted layers are 250 and 220 nm, respectively. 1

Figure 29: Sensor responses of MIP-MA46 [methacrylic acid 46% by weight crosslinked with 54% Ethylene glycol dimethacrylate] imprinted with 8.2 % ter-butylazine (TBA) for concentrations ranging from 0.35 mg/L to 7 mg/L at 28°C. The heights of the imprinted and non-imprinted layers are 225 and 215nm, respectively. . 1

Figure 30: Selectivity of MIP-MA30 [methacrylic acid 30 % by mass crosslinked with 70 % Ethylene glycol dimethacrylate] imprinted with 10 % Atrazine (ATR) tested for, 7 ppm of Atrazine (ATR), Des-ethyl atrazine (DEA), Des-ethyl-Des-isopropyl atrazine (DEDIA), Des-isopropyl atrazine (DIA), Simazine (SIM), Terbutylazine (TBA) and Propazine (PRO) was tested. Thickness of the imprinted and non-imprinted layers was 220 and 235 nm, respectively. 1

Figure 31: Cross-Selectivity responses of MIPs-MA46 [methacrylic acid 46% crosslinked with 54% ethylene glycol dimethacrylate imprinted by 10% of Atrazine] layers at 28°C, imprinted with Des-isopropyl atrazine (DIA), Atrazine (ATR), Terbutylazine (TBA) and Propazine (PRO) respectively. Frequency shifts were normalized for layer thickness and subtracted from frequency shifts of reference electrode with non-imprinted polymer in each case..... 1

Figure 32: Selectivity analysis for Atrazine by MIP-ME35 [imprinted copolymer of 28 % methacrylic acid and 7% methacrylate by weight crosslinked with 58 % ethylene glycol dimethacrylate imprinted with 10% of Atrazine as template]. Sensor signals are shown for 7ppm of Atrazine (ATR), Des-ethyl atrazine (DEA), Des-ethyl-Des-isopropyl atrazine (DEDIA), Des-isopropyl atrazine (DIA), Simazine (SIM), Terbutylazine (TBA) and Propazine (PRO) by imprinted, non imprinted electrodes and the net shift in frequency by polymer coatings of 189 nm and 200 nm respectively..... 1

Figure 33: Sensor measurements at 28°C for cross selectivity by MIP-ME42 [imprinted copolymer of 35% methacrylic acid and 7% methacrylate crosslinked with 58% Ethylene glycol dimethacrylate by weight imprinted with 10% of Atrazine as template] with layer thickness of 185 nm for imprinted and 207nm for reference channel. 7ppm of Atrazine (ATR), Des-ethylatrazine (DEA) Des-ethyl-Des-isopropyl atrazine (DEDIA), Des-isopropyl atrazine (DIA), Simazine (SIM), Terbutylazine (TBA) and Propazine (PRO) was analyzed..... 1

Figure 34: Sensor response of MIP-ME42 [imprinted copolymer of 35 % methacrylic acid and 7% methacrylate crosslinked with 58% Ethylene glycol dimethacrylate by weight imprinted with 10% of Atrazine as template] and non imprinted polymer film for different concentrations of Atrazine in water at 28°C. The heights of the imprinted and non-imprinted layers are 185 and 205nm, respectively..... 1

Figure 35: Sensitivity of MIP-ME42 [35 % methacrylic acid &7% methacrylate crosslinked with 58 % Ethylene glycol dimethacrylate by weight imprinted with 10% of Atrazine as template] and non imprinted polymer film for different concentrations

of Atrazine in water at 28°C. The heights of the imprinted and non-imprinted layers are 185 and 205nm, respectively. 1

Figure 36: Sensor response of MIP-ME42 [imprinted copolymer of 35% methacrylic acid and 7% methacrylate by weight crosslinked with 58% Ethylene glycol dimethacrylate imprinted with 10% of Atrazine as template] and non imprinted polymer film for different concentrations of Atrazine in water at 28°C. The heights of the imprinted and non-imprinted layers are 185 and 205nm, respectively. 1

Figure 37: Effect of concentration of Atrazine on Frequency Shift measured at 28°C by MIP-ME42 layer of 185nm at flow rate of 1.5mL/min. 1

Figure 38: AFM Scan of 10µL scan size in contact mode surface study of imprinted polymer layer MIP-ME42 after sensor measurements [imprinted copolymer of 35% methacrylic acid and 7% methacrylate by weight crosslinked with 58% ethylene glycol dimethacrylate imprinted with 10% of Atrazine as template]..... 1

Figure 39: Effect of methanol on mass of synthetic imprinted and reference coatings for removal of Atrazine including MIPs-MA46 [methacrylic acid 46% crosslinked with 54% ethylene glycol dimethacrylate imprinted by 10% of Atrazine], MIPs-MA30 [methacrylic acid 30% crosslinked with 70% ethylene glycol dimethacrylate imprinted by 10% of Atrazine], MIP-ME33 [imprinted copolymer of 28% methacrylic acid and 5 % methacrylate crosslinked with 58% ethylene glycol dimethacrylate by weight imprinted with 10% of Atrazine as template] & MIP-ME42 [imprinted copolymer of 35% methacrylic acid and 7% methacrylate crosslinked with 58% Ethylene glycol dimethacrylate imprinted by weight with 10% of Atrazine as template]. 1

Figure 40: Cross selectivity comparison of MIPs-MA30 [methacrylic acid 30% crosslinked with 70% ethylene glycol dimethacrylate imprinted by 10% of Atrazine], MIPs-MA46 [methacrylic acid 46% crosslinked with 54% ethylene glycol dimethacrylate imprinted by weight and 10% of Atrazine as template], MIP-ME42 [imprinted copolymer of 35% methacrylic acid and 7 % methacrylate crosslinked

with 58% ethylene glycol dimethacrylate by weight imprinted with 10% of Atrazine as template], MIP-ME35 [imprinted copolymer of 28% methacrylic acid and 5% methacrylate crosslinked with 58 % ethylene glycol dimethacrylate by weight imprinted and 10% of Atrazine as template]..... 1

Figure 41: AFM scan (in contact mode with Silicon Nitride tip) of 1mg of molecularly imprinted nanoparticles precipitated from MIP-ME42 [imprinted copolymer of 35 % methacrylic acid and 7% methacrylate crosslinked with 58 % ethylene glycol dimethacrylate by weight imprinted with 10% of atrazine as template] in 10mL of Acetone..... 1

Figure 42: Three dimensional AFM image narrowly distributed imprinted nanoparticles (1mg) in 10 mL of acetone..... 1

Figure 43: AFM image (in contact mode with Silicon Nitride tip) of narrowly distributed nanoparticles with a concentration of 1 mg in 20 mL of Acetone. The maximum size of the particle was in range of 200-220 nm. 1

Figure 44: AFM image taken in contact mode of molecularly imprinted nanoparticles (1mg) diluted in 50 mL of Acetone..... 1

Figure 45: AFM image recorded (in contact mode with Silicon Nitride tip), of Imprinted nanoparticles (1mg) diluted in 200 mL of acetone with excellent distribution ranging from 55-81 nm in size..... 1

Figure 46: FTIR Spectra of washings of Nanoparticles in methanol for removal of Atrazine used as template and of methanol as reference. Peaks at 3394cm^{-1} and 1623cm^{-1} are observed for $-\text{NH}$ group and aromatic carbon of the triazine ring indicating presence of Atrazine in the solvent. 1

Figure 47: Screen image of damping spectra of QCM before and after coating nanoparticles..... 1

Figure 48: Damping spectra of QCM before and after coating imprinted nanoparticles recorded at frequency span of 50 kHz. Decrease in the resonance frequency was 5.219

kHz indicating mass load of 208 nm thick layers of nanoparticles extracted from MIP-ME42 [imprinted copolymer of 35 % methacrylic acid and 7% methacrylate crosslinked with 58 % Ethylene glycol dimethacrylate imprinted by weight with 10% of Atrazine as template]..... 1

Figure 49: AFM image showing deflection of Silicon Nitride tip while scanning in contact mode the Imprinted particles as coated on gold electrode of quartz substrate. 1

Figure 50: Image of running measurement in WINSENS XP for sensitivity response of imprinted nanoparticles layer (208nm) and reference polymer ME42 coatings (225 nm) as recorded by WINSENS XP software. The curve in second window presents the net sensor response. The size of imprinted nanoparticles used in layer was 45-81 nm. 1

Figure 51: Size of Imprinted Nanoparticles 45-81 nm as illustrated in AFM image (recorded in contact mode with Silicon Nitride tip), of particles precipitated from solution C (15 μ L of MIP-ME42 in 6 mL of Acetonitrile) 1

Figure 52: AFM image (in contact mode with Silicon Nitride tip), of imprinted Nanoparticles in 3-D with size range of 45-81 nm precipitated by solution B (15 μ L of MIP-ME42 in 6 mL of Acetonitrile)..... 1

Figure 53: Size of Imprinted Nanoparticles 90-140 nm as shown in AFM image (taken in contact mode with Silicon Nitride tip with Silicon Nitride tip) of particles precipitated from solution B (30 μ L of MIP-ME42 in 6 mL of Acetonitrile)..... 1

Figure 54: AFM image (in contact mode with Silicon Nitride tip), of imprinted Nanoparticles in 3-D with size range of 90-140 nm precipitated by solution B (30 μ L of MIP-ME42 in 6 mL of Acetonitrile)..... 1

Figure 55: Size of Imprinted Nanoparticles 100-170 nm as shown in AFM image (taken in contact mode with Silicon Nitride tip with Silicon Nitride tip) of particles precipitated from solution A (60 μ L of MIP-ME42 in 6 mL of Acetonitrile) 1

Figure 56 AFM image (recorded in contact mode with Silicon Nitride tip), of Imprinted Nanoparticles with size range of 100-170 nm precipitated from Solution A (60 μ L of MIP-ME42 in 6 mL of Acetonitrile).....	1
Figure 57: Sensor response recorded at 28°C with Nanoparticles of different sizes for 7mg/L of Atrazine.	1
Figure 58: Measurement of sensitivity of imprinted nanoparticles 28°C with flow rate of 1.5mL/min for different concentrations of Atrazine in water by imprinted nanoparticles of size 45-81nm precipitated from MIP-ME42 [imprinted copolymer of 35 % methacrylic acid and 7% methacrylate crosslinked with 58 % Ethylene glycol dimethacrylate by weight imprinted with 10% of Atrazine as template] with layer height of 168nm and reference layer of non-imprinted polymer ME42 with layer height of 180nm.....	1
Figure 59: Sensor response recorded at 28°C with flow rate of 1.5 mL/min for different concentrations aqueous solution of Atrazine by imprinted nanoparticles of size 45-81nm precipitated from MIP-ME42 [imprinted copolymer of 35% methacrylic acid and 7 % methacrylate by weight crosslinked with 58% Ethylene glycol dimethacrylate imprinted with 10% of Atrazine as template] with layer height of 208 nm and reference layer of non-imprinted polymer ME42 with layer height of 220 nm.	1
Figure 60: Sensitivity of imprinted nanoparticles 28°C for different concentrations of Atrazine in water, by imprinted nanoparticles of size 45-81nm precipitated from MIP-ME42 [imprinted copolymer of 35 % methacrylic acid and 7 % methacrylate by weight crosslinked with 58 % Ethylene glycol dimethacrylate imprinted with 10% of Atrazine as template] with layer height of 208 nm and reference layer of non-imprinted polymer ME42 with layer height of 220 nm.....	1
Figure 61: Comparison of normalized Frequency shifts recorded at 28°C by imprinted polymer MIP-ME42 [35 % methacrylic acid and 7% methacrylate crosslinked with 58 % ethylene glycol dimethacrylate by weight imprinted with 10%	

of Atrazine as template] and imprinted nanoparticles precipitated from MIP-ME42 for various concentrations of Atrazine at flow rate of 1.5mL/min 1

Figure 62: Selectivity measurement for Atrazine at 28°C with flow rate of 1.5mL/min for (7mg/L) Atrazine by imprinted nanoparticles of size 45-81nm precipitated from MIP-ME42 [imprinted copolymer of 35 % methacrylic acid and 7% methacrylate crosslinked with 58% Ethylene glycol dimethacrylate by weight imprinted with 10% of Atrazine as template] against 7mg/L of Terbutylazine (TBA) and Desisopropylazine (DIA)..... 1

Figure 63: Selectivity measurement for Atrazine at 28°C with flow rate of 1.5mL/min for (7ug/l) Atrazine by imprinted nanoparticles of size 45-81nm precipitated from MIP-ME42 [imprinted copolymer of 35 % methacrylic acid and 7% methacrylate by weight crosslinked with 58 % Ethylene glycol dimethacrylate imprinted with 10% of Atrazine as template] against 7mg/L of Des-ethyl atrazine (DEA), Simazine (SIM), Des-ethyl- des isopropyl atrazine (DEDIA) and Propazine (PRO)..... 1

Figure 64: Mass sensitive sensor signals for selectivity of molecularly imprinted synthetic antibodies for Atrazine (ATR) against Des-ethyl atrazine (DIA), Des-ethyl-isopropyl atrazine (DEDIA), Des-isopropyl atrazine (DIA), Terbutylazine (TBA), Propazine (PRO) and Simazine (SIM). 1

Figure 65: AFM image taken in contact mode showing surface of electrode coated with imprinted NPs used for sensor measurement. 1

Figure 66 : A three dimensional view of the sensor layer of imprinted NPs coated on gold electrode of QCM..... 1

Figure 67: Immobilization of Natural Antibody (Atrazine) within measuring cell after attaining equilibrium in water pumped at 1.5mL/min by injecting and sucking back antibody solution with 200 µL Gilson pipette , generating a layer of 128nm as illustrated by frequency shift of 3.2 KHz. 92

Figure 68: Sensor Response by natural antibody (Atrazine) having layer thickness of 128 nm at room temperature for concentrations starting from 7ppm down to 4ppm of Atrazine solution in water pumped at constant flow rate of 1.5 mL/min..... 1

Figure 69: Sensitivity of Natural antibody at room temperature with a layer thickness of 128nm for Atrazine solutions with concentrations from 3.5ppm down to 0.5ppm reaching signal to noise ratio ≥ 3 1

Figure 70: Sensitivity of natural antibody layer of 128 nm towards different concentration of Atrazine in water pumped at 1.5 mL/min, ranging from 0.5mg/L to 7mg/L at room temperature. 1

Figure 71: Cross sensitivity measurement curves by Natural antibody Atrazine layer (128nm) for Ter-buthylazine (TBA) 7mg/L, Propoxur (PROP) 7 mg/L, Propazine (PRO) 7 mg/L at room temperature in flow mode at the rate of 1.5 mL/min. 96

Figure 72: Chemical structure of Popoxur (Carbamate Insecticide)..... 1

Figure 73: Cross sensitivity measurement curves by Natural antibody Atrazine layer (128 nm) for Terbutylazine (TBA) 7 mg/L, Propoxur (PROP) 7mg/L, Propazine (PRO) 7 mg/L at room temperature in flow mode at the rate of 1.5 mL/min. 1

Figure 74: Surface scan in contact mode by AFM of sensor layer on gold electrode of QCM comprising natural antibody of Atrazine..... 1

Figure 75: AFM image in contact mode scanning scratch in the sensor layer of natural antibody of Atrazine for investigating layer height 1

Figure 76: Cross section of thin film of natural antibody on gold electrode of QCM after sensor measurement to investigate mechanical loss of the layer. 1

Figure 77: Normalized sensitivity signals of synthetic and natural antibodies for atrazine solutions in water ranging from 0.5 mg/L to 7mg/L at room temperature. Synthetic antibodies include Imprinted MA46 [methacrylic acid (46 %) crosslinked with (54 %) ethylene glycol dimethacrylate with 10% Atrazine], Imprinted ME42

[copolymer of methacrylic acid (35 %) and methylacrylate (7 %) crosslinked with ethylene glycol dimethacrylate 58 % by weight & 10% Atrazine], and Imprinted (NPs) nanoparticles (size: 65-85nm) extracted from MIP-ME42. 1

Figure 78: Selectivity of synthetic and natural antibodies for atrazine solutions in water for Atrazine (ATR) and its structural analogues des-ethyl atrazine (DEA), des-ethyl-des-isopropyl atrazine (DEDIA), Des-isopropyl atrazine (DIA), Terbutylazine (TBA), Propazine (PRO), and Simazine (SIM) at 28°C. Synthetic antibodies include Imprinted MA46 [methacrylic acid (46%) crosslinked with (54%) ethylene glycol dimethacrylate with 10% Atrazine] Imprinted ME42 [copolymer of methacrylic acid (35%) and methylacrylate (7%) crosslinked with ethylene glycol dimethacrylate 58% by weight], and (NPs) nanoparticles (size: 65-85nm) extracted from imprinted ME42. 1

REFERENCES

- ¹ C.D.S. Tom Lin, ed., *A World Compendium: The Pesticide Manual*, 11th ed., British Crop Protection Council, Farnham, Surrey, UK, (P.451), 1997
- ² M. Younes, H. Galal-Gorchev, *Food Chem. Toxicology*, 2000, 38, S87–S90.
- ³ Ali, Imran, Jain. C. K., *Current Science* 1998, 75,10, 1011-1014.
- ⁴ Wegorek, Wladyslaw Trojanowski, Henryk Dabrowski, Jerzy, *Materialy Sesji Naukowej Instytutu Ochrony Roslin (Poznan)* 1990, 30(1), 23-38.
- ⁵ Mladinic Marin, Perkovic Petra, Zeljezic Davor, *Toxicol. Letters*, 2009,189 ,2,130-7.
- ⁶ J. Doull, American Chemical Society, Washington DC, 1989.
- ⁷ http://ec.europa.eu/environment/water/water-drink/index_en.html
- ⁸ C. Cacho, E. Turiel , A. Martin Esteban, C. Perez Conde, C. Camara, *Anal Bioanal Chem.*, 2003, 376, 491–496.
- ⁹ Jenkins, Amanda L., Yin Ray, Jensen, Janet L., *Analyst* 2001, 126, 6, 798-802.
- ¹⁰ Martin Siemann, Lars I. Andersson, and Klaus Mosbach, *J. Agric. Food Chem.* 1996, 44, 141-145
- ¹¹ Dickert F.L., Lieberzeit P., Tortschanoff M., *Sensors and Actuators, B*: 2000, B65 1-3, 186-189.
- ¹² Dickert F.L., Bulst,W., E. Hayden Oliver, Ping Liu, AchATR, Paul, Sikorski, Renuatus; Wolff, Ulrich, *Proceedings of SPIE-The International Society for Optical Engineering* 2001, 4205(Advanced Environmental and Chemical Sensing Technology), 57-64.

-
- ¹³ Dickert F.L, Bulst, W. E., Hayden, Oliver, Ping Liu, AchATR, Paul Sikorski, Renatus, Wolff, Ulrich , *Advanced Environmental and Chemical Sensing Technology*, 2001, 4205, 57-64.
- ¹⁴ United States Patent 6890486, Penelle, Jacques (Hadley, MA, US).
- ¹⁵ http://www.pesticideinfo.org/Detail_Chemical.jsp?Rec_Id=PC35769
- ¹⁶ http://www.chbr.noaa.gov/easi/data/contaminant_detail.aspx?contamid=443
- ¹⁷ Homer M. LeBaron, Janis E. McFarland and Orvin C. Burnside, *The Triazine Herbicides 50 years Revolutionizing Agriculture*, 2008, 31-77.
- ¹⁸ Verschueren Karel, *Handbook of Environmental Data on Organic Chemicals*, 4th edition, John Wiley & Sons, Inc., New York, 1983.
- ¹⁹ Peter Gründler, *Chemical Sensors*, 2007.
- ²⁰ Dissertation Dr. A. Afzal
- ²¹ Franz L. Dickert, *Anal Bioanal Chem*, 2007, 389, 353-354
- ²² Pejic B, Lieberzeit PA, Dickert FL, *Anal and Bioanal Chemistry* 2007, 387, 237–247
- ²³ F. L. Dickert, K. Halikias, O. Hayden, L. Piu, R. Sikorski, *Sensors and Actuators B*, 2001, 76, 295.
- ²⁴ Frank Eichelbaum, Ralf Borngräber, Jens Schröder, Ralf Lucklum, Peter Hauptmann, *Review of Scientific Instruments*, 1999, 70, 5.
- ²⁵ Franz L. Dickert, Peter Lieberzeit, Oliver Hayden, *Analytical and Bioanalytical Chemistry* 2003, 377.

-
- ²⁶ GZ. Sauerbrey, Mitteilung aus dem ,Physikalischen Institut der TU Berlin A.E.U. 1964,18.
- ²⁷ Peter A. Lieberzeit, Sylwia Gazda-Miarecka, Konstantinos Halikias, Christian Schirk,, Jörg Kauling, Franz L. Dickert, *Sensors and Actuators B*, 2005,111–112.
- ²⁸ Mosbach, 1994, Andersson et al.,1995.
- ²⁹ F. L. Dickert, P. A. Lieberzeit, *Encyclopaedia of Analytical Chemistry*, R. A. Meyers (Ed.), John Wiley and Sons Ltd. Chichester, 2000, P. 3831-3855.
- ³⁰ A. Afzal, F. L. Dickert, *Nanotechnological Applications of Novel Polymers* 2009, 165-182
- ³¹ Daimay Lin-Vien, Norman B. Colthup, William G. Fateley, Jeanette G. Grasselli, *The Handbook of Infrared and Raman Characteristic Frequencies of Organic Molecules*, Academic Press Inc.,1991.
- ³² O. Hayden, R. Bindeus and F. L. Dickert, *Sci. Technol.* 2003, 14,1876-1881.
- ³³ Peter A. Lieberzeit, Abdul Rehman, Sadaf Yaqub & Franz I. Dickert. *NANO*, 2008, 3, 4, 205–208.
- ³⁴ Dickert, O. Hayden, P. Lieberzeit, C. Palfinger, D. Pickert, U. Wolff, G. Scholl, *Sensors and Actuators B*, 2003, 95, 20.
- ³⁵ Peter A. Lieberzeit , A. Afzal, A. Rehman, Franz L. Dickert, *Sensors and Actuators B*, 2007, 127.
- ³⁶ Lieberzeit, A. Afzal, D. Podlipna, S. Krassnig, H. Blumenstock, F. L. Dickert, *Sensors and Actuators B* , 2007, 126, 153–158.
- ³⁷ Zhao Li, Jianfu Ding, Michael Day, Ye Tao, *Macromolecules* 2006, 39.

³⁸ Abbas, Lichtman, Prober, Cellular and Molecular Immunology, W.B. Saunders 1999

³⁹ R. Schirhagl, A. Seifner, F. T. Husain, M. Cichna-Markl, P. A. Lieberzeit, and F. L. Dickert , Sensor Lett., 2010, 8, 399-404.

⁴⁰ Romana Schirhagl, Peter A. Lieberzeit, and Franz L. Dickert
Advanced Materials (Weinheim, Germany) , 2010, 22, 18, 2078-2081.

Curriculum Vitea

Personal

Name	Sadaf Yaqub
Date of Birth	16.12.1979
Place of Birth	Attock
Nationality	Pakistani
Gender	Female

Education

1985-1995	Higher Secondary School
1995-1997	Senior Higher Secondary School
1997-1999	Bachelors of Science
1999-2001	Masters of Chemistry

Scientific Work Experience

2000 - 2001	Master's research work with Title "Synthesis of some Glycosylamides & their derivatives as potential surfactants"
2002 - 2007	"Study of establishing novel chemical decontamination methods in power reactors" & QA/QC work as Junior Scientist, PIEAS, Islamabad, Pakistan
2007-to-date	PhD studies under supervision of Prof. Dr. F. L. Dickert at Institute of Analytical Chemistry & Food Chemistry

Awards

1990-1993	Federal board & POF scholarship for distinction at primary & secondary level Higher Secondary School
1998	President talent scholarship at graduation level
2007	PhD scholarship for Austria awarded by higher education